UNIVERSITÀ DEGLI STUDI DI PALERMO

DIPARTIMENTO DI ENERGIA, INGEGNERIA DELL'INFORMAZIONE E MODELLI MATEMATICI (DEIM)

Corso di Dottorato di Ricerca in Ingegneria Elettrica - XXIV CICLO
S.S.D. ING-INF/07 – Misure Elettriche ed Elettroniche

Tesi di Dottorato

# Study and development of innovative measurement methods and systems for anti-islanding protection in smart grids

NGUYEN Ngoc Trung

**Tutor**
prof. Antonio Cataliotti

**Coordinatore del corso di Dottorato**
prof. Mariano Giuseppe Ippolito

Dicembre 2013

**ACKNOWLEDGMENTS**

I would never have been able to finish my dissertation without the guidance of my committee members, help from friends, and support from my family and wife.

I cannot express enough thanks to my professor, supervisor for his continued support and encouragement: Prof. Antonio Cataliotti.

I would like to thank Dr.Ing Cosentino Valentina, who always patiently listens to me, carefully explains every issues and spent her holiday time to correct my thesis.

My completion of this project could not have been accomplished without the support of my colleagues: Salvatore, Antonio, Dario, Giovanni and all the other colleagues in our laboratory – thank you for allowing me time away from you to research and write, as well as other things about life in Palermo which is always new and amazing with me.

Finally, to my caring, loving, and supportive wife, Linh: my deepest gratitude and my *picolino Ciccio.* Your encouragement when the times got rough are much appreciated and duly noted. It was a great comfort and relief to know that you were willing to provide management of our household activities while I completed my work. My heartfelt thanks.

# TABLE OF CONTENTS

## LIST OF SYMBOLS AND ABBREVIATIONS

### Pollutants symbols

### Abbreviations - Glossary

| | |
|---|---|
| ADC | Analogue to digital converter |
| AFD | Active Frequency Drift Anti-islanding Method |
| CMR | Common mode rejection |
| CRV | Constant reference voltage |
| CSI | Current source inverter |
| DG | Distributed generation |
| DGPS | Distributed generator power system |
| DPF | Displacement Power Factor |
| DRMAC | Difference in root mean absolute of wavelet coefficients |
| DSP | Digital signal processor |
| DWT | Discrete wavelet transform |
| EMC | Electromagnetic Compatibility |
| ENS | Selbsttaetig wirkende Freischaltstelle mit 2 voneinander unabhängigen Einrichtungen zur Netzueberwachung mit zugeordneten allpoligen Schaltern in Reihe (also See MSD) |
| FCC | Federal Communications Commission |

| | |
|---|---|
| GTI | Grid-tie inverter |
| GUI | Graphical user interface |
| Hz | Hertz (cycles per second) |
| ICT | Incremental conductance technique |
| IEA | International Energy Agency |
| IEC | International Electrotechnical Commission |
| IEEE | Institute for Electrical and Electronics Engineers |
| IGBT | Insulated Gate Bipolar Transistor |
| Islanding | Islanding is a condition in which a portion of the utility system, which contains both load and generation, is isolated from the remainder of the utility system and continues to operate via a photovoltaic power source. |
| MPP | Maximum power point |
| MPPT | Maximum Power Point Tracking |
| MSD | Mains Monitoring Units with Allocated All-pole Switching Devices Connected in Series (also see ENS) |
| NDZ | Non-Detection Zone |
| OFP | Over Frequency Protection Device or Method |
| OFP/UFP | Over/Under frequency protection |
| OVP | Over Voltage Protection Device or Method |

| | |
|---|---|
| OVP/UVP | Over/Under voltage protection |
| P&O | Perturb and observe |
| PCC | Point of Common Coupling |
| PCS/PCU | Power conditioning system/unit |
| PJD | Phase Jump Detection Anti-islanding Method |
| PLCC | Power-line Carrier Communications |
| PLL | Phase Lock Loop |
| PV | Photovoltaic |
| PWM | Pulse width modulation/modulated |
| Qf | Quality Factor of a Resistor, Inductor, Capacitor (RLC) Circuit |
| RFI | Radio Frequency Interference |
| RMAC | Root mean absolute of wavelet coefficients |
| SCADA | Supervisory Control and Data Acquisition |
| SFS | Sandia Frequency Shift Anti-islanding Method |
| SMS | Slip Mode Phase Shift Anti-islanding Method |
| ST | Shoot-through |
| SVS | Sandia Voltage Shift Anti-islanding Method |
| T&D | Transmission and distribution |

| | |
|---|---|
| THD | Total Harmonic Distortion |
| UFP | Under Frequency Protection Device or Method |
| UL | Underwriters Laboratories, Inc. |
| UVP | Under Voltage Protection Device or Method |
| VCO | Voltage Controlled Oscillator |
| VSC | Voltage Source Converter |
| VSI | Voltage source inverter |
| WBA | Wavelet based analysis |
| Z | Impedance |
| ZSI | Z-source inverter |

# CHAPTER 1. INTRODUCTION

## 1.1 BACKGROUND AND MOTIVATION

One of the most important challenges in the near future is the complete integration of the distributed generators (DGs) in electric power systems, especially at distribution level (i.e. in medium and low voltage networks). In fact, the most feasible way to achieve the 20-20-20 target (20% reduction of greenhouses gas emissions, 20% increase of energy efficiency, 20% increase of renewable sources) is the increase of DG by means of renewable sources (RS), which are available on the territory and otherwise not exploitable. This implies a complete rethinking of the management and control of electricity networks, which have to move from passive systems to new active "smart grids". The existing passive systems are characterized by unidirectional energy flows and a limited amount of intelligent and automation functions. On the contrary, in the smart grids concept, energy flows are bi-directional and smart metering technologies and capabilities are needed, also with a two-way communications network and a number of other intelligent field devices, providing for monitoring, automation, and protection and control actions.

The European Union and also other Countries worldwide have endorsed the smart grid vision, with a particular attention at distribution networks, as they have a widespread diffusion on the territory, thus they can allow to fully exploit the RS. However these networks are more exposed than the transmission networks to the technical problems related to the DG, which are related not only to the possibility of energy flows direction changing but also to the amount of power flows, other technical bindings (slow and rapid voltage changes, thermal rate limits on the electricity lines, increase of short circuit currents and so on) and the islanding occurrence.

The term "islanding" refers to the condition in which a DG continues to power a part of the grid even if power from electric utility is no longer present. Islanding is an unwanted condition because of its adverse and potentially dangerous effects concerning power quality deterioration, grid protection interference, equipment damage, and personnel safety hazards. Thus, DGs have to be equipped with a proper anti-islanding protection system, which should be able to detect the islanding occurrence and promptly disconnect the DGs themselves from the utility grid (conventional anti-islanding protection). In recent times there has been also an increasing interest in a sort of "intentional" islanding operation, as well as in the so-called micro-grids. In these cases the distribution grid (or a part of it) can still operate in controllable islanding conditions, decoupled from the main grid. This can allow the improvement of power

quality in terms of supply continuity. In such condition the islanding detection is still important in order to switch the DGs' control mode from the simple power injection to the voltage and frequency control.

Some initiatives are in course at European Community level, to face the issues related to the DG integration in distribution networks. The Network Code Development by ENTSO-E (European Network of Transmission System Operators for Electricity) concerns the technical rules for DGs connection to and operation with electricity networks. The European Commission Smart Grid Mandate, M/490 EN, is aimed at developing or updating the European standardization for smart grids, concerning DGs connection, network automation and so on. All these activities involve a number of IEC and CENELEC Standards and Technical Specifications. For example, the CENELEC Technical Committee TC8X WG3 is currently working on some documents concerning the Requirements for the connection of micro-generators (up to 16 A) and generators (above 16 A) to distribution networks. At national level, some standards are available on these topics, such as the standard CEI 0-21 in Italy or the VDE-AR-N 4105 in Germany, whose approaches are very similar to the European standards projects. Furthermore, at international level, some IEC and IEEE standards are available, which define the requirements for connection of DGs and utility grid and the characteristics of the related interface devices (IDs). Generally speaking, these standards address the normal voltage and frequency operation range, some power quality issues, and safety related matters, in most cases including the issue of the unwanted islanding. As regards this last point, the anti-islanding requirements are essentially based on local measurements of conventional parameters, such as voltage or frequency; the thresholds for the disconnection of DGs are usually fixed in terms of over/under voltage and frequency. The standard CEI 0-21 introduces the possibility for the utility to remotely command the disconnection of the DGs or to modify the aforementioned thresholds, in order to avoid the operation in islanding conditions. The same standard considers also an "intentional islanding" issue, in which the utility can allow the temporary islanding operation of a part of the distribution grid (for preferential loads or maintenance reasons). Furthermore, this standard introduces some new features related to the possibility for DGs to participate to the voltage and frequency regulation, by means of the implementation of proper control strategies, based on the remote control by the utility.

As regards the islanding detection methods, several methods can be found in literature, which can be classified into passive, active and communications-based methods. Passive methods are based on the local monitoring of one or more grid variables (such as frequency, voltage or

phase angle, THD levels) and their comparison with some thresholds set for the measured parameters. As already mentioned, the anti-islanding protection considered by the current standards is based on passive methods. Such methods have the advantage of an easy and low-cost implementation; furthermore they do not deteriorate the power quality levels at the metering section. However, they can have a large "non-detection zone" (NDZ), i.e. they can fail when there is an almost balanced condition between the DG's generated power and the power consumed by the loads connected to the supplied part of the network. For this reason, passive methods are generally considered to be insufficient for the anti-islanding protection. Active methods are based on the injection at the point of common coupling (PCC) of a small disturbance (such as voltage, frequency or phase jumps; injection of current harmonics, interharmonics or negative-sequence components, active and reactive power variations) and on the monitoring of the resulting grid response. If the injected disturbance causes a significant change in system parameters at the PCC, it means that there is an islanding condition; otherwise, if the grid supply is present, the injected disturbance should be corrected by the grid voltage and frequency control. Active methods can reduce the NDZ, but they determine power quality problems and their effectiveness can be negatively affected by the presence of several DGs in the same grid. Moreover, their practical implementation would require a rethink of the control systems of the inverters (i.e. they cannot be easily implemented on an inverter already installed in a DG, since its control system is not adjustable for such purpose). The communication-based methods involve a transmission of data between the DG and the grid, and these data are used by the DG to determine when to disconnect. These methods are reliable and easy to be simplemented, they are theoretically NDZ free and they do not cause power quality problems; moreover they are not affected by the number of inverters on the system and they would be effective at any penetration level, with any size system, and with any type of DGs. However, they need a proper two-ways communication infrastructure (which is still missing, especially at distribution grid level) and their implementation can be expensive, depending on the adopted communication system.

## 1.2 OUTLINE OF THE THESIS

At the light of the aforesaid considerations, this work has been focused on the development of a hybrid solution for the islanding detection, which makes use of both passive methods (local measurements) and communications between the DGs and the distribution grid.

More in detail, the proposed solution has been developed starting from some existing standard requirements for local measurements and improving their effectiveness by both monitoring more than one parameter. In fact, most standards fix some thresholds for the disconnection of

DGs in terms of over/under voltage and frequency. Such limits determine the NDZ, i.e. the condition in which islanding cannot be detected because voltage and frequency remain within these limits, To reduce the NDZ, the measurements of other parameters can be added to the over/under voltage and frequency. A preliminary simulation study has been carried out concerning the usefulness of some parameters (such as the harmonic distortion, the phase jumps and the voltage unbalance), for their employment for the purpose of islanding detection and the reduction of the NDZ. This preliminary study has been carried out on a simple test system, in which a DG is connected to the point of common coupling (PCC) between the grid and the load. The usefulness of the considered parameters has been investigated in different scenarios, with both sinusoidal and nonsinusoidal supply voltage and both linear and nonlinear loads. Starting from the results of the study, a combined approach has been formulated, which is based on the simultaneous monitoring of the different parameters, obtaining a mix of information which allows to reduce the NDZ. Furthermore, when the aforesaid local measurements give an uncertain result (i.e. in NDZ situations), communications between the grid and the DG can be used to send utility status information back to the DG (in order to detect the status of the PCC breaker). In such cases the communications are used to support the decision, in order to avoid the unwanted operation of DGs in islanded conditions. On the other hand, the local measurements could help if a communication fail occurs.

The effectiveness of the proposed hybrid solution has been analyzed in the real case of the Ustica Island's distribution network. The model of the simulated network has been implemented in Matlab/Simulink environment and the presence of the DG was simulated at the low voltage side of a secondary substation of the distribution network. The analysis has been carried out in several scenarios, which were obtained by varying the load conditions (both linear and non linear), the DG's configuration (presence of one or more generators) and the supply voltage (sinusoidal or nonsinusoidal).

The proposed hybrid solution for islanding detection can be implemented in a real system, by integrating local measurements and communication in the DG interface device (ID) and developing a proper communication architecture for smart grid applications. In this viewpoint, the study herein presented has been carried out in conjunction with the following research projects (both under the Scientific Responsibility of prof. Antonio Cataliotti):

- PO FESR 2007-13 Sicily, Line 4.1.1.1, Project: REIPERSEI Title: "Reti Elettriche Intelligenti per la Penetrazione delle Energie Rinnovabili nei Sistemi Elettrici delle Isole

minori" (Smart grids for the exploitation of renewable energy sources in the little islands of the Mediterranean Sea),

- PO FESR 2007-13 Sicily, Line 4.1.1.2, Project: SERPICO Title: "Sviluppo E Realizzazione di Prototipi di Inverter per impianti fotovoltaici a COncentrazione" (Development of new inverters prototypes for concentration photovoltaic systems).

In the framework of the aforesaid projects a new ID prototype has been developed for distributed generation, which is able to integrate both measurement and communication functions. Furthermore, different possible solutions have been investigated concerning the communication architecture, mainly using the power line communication technology, even integrated with other wireless solutions, in the framework of a SCADA (Supervisory Control and Data Acquisition) architecture. The proposed hybrid anti-islanding protection can be implemented in such systems, obtaining a mix of information (even redundant), which can help to improve the effectiveness of the traditional anti-islanding protection, without introducing power quality problems (as active methods do) and without depending on the number or type of DG connected to the power system. The proposed approach can also allow the utility to remote control the DGs, in the perspective of their active participation to the power grid stability and control. In this way, it would be possible to move towards a complete integration of DGs with the utility systems, implementing not only protection functions, but even more, contributing to power grid stability and control.

The thesis is divided as follows.

- In the first chapter the motivation and scientific goals of the thesis have been described.
- The second chapter summarizes the main regulations and standards concerning the DG integration in distribution networks and the anti-islanding protection requirements. Furthermore, an overview is given concerning the main features, advantage and drawbacks of the islanding detection methods already proposed in literature.
- In the third chapter the proposed combination of local measurements are introduced; the reduction of the NDZ is also investigated and the results of the preliminary study on the simple test system are presented and discussed. Starting from this, the proposed hybrid solution is formulated, in conjunction with its implementation on the new ID prototype and the communication system architecture.
- The fourth chapter reports the results of the simulations which have been carried out on the real test system of the Ustica's distribution network.
- The source code implementation of the proposed solution is reported in the appendix.

# CHAPTER 2. ISLANDING DETECTION. STATE OF THE ART

## 2.1 INTRODUCTION

Nowadays, sustainable development is a global strategy, in particular, in the field of energy such as the electric power system, the trend is to improve new processes and technologies; they boosted and accelerated rapidly the roll out of "smart active grids" which use information and communication techniques. The photovoltaic (PV) is the main type of distributed generation technology interconnected to the utility grid and PV systems, considering the fast growth and widespread development of PV systems embedded in the distributed generation power system (DGPS). It is important that interconnection produces as streamlined as possible to avoid unnecessary interconnection studies, cost and delays.

One of the most important challenges in the near future is the complete integration of the distributed generators (DGs) in electric power systems, especially at distribution level (i.e. in medium and low voltage networks). In fact, such integration would allow the best use of the renewable sources (RS) available on the territory and otherwise they could not be exploitable. This implies a complete rethinking of the management and control of electricity networks, which have to move from passive systems to new active "smart grids" [1-6]. The existing passive systems are characterized by unidirectional energy flows and a limited amount of intelligent and automation functions. On the contrary, in the smart grids concept, energy flows are bi-directional and smart metering technologies and capabilities are needed, also with a two-way communications network and a number of other intelligent field devices, providing for monitoring, automation, and protection and control actions [7-9]. In this study, proposing of a novel IDM is one of the most important features. The term "islanding" refers to the condition in which a DG is continuing to operate with local load that means DG continues to power a part of the grid even if power from electric utility is no longer present [8, 10, 11].

Islanding can be either intentional or unintentional. However, islanding condition must be detected, unless this is an undesirable condition. This is necessary for the system to have immediate responses after islanding occurred, in order to ensure the safety of utility maintenance personnel and the general public and also to avoid damage to connected equipment; because of this situation's adverse and potentially dangerous affects concerning power quality deterioration, grid protection interference, personnel safety hazards, and equipment damage. In this case, some kinds of DGs (i.e. the PV inverters) need to disconnect from the grid in case of abnormal grid conditions of voltage and frequency. Thus, DGs have

to be equipped with a proper anti-islanding protection system, which should be able to detect the islanding occurrence and promptly disconnect the DGs themselves from the utility grid.

## 2.2 INTERNATIONAL REGULATIONS

Although each electric power system (EPS) will have their own specific guidelines according to the features of each particular region, there are some international standards available that can be used as regulations. There are lots of international regulations for the connection of DGs and utility grid. The most important standards are as follows:

- IEEE929 Recommended Practice for Utility Interface of Photovoltaic (PV) Systems [1].
- IEEE1547 Series of Standards for Interconnection of Distributed Resources with Electric Power Systems from 2003 to 2009 (DG<10MVA) [7].
- UL1741, Standard for Inverters, Converters, and Controllers for Use in Independent Power Systems, elaborated by Underwriters Laboratories Inc., an important standardization body in the US. In terms of grid requirements UL 1741 acknowledges IEEE 1547 [10].
- EN 50160 Voltage Characteristics in Public Distribution Systems [12] and CEI 0-21- Reference technical rules for the connection of active and passive users to the LV electrical Utilities [13].
- IEC61727 Characteristics of Utility Interface and Series of IEC 61000 - Electromagnetic Compatibility (EMC – low frequency). In Europe, according to [10] current harmonic limits set by IEC 61000-3-2 (class A).
- VDE 0126-1-1 Safety is used for the utility in Germany.

The Europeans apply the standard IEC61727 meanwhile the recommendations for United State are IEEE929-Recommended Practice for Utility Interface of Photovoltaic (PV) Systems and IEEE1547-Series of Standards for Interconnection of Distributed Resources with Electric Power Systems from 2003 to 2009 (DG<10MVA); in Germany, the standard is VDE 0126-1-1 [1],[7],[10],[12]. When the utility voltage is over certain limits (typically around ± 15%) the inverter should cease to energize within 0.2s to 2s (depending on the standards). According to the IEC61727, CEI 0-21 [13], the power system operates continuously when the voltage at the point of utility connection is in the middle 85% and 110%; those are detailed below [10, 14-16].

| IEEE 1547 | | IEC61727 | | VDE0126-1-1 | |
|---|---|---|---|---|---|
| Voltage range (%) | Disconnection time (s) | Voltage range (%) | Disconnection time (s) | Voltage range (%) | Disconnection time (s) |
| V < 50 | 0.16 | V < 50 | 0.10 | 110 ≤ V < 85 | 0.2 |
| 50 ≤ V < 88 | 2.00 | 50 ≤ V < 85 | 2.00 | | |
| 110 < V < 120 | 1.00 | 110 < V < 135 | 2.00 | | |
| V ≥ 120 | 0.16 | V ≥ 135 | 0.05 | | |

***Table 2.1 International regulation of disconnected time for voltage variations***

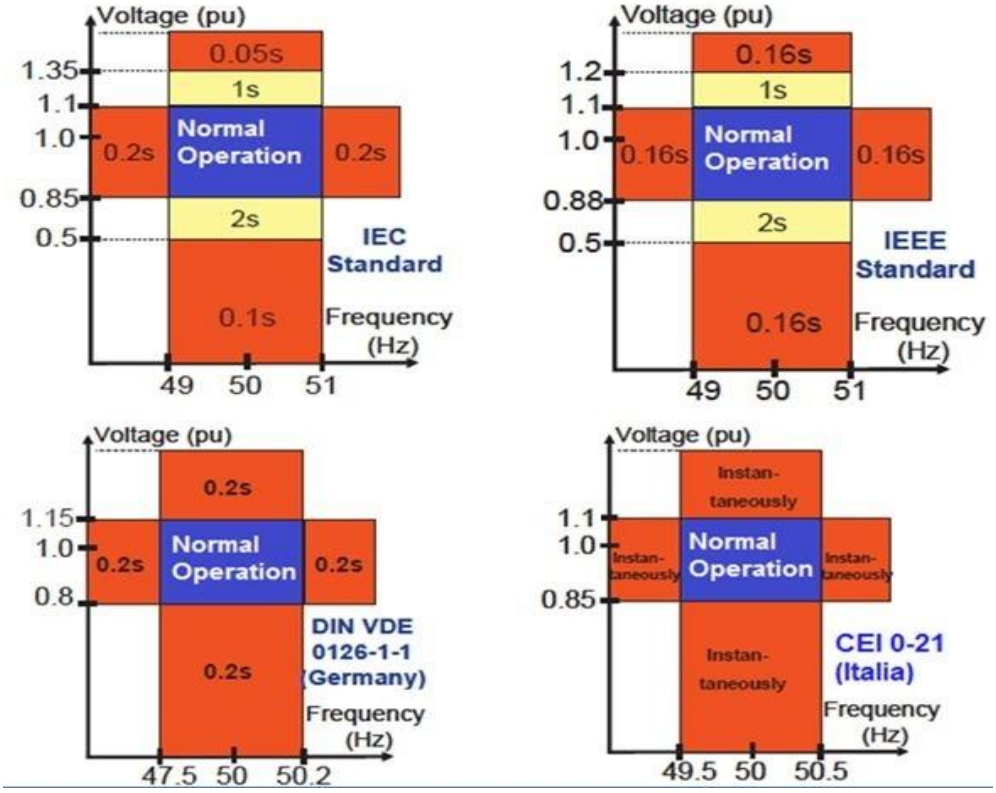


Fig.2.1. ***Requirements for anti-islanding detection on LV network (voltage and frequency) by IEC, IEEE, Germany and Italia***

### 2.2.1 ANTI-ISLANDING PROTECTION REQUIREMENTS

According to IEEE 1547 and CEI 0-21 standard suggests that if the circuit breaker (CB) supplying the feeder connected to the DG at PCC is tripped; DRs should be disconnected from the utility distributed system [17]. This is known as a mandatory feature in the inverter interfaces for DGs, as well as the characteristic of "anti-islanding" protection. Thus, DGs have to be equipped with a proper anti-islanding protection system, which should be able to detect the islanding occurrence and promptly disconnect the DGs themselves from the utility grid and to prevent any out of synchronism reclosing. Anti-islanding systems are mainly used to ensure safety for DPS. Meaning that this system can safe the utility

maintenance personnel and the general public and also to avoid damage to connected equipment.

### 2.2.2 RECONNECTED CONDITIONS

A novel suitable isolated control procedure will provide reconnection detection signal for synchronous type DGs and must be used for proper operation of DGs in order to maintain power quality and reliability when working in parallel with the grid, as well as working stand-alone. In [10] the inverter can be reconnected after trip by abnormal, voltage or frequency deviations and DC current injection limitation of the rated RMS current should compliance with requirements of IEC 61727, CEI 0-21 standard as $85<V<110$ (%), $f_n-1<f<f_n+1$ (Hz) and minimum delay of 3 seconds and $I_{DC}<1$ (%).

In order to avoid unnecessary loss of supply especially for high priority loads, DGs stand-alone operation is getting more attention. However, to ensure more reliability, the islanded distribution network must reconnect to the grid as soon as the quality of supply from grid is refined. As the circuit breaker (CB) which had been opened for unintentional/intentional islanding operation is often so far from the DG, introducing a reliable method for localized reconnection detection and proper DG control mode activation will be an interesting issue. Such a method could be implemented via a micro-processor based relay as a low cost alternate for the expensive communication means required between all of the CBs that may initiate the islanding and the DG [18].

## 2.3 OVERVIEW OF ANTI-ISLANDING DETECTION METHODS

### 2.3.1 INTRODUCTION

The intentional islanding refers to the case of the DGPS in which one or several distributed energy resources are allowed to work *independently* to *continue energize* load location or a part of the grid even if power from the main grid is no longer present. For some period of time, this section is separated from the rest of the utility grid.

When DGs are connected into the distributed power system (DPS), which converts the radial power line to complicated ones, as well as the dynamic behaviors of the DGs affect the steady state operation condition of DPS. In the following, the various influences of the utility grid-connected by DGs on the existing protection system are listed [17]:

- blinding of protection
- changing of fault levels with connection and disconnection of DERs

- unwanted islanding (i.e. DC-link such as PV, fuel cell)
- false tripping or nuisance tripping
- prevention of automatic reclosing or unsynchronized reclosing

For safe operation of DPS connected by DG, anti-islanding detection methods should be applied to change the DG operating condition to stand-alone situation and vice-versa. Detecting the absence of power from the grid is complicated by two items:

- The distributed generator itself is a source of power whose voltage is by definition identical to the voltage from the grid, so it is hard to distinguish the two
- A nearby motor may continue to spin and act as a generator, creating a frequency similar to the original line frequency (50 or 60 Hz). That may be also true if the load in the building forms a resonant circuit at the line frequency.

In the following, IDMs are briefly described, as well as their non-detection zone (NDZ) is discussed. Islanding condition might be detected passively, actively or by utility notification. For this issue, the utility grid must know when it removes power to the load, and send a trip signal to the DGs to stop generating power. These methods can be classified in three main categories, also the methods can be found in literature [8, 10-20] concerning the islanding detection, which can be classified into:

- Passive methods
- Active methods
- Communication based methods
- Hybrid methods

In Fig. 2.2 a summary of the state of the art of islanding detection methods is presented with a brief comparison in Table 2.2 .

First, passive detection is done by detecting that the line voltage and frequency are no longer within certain limits. One principle is that, once the grid is no longer establishing the line voltage that voltage will change (it will usually drop, but not necessarily). The other principle is that, even if a motor is creating a line frequency, it will slow down, and therefore do so at lower frequency than the standard line frequency.

Second, active detection is done by purposely adding a disturbance to the line, and seeing its effect: The principle is that the grid offers essentially zero ohm impedance. In the

absence of the grid, the impedance that is seen is the load in the building, which is substantially higher.

Third, remote islanding detection techniques are based on communication modes between utilities and DGs. Although these techniques may have better reliability than local techniques, however, they are expensive to implement and hence uneconomical. Among them, power line communication (PLC) is the only wire line technology that has cost comparable to wireless, since the lines are already present (i.e., the power lines), and it has no service cost. As regards this last aspect, a large variety of communication technologies can be involved in the realization of smart grid infrastructures, each one having its own advantages and drawbacks [8, 10, 11, 14, 16, 20-28].

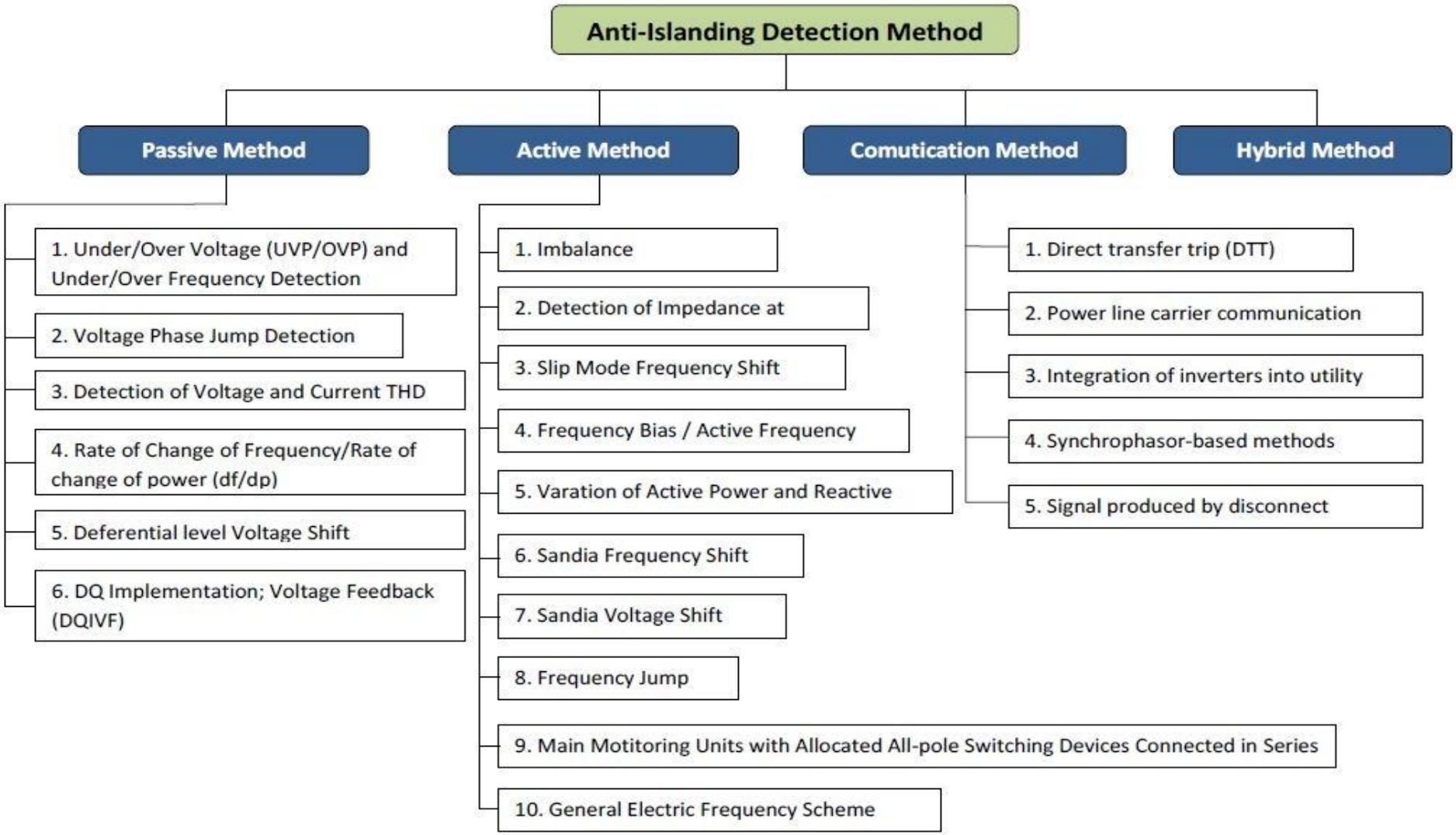


Fig.2.2. ***Anti-islanding detection methods overview***

| Islanding Detection Methods | Strengths | Weaknesses | Grid friendly | Examples |
|---|---|---|---|---|
| **Passive Methods** | - Short islanding detection time<br>- Do not perturb the system<br>- Accurate when there is a large mismatch in generation and demand in the islanded system<br>- Grid friendly<br>- Easy and cheap to implement | - Difficult to detect islanding when the load and generation in the islanded system closely match<br>- Special care has to be taken while setting the thresholds<br>- If the setting is too aggressive then it could result in nuisance tripping<br>- NDZ larger compared to others | - Yes | - Rate of change of output power scheme[22, 29]<br>- Rate of change of frequency scheme [26]<br>- Rate of change of frequency over power scheme [30]<br>- Change of impedance scheme [31, 32]<br>- Voltage unbalance scheme [26, 33]<br>- Harmonic distortion scheme [30, 33, 34] |
| **Active Methods** | - Can detect islanding even in a perfect match between generation and demand in the islanded system (Small NDZ - low NDZ)<br>- some easy to implement | - Introduce perturbation in the system. It often degrades the power quantity (may create power quality problems) and if significant enough, it may degrade the system stability even when connected to the grid.<br>- Detection time is slow as a result of extra time needed to see the system response for perturbation.<br>- can lead to nuisance trip<br>- some difficult to implement<br>- possible interaction between converters in the same grid | - suitable for a finite number of generators | - Reactive power export error detection scheme [35]<br>- Impedance measurement scheme [31, 36, 37]<br>- Phase (or frequency) shift schemes (like SMS, AFD, AFDPF and ALPS) [38, 39] |
| **Communication Methods** | - Highly reliable<br>- some easy to implement<br>- theoretically no NDZ | - Expensive to implement especially for small systems<br>- need communication infrastructure<br>- need involvement of utility | - Yes | - Transfer trip scheme [8, 28]<br>- Power line signalling scheme [8, 20, 24, 40, 41] |
| **Hybrid Methods** | - Have small NDZ.<br>- Perturbation is introduced only when islanding is suspected. | - Islanding detection time is prolonged as both passive and active technique is implemented | - Yes | - Technique based on positive feedback and voltage imbalance [8]<br>- Technique based on voltage and reactive power shift [25] |

***Table 2.2 Brief comparison of islanding detection methods***

### 2.3.2 PASSIVE METHODS

These methods are based on a local monitoring of grid variables such as frequency, voltage and/or their characteristics, as the phase angle, particular harmonics or the total harmonic distortion (THD) levels. If the monitoring algorithm detects large or sudden changes of these variables at the point of common coupling (PCC) of the DG with the utility grid, the DG is commanded to disconnect. The discrimination between the islanding and grid connected condition is based upon some thresholds set for the measured parameters [8, 11, 15, 19, 22, 30].

- Over/under voltage – monitors whether or not the grid voltage goes out of the limits established by the relevant standards.
- Over/under frequency – monitors whether or not the grid frequency goes out of the limits imposed by the relevant standards.
- Monitoring rate of change of frequency (ROCOF) and voltage (ROCOV).
- Phase monitoring – monitors fast jumps of grid voltage phase
- Voltage harmonic – monitors selective (3rd, 5th, etc.) or total harmonic distortion (THD) of grid voltage.

*Comparison and Evaluation:* Passive methods have the advantage of an easy and low-cost implementation; furthermore they do not deteriorate the power quality levels at the metering section. However, they can have a large "non-detection zone" (NDZ), i.e. they can fail when there is an almost balanced condition between the DG's generated power and the power consumed by the loads connected to the supplied part of the network. For this reason, passive methods are generally considered to be insufficient for the anti-islanding protection [8].

### 2.3.3 ACTIVE METHODS

These methods are based on the injection at the PCC of a small disturbance (such as voltage, frequency or phase jumps; injection of current harmonics, inter-harmonics or negative-sequence components, active and reactive power variations, etc.) and on the monitoring of the resulting grid response, in order to decide whether or not an islanding condition is present. In fact, in case of grid connected situation, the injected disturbance should be corrected by the grid (by the voltage and frequency control); on the contrary, if the injected disturbance causes a significant change in system parameters at the PCC, it means that there is an islanding condition.

In most cases the disturbance should be injected by acting on the control system of the DG inverter [8, 10, 11, 14-16, 19, 23].

- Positive feedback inside the DG control – the controller tries to alter grid variables such as frequency, phase or voltage magnitude [37, 42-46].
- Impedance detection – active method which has been promoted by the requirements in the German standard. A current spike is periodically injected at the point of common coupling by a grid tied power converter. Based on the voltage response to this disturbance, the grid impedance value is determined using Fourier transform. The influence of non-linear loads connected close to the point of common coupling (PCC) is also addressed and as a consequence additional signal processing method is necessary in order to obtain accurate results [11, 31, 32, 35, 36].

*Comparison and Evaluation:* In comparison with the passive methods, the main advantage of the active methods is the reduction of the NDZ. As regards this, in literature some hybrid solutions have been proposed, based on passive and active methods, in order to reduce the NDZ [11, 16]. However, active methods determine power quality problems, as they disturb the delivered power in order to detect islanding conditions; furthermore their effectiveness can be negatively affected by the presence of several DGs in the same grid. Finally, the practical implementation of an active method would require a rethink of the control systems of the inverters (i.e. they cannot be easily implemented on an inverter already installed in a DG, since its control system is not adjustable for such purpose) [8].

### 2.3.4 COMMUNICATION METHODS

Another category of methods for detecting islanding is based on communication between DG and the utility grid. The communication-based methods involve a transmission of data between the DG and the grid, and these data are used by the DG to determine when to disconnect [8, 14, 20, 27]. Three main methods using communication are detailed:

- Power line used as carrier for communication between the PV inverter and utility grid. A continuous signal is transmitted by utility network via the power line. A receiver is necessary to be connected to the DG for detecting the loss of this signal and hence determining islanding conditions.

- Signal produced by disconnects. This method assumes that the utility reclose is equipped with a transmitter which communicates with DG when opens.
- SCADA based method uses placement of voltage sensors at the location where DG is connected and integration of those sensors in the SCADA system for monitoring and alarming the PV system to disconnect in case of islanding. With an increasing number of DGs connected to the grid, real time monitoring of voltage for each generator in distribution grid can be a cumbersome process.

*Comparison and Evaluation**:*** These methods are reliable and easy to be implemented, they are theoretically NDZ free and they do not cause power quality problems; moreover they are not affected by the number of inverters on the system and they would be effective at any penetration level, with any size system, and with any type of DGs [8].

In particular, the PLC-based methods entail the use of the power line as a communication channel [8, 14, 20, 27] . A continuous low-energy signal is transmitted between a transmitter located on the side of the grid and receiver located on the side of the DG. Thus the PLC signal is used to perform a continuity test of the line. When the communication is interrupted, this indicates a break in the continuity of the line and the receiver command the disconnection of the DG. Because the series inductances of transformers block high-frequency signals, the methods proposed in literature are based on the use of low-frequency signals or even sub-harmonic signals, unless both the transmitters and the receivers are all installed in the medium voltage network. As regards this, in previous works the authors have investigated the use of PLC in MV-LV networks, showing the feasibility of the communication at both MV and LV level.

### 2.3.5 HYBRID METHODS

Hybrid anti-islanding is the better way to overcome all islanding problems. The method based on a hybrid method using the passive and the active techniques can detect the islanding condition effectively without decreasing the power quality interconnected DG because it injects of small amount of disturbance. The active methods is implemented and operated only when the islanding is suspected by the passive technique. The islanding can be detected quickly (in just a few milliseconds) and the distributed generation can be shut down quickly and this method can reduce the NDZ [38].

### 2.3.6 DISCUSSION

There is no single islanding detection technique which works sufficiently and perfectly for all systems under every operated condition. The available choice of the islanding detection methods mainly depends on the type of the DG and the utility grid features. The passive methods based on the local measurement techniques are the protection of fundamental groups of DG connected to grid. Recently, active methods are preferred because of their low NDZ. However, active techniques always introduce a perturbation in the system so it may degrade the system stability and create power quality problems. Nowadays, the utility grid may facilitate a move towards the use of communication techniques and hybrid based methods for islanding detection, which makes use of both passive methods (local measurements) and communications with the grid [8] and will be presented in the following chapters. It has been developed starting from standard requirements and improving the effectiveness of the passive methods by monitoring more than one parameter. In fact, apart from the measurements of over/under voltage and frequency (considered in the standard requirements), the monitoring of other parameters is used, in order to reduce the NDZ. Furthermore, also the communications are used between the DG and the grid, in accordance with the standards. The communication is always operated and trip signal will be sent immediately when the islanding is suspected by the local measurement technique. In this way, a mix of information can be obtained (even redundant) in order to avoid misleading situations. In critical cases (i.e. in NDZ situations) the communications should support the decision, in order to avoid the unwanted operation of DGs in islanded conditions. On the other hand, the local measurements could help if a communication fail occurs.

# CHAPTER 3. THE PROPOSED SOLUTION FOR ISLANDING DETECTION

## 3.1 INTRODUCTION

In the previous chapter an analysis has been carried out of the main advantages and drawbacks of the different approaches which have been proposed in literature for the islanding detection (passive, active and communication-based methods). It was shown that passive methods have the advantage of an easy and low-cost implementation and they do not deteriorate the power quality levels at the metering section; however, they can have a large "non-detection zone" (NDZ). Active methods can reduce the NDZ, but they determine power quality problems and their effectiveness can be negatively affected by the presence of several DGs in the same grid; moreover, their practical implementation would require a rethink of the control systems of the inverters (i.e. they cannot be easily implemented on an inverter already installed in a DG). Communication-based methods are reliable and easy to be implemented, they are theoretically NDZ free and they do not cause power quality problems; moreover they are not affected by the number of inverters on the system and they would be effective at any penetration level, with any size system, and with any type of DGs; their main limit is that they need a proper two-ways communication infrastructure (which is still missing, especially at distribution grid level).

At the light of the aforesaid considerations, the work has been focused on the feasibility of a hybrid solution for the islanding detection, which makes use of a combined passive method (local measurements) integrated with the communications between the DGs and the distribution grid.

The combined passive method has been developed starting from the requirements of the CEI 0-21 standard requirements for local measurements and improving their effectiveness by both monitoring more than one parameter. In fact, most standards fix some thresholds for the disconnection of DGs in terms of over/under voltage and frequency (OUV and OUF, respectively), which are measured at the point of common coupling (PCC) between the DG and the distribution grid. Such limits determine the NDZ, i.e. the condition in which islanding cannot be detected because voltage and frequency remain within these limits, To reduce the NDZ, the measurements of other parameters can be added to the over/under voltage and frequency. A preliminary investigation was already carried out concerning the usefulness of some parameters (such as the harmonic distortion), for their employment for the purpose of islanding detection. Starting from the results of the aforesaid preliminary studies, a combined approach has been

formulated, which is based on the simultaneous monitoring of the following quantities: over/under voltage and frequency (OUV, OUF), voltage phase jump (PJ), voltage unbalance (VU) and voltage total harmonic distortion (THD). It has been demonstrated that the mix of such measurements can reduce the NDZ.

On the other hand, the work has shown that, in some cases, the measurements of the considered parameters can give an uncertain result (i.e. the variations of some parameters could be too small, or within the measurement uncertainty range). This is also related to the fact that, for the practical implementation of the proposed solution, it is necessary to fix the proper thresholds for the parameters variations, in order to provide a reliable islanding detection. For the considered parameters some limits are already fixed by the current standards concerning the voltage and power quality levels in distribution networks and they can be considered as a first reference for the thresholds. However, some "site-specific" conditions can occur, such as the starting of some typical loads (such as motors, which can cause transient phase jumps) or the presence of nonlinear and/or time-varying loads (which can modify the harmonic distortion level at PCC during their normal operation). Such conditions can cause significant variations on the monitored parameters and can lead to incorrect information for the islanding detection purpose. Thus, the islanding detection strategy should take into account these situations, in order to adjust itself to the measurement site. A possible solution to this problem can be achieved if the local measurements are implemented in a recursive algorithm, which can allow to properly fix the thresholds.

Furthermore, the combined passive method has been integrated with the communications (hybrid method), in order to improve the effectiveness of the islanding detection. In fact when the local measurements give an uncertain result (i.e. in NDZ situations), communications between the grid and the DG can be used to send utility status information back to the DG (in order to detect the status of the PCC breaker). In such cases the communications are used to support the decision, in order to avoid the unwanted operation of DGs in islanded conditions. On the other hand, the local measurements could help if a communication fail occurs. The proposed hybrid solution for islanding detection can be implemented in a real system, by integrating local measurements and communication in the DG interface device (ID) and developing a proper communication architecture for smart grid applications.

The following sections describe the development of both the combined passive method and the hybrid solution.

## 3.2 INDICES TO DETECT ISLANDING

In this study, we select four system parameters including three conventionally used parameters (voltage magnitude, phase, and frequency) and newly proposed one (total harmonic distortion of current) and define the indices for detecting islanding operations. In the following, each considered index is introduced and a flow chart of its measurement is reported; the flow charts include also the approach for fixing the thresholds, which is developed in accordance with the standard requirements (if any) or in a recursive way (for the indices which are not considered in the standards).

### 3.2.1 INDEX OF THE VOLTAGE MAGNITUDE

The index is defined as the root-mean square (rms) value of voltage of one period

$$V_{rms,t} = \frac{1}{N}\sum_{i=0}^{N-1} V_{i-1}^2 \quad (3.1)$$

*Where,*

N is a sampling number of one cycle in the monitoring time,

v is an instantaneous voltage,

t is the monitoring time.

For this index the standards already provide some thresholds, which are also related to the trip time for the disconnection of the DG.

The maximum disconnection times laid down in the standard such as IEEE1547, EN50160 and CEI 0-21.

- $V < 0.5 \times V_n$ - 0.1 s ($V_n$ is the nominal voltage)
- $V \leq 0.85 \times V_n$ -2.0 s
- $V > 1.1 \times V_n$ - 2.0 s
- $V \geq 1.35 \times V_n$ - 0.05 s

Once any grid power is restored, the inverter should not connect for some time. This is typically between 20 seconds to 5 minutes and should be agreed with the utility provider.

In the following figure there is reported the flow chart of the implementation of the rms index measurement

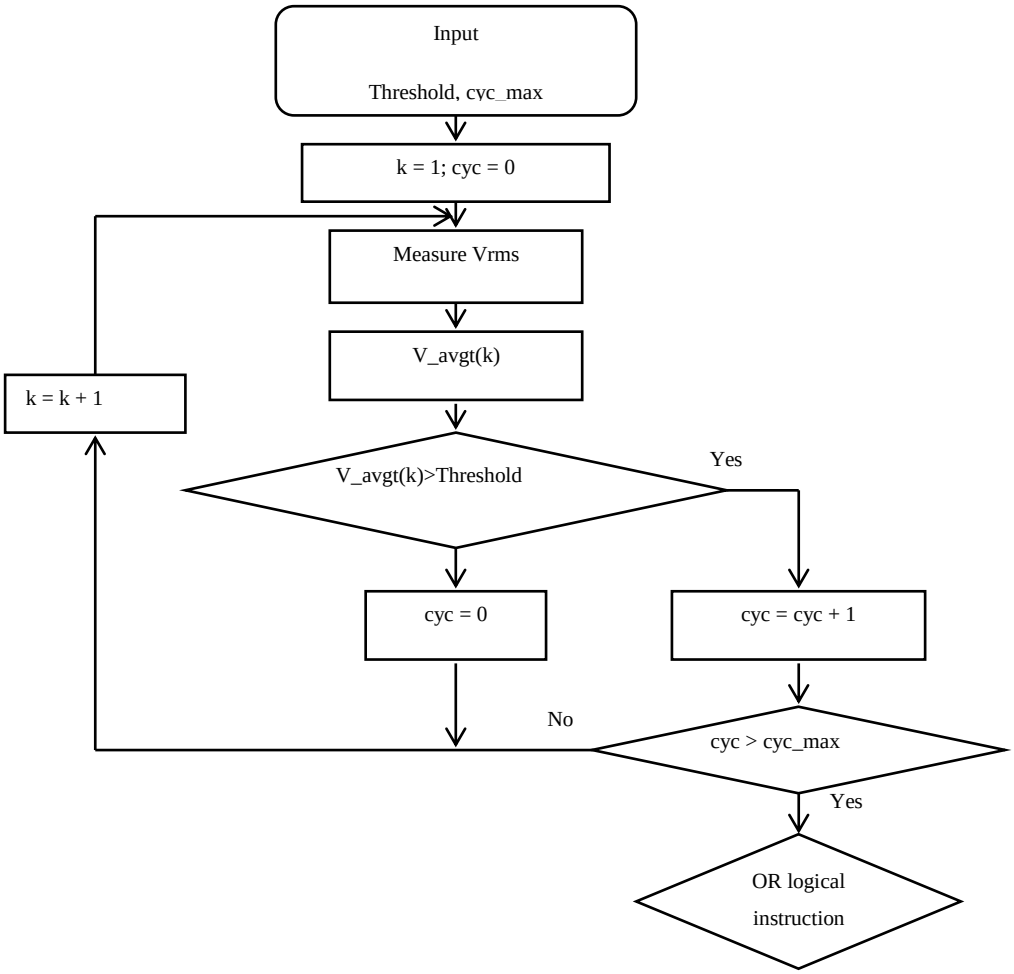


***Fig.3.1 Over/Under Voltage Detection method Algorithm***

### 3.2.2 INDEX OF THE PHASE DISPLACEMENT

The index is defined as the phase difference of voltage and current in the one-cycle

$$Ph_{avg,t} = \frac{1}{N}\sum_{i=0}^{N-1} Ph_{t-i} \quad (3.2)$$

The phase displacement index is used to quantify how much the monitored phase difference changes from the steady state and normal loading conditions, as reported the following equation

$$\Delta Ph_t = Ph_{avg,s} - Ph_{avg,t} \quad (3.3)$$

Where,

N is a sampling number of one cycle in the monitoring time,

t is the monitoring time,

$Ph_{avg,s}$ is the reference for the phase difference of the steady state and normal loading conditions,

$Ph_{avg,t}$ is the phase of voltage in the normal condition.

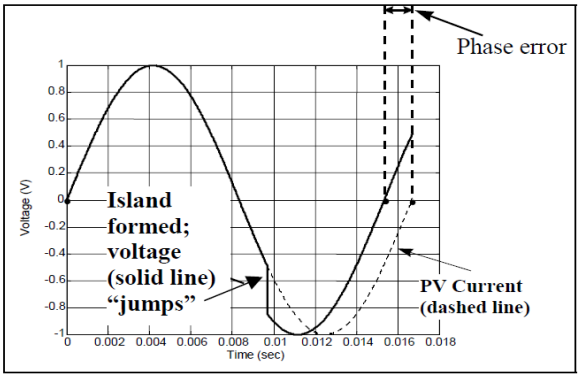


***Fig.3.2 The operation of phase difference of voltage and current in the one-cycle***

In the following figure there is reported the flow chart of the implementation of the phase displacement (or Phase Jump-PJ) index measurement

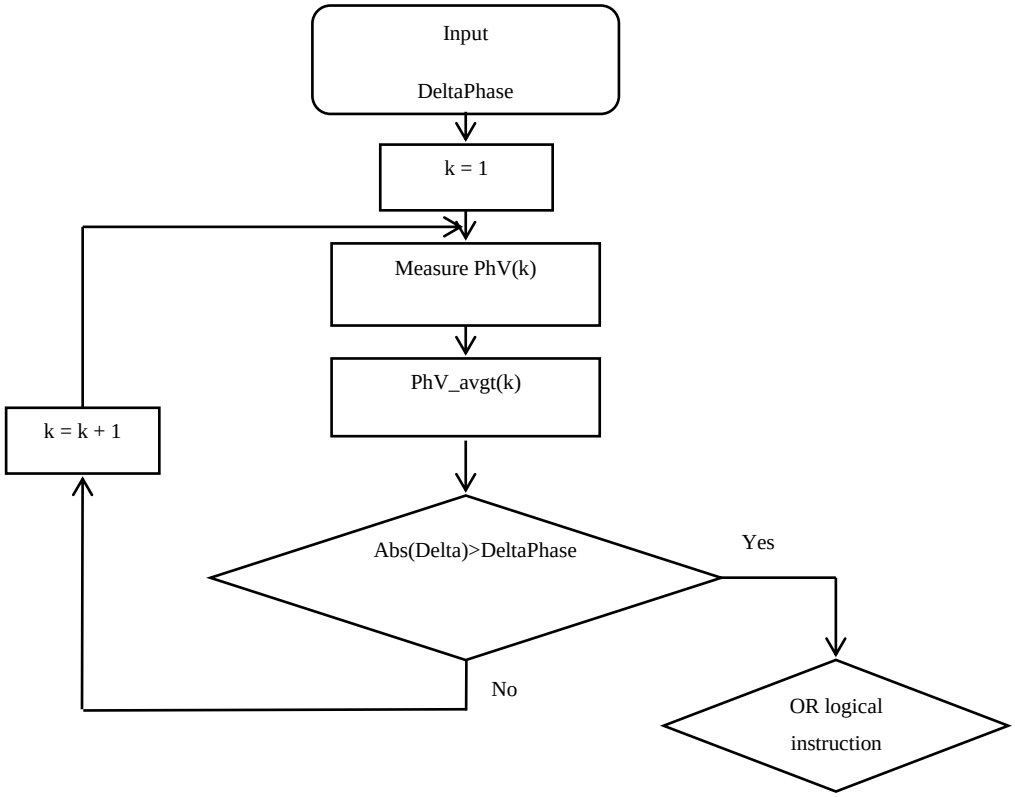


***Fig.3.3 Voltage Phase Jump Detection method Algorithm***

### 3.2.3 INDEX OF THE RATE OF CHANGES IN FREQUENCY

The index is defined as changes in frequency of one second:

$$Cf_t = \left| f_t - f_{t-(1s)} \right| \quad (3.4)$$

where, $f_t$ is the frequency at the monitoring time of t.

For this index the standards already provide the following threshold, which is also related to the trip time for the disconnection of the DG. The frequency variation is limit (with respect to the rated value) ±1 Hz - 0.2s.

### 3.2.4 INDEX OF CHANGES IN TOTAL HARMONIC DISTORTION OF VOLTAGE AT PCC.

The changes in the load of DR due to loss of main source power obviously result in the changes in the harmonics of current. So, we introduce the total harmonic distortion of current as one of indices for detecting islanding operations. Therefore, it is possible to detect an islanding operation of DR by monitoring the variance of harmonic quantity of current. The total harmonic distortion of current at the monitoring time *t* can be defined as follows,

$$THD_t = \frac{\sqrt{\sum_{h=2}^{\infty} V_h^2}}{V_1} . 100 \quad (3.5)$$

And, the average of *THDt* over one-cycle is defined as follows,

$$THD_{avg,t} = \frac{1}{N} \sum_{i=0}^{N-1} THD_{t-i} \quad (3.6)$$

The index of changes in THD is also defined as follows which measures how much the monitored THD at t deviates from the steady state and normal loading conditions,

$$Theta\ (\theta) = |\Delta THD_t| = \left| \frac{THD_{avg,s} - THD_{avg,t}}{THD_{avg,s}} \right| . 100 \quad (3.7)$$

*Where*,

*h* means the harmonic component.

N is a sampling number of one cycle in the monitoring time

THDavg,s is the THD reference value the steady state and normal loading conditions.

After THDavg,s is initially set, in order to adapt the normal load variation, if ΔTHDt remains within –100% through +75% for one-cycle, it is updated by THDavg,t. And also, to *avoid inaccurate decisions during too short transient state, if there are abrupt changes in THDavg,t above 0.1% during 1/4 cycle, as defined in following equation, this method discards the value and goes to the next time step.*

$$THD_{defined,t} = THD_{avg,t} - THD_{avg,t-p} \quad (3.8)$$

*Where,* p is set to be ¼ cycles that is 5 ms.

In the following figure there is reported the flow chart of the implementation of the THD index measurement

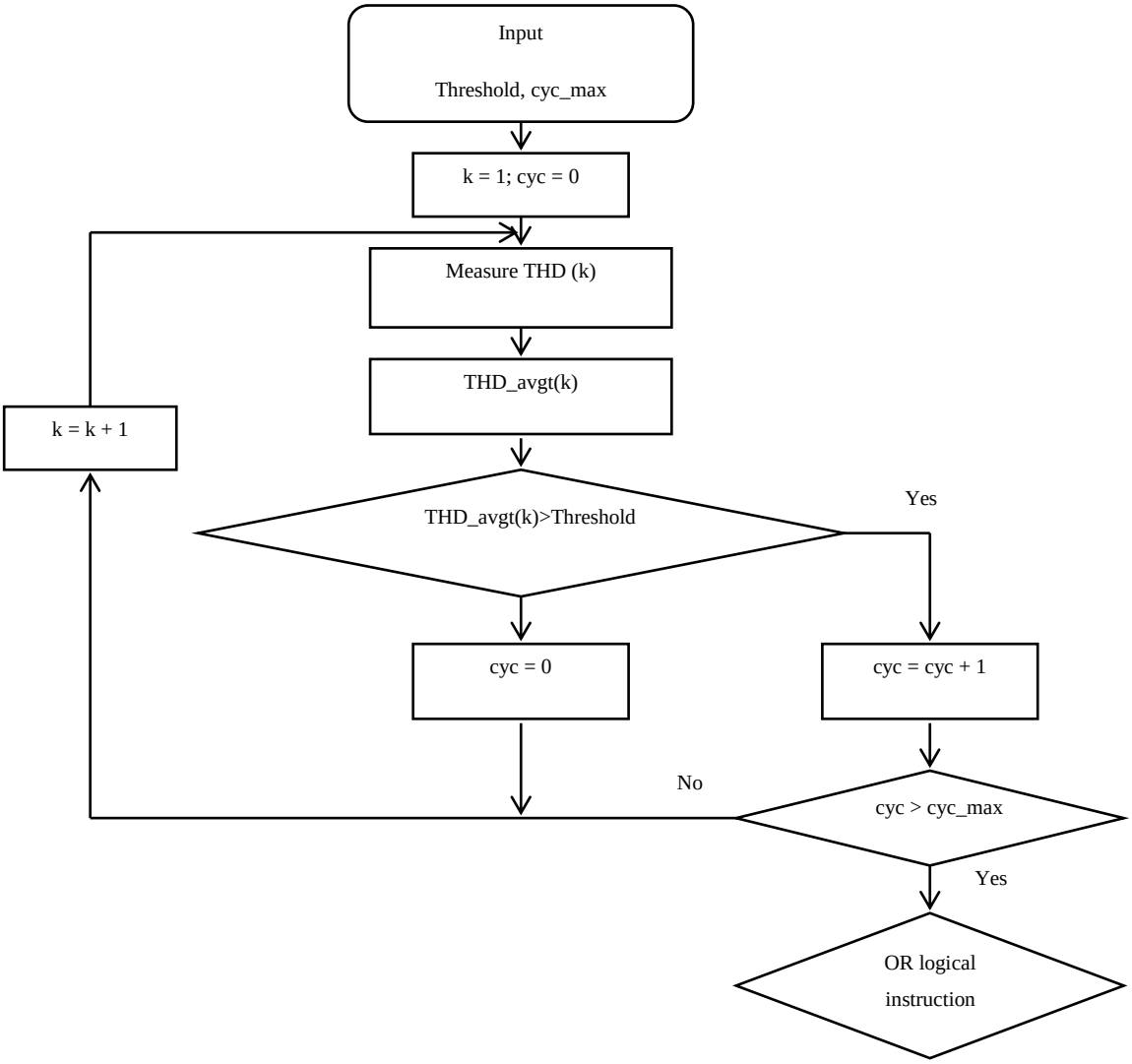


***Fig.3.4 Voltage THD Detection method Algorithm***

As regards the thresholds for the THD, the standard requirements for the utility interconnected distributed generators can be used as a reference.

For example, the IEC 61727 specifies the main requirements for the interconnection of photovoltaic (PV) systems to the utility distribution system (for PV connections of 10 kVA or less). Most of the requirements concern the PV systems inverter. When the utility limits move outside normal operational bounds the inverter should disconnect itself from the grid. The considered limits are reported below.

Inverter Output Power Quality - the output of any inverter should operate within the following limits:

- the inverter must limit the injection of any d.c. current into the utility to less than 1% of its rated output
- the total harmonic current distortion should be less than 5%
- harmonic current distortion for each individual harmonic should be less than those given in the standard
- the inverter must control flicker to be in line with IEC 61000
- when the inverters output is greater than 50%, the power factor must be greater than 0.9

### 3.2.5 VOLTAGE UNBALANCE VARIATION

Generally, even though the loading for DG has little changed after the loss of main source, due to the topology changes of the networks and the load, the voltage unbalance varies. So, if we keep monitoring the unbalance of three-phase output voltage of the DG, then it is possible to effectively detect an islanding operation of DG [26, 33]. In order to do this, we define the voltage unbalance at the monitoring time by

$$VU_t = \frac{NS_t}{PS_t}.100 \tag{3.9}$$

*Where,*

$NS_t$ and $PS_t$ mean the magnitude of negative and positive sequence of voltage at t, respectively.

This study defines the one-cycle average of voltage unbalance, and also defines the voltage unbalance variation, which measuring how much the monitored voltage unbalance deviates from the steady state and normal loading conditions.

$$\boldsymbol{VU}_{avg,t} = \frac{\mathbf{1}}{\boldsymbol{N}} \sum_{i=0}^{N-1} \boldsymbol{VU}_{t-i} \tag{3.10}$$

$$\Delta VU_t = \frac{VU_{avg,s} - VU_{avg,t}}{VU_{avg,s}}.100 \tag{3.11}$$

*Where,*

N is the sampling number of one-cycle, t is the monitoring time, and $VU_{avg,s}$ is the VU reference value initially set for the steady-state and normal loading conditions.

After $VU_{avg,s}$ is initially set, if $\Delta VU_t$ remains within -100% through +50% for one-cycle, the $VU_{avg,s}$ is updated by the $VU_{avg,t}$ in order to adapt to the normal load variation.

In the following figure there is reported the flow chart of the implementation of the VU index measurement.

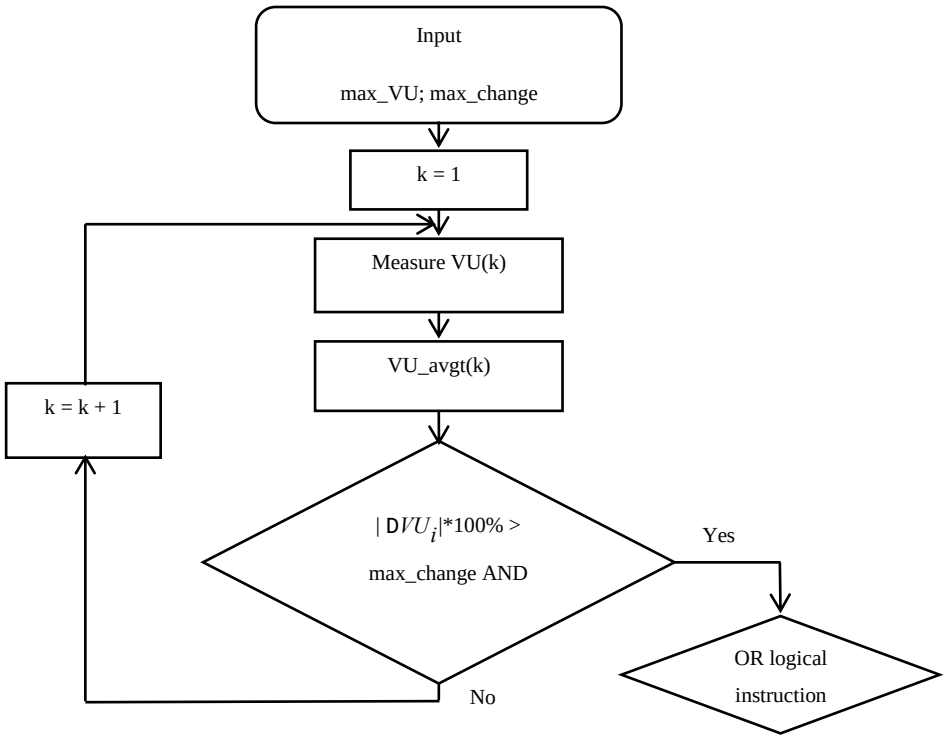


***Fig.3.5 Voltage Unbalance Detection method Algorithm***

## 3.3 NON DETECTION ZONE (NDZ) REDUCTION

### 3.3.1 NDZ OF OUV, OUF AND VOLTAGE PHASE DETECTION (PHASE JUMP PJ)

The amplitude and phase angle of RLC parallel load impedance are defined that can be represented as.

$$|Z| = \frac{1}{\sqrt{\frac{1}{R^2} + (\frac{1}{\omega L} - \omega C)^2}} = \frac{R}{\sqrt{1 + Q_f^2(\frac{f_0}{f} - \frac{f}{f_0})^2}}$$

$$R = \frac{V^2}{P_{load}}$$

$$L = \frac{V^2}{(2\pi . f . Q_f . P_{load})}$$

$$C = \frac{Q_f . P_{load}}{(2\pi . f . V^2)}$$

$$\varphi_{load} = tan^{-1}\left[R\left(\frac{1}{\omega L} - \omega C\right)\right] = tan^{-1}\left[Q_f\ (\frac{f_0}{f} - \frac{f}{f_0})\right]$$

Where,

Resonant frequency $f_0 = \frac{1}{2\pi\sqrt{LC}}$

$\omega_0 = \frac{1}{\sqrt{LC}}$

Quality factor $Q_f = R\sqrt{\frac{C}{L}}$

Formulation of NDZ based on the power mismatch.

After the grid disconnected, the load impedance and the new load resonant frequency are derived as

$$|Z| = \frac{1}{\sqrt{\frac{1}{(R+\Delta R)^2} + [(\frac{1}{\omega(L+\Delta L)} - \omega(C+\Delta C)]^2}}$$

$$f' = \frac{1}{2\pi\sqrt{(L+\Delta L).(C+\Delta C)}}$$

The following formula can be obtained

$$\frac{f^{'} - f}{f} = \frac{\frac{1}{2\pi\sqrt{(L+\Delta L).(C+\Delta C)}} - \frac{1}{2\pi\sqrt{LC}}}{\frac{1}{2\pi\sqrt{LC}}} = \frac{\sqrt{LC}}{\sqrt{(L+\Delta L).(C+\Delta C)}} - 1$$

Given the frequency thresholds, $f_{max}$ and $f_{min}$, in order for f' to be within thresholds that means f' be within the limited value [$f_{min}$, $f_{max}$]. Under the frequency thresholds of Over/Under Frequency method (OUF), the equation above must be met below

$$\frac{f_{min}-f}{f} \leq \frac{\sqrt{LC}}{\sqrt{(L+\Delta L).(C+\Delta C)}} - 1 \leq \frac{f_{max}-f}{f}$$

$$\frac{f_{min}}{f} - 1 \leq \frac{\sqrt{LC}}{\sqrt{(L+\Delta L).(C+\Delta C)}} - 1 \leq \frac{f_{max}}{f} - 1$$

$$\frac{f_{min}}{f} \leq \frac{\sqrt{LC}}{\sqrt{(L+\Delta L).(C+\Delta C)}} \leq \frac{f_{max}}{f}$$

$$(\frac{f_{min}}{f})^2 \leq \frac{LC}{(L+\Delta L).(C+\Delta C)} \leq (\frac{f_{max}}{f})^2$$

$$(\frac{f}{f_{max}})^2 \leq \frac{(L+\Delta L).(C+\Delta C)}{LC} \leq (\frac{f}{f_{min}})^2$$

$$(\frac{f}{f_{max}})^2 \leq \frac{LC + L\Delta C + C\Delta L + \Delta L\Delta C}{LC} \leq (\frac{f}{f_{min}})^2$$

If the approximations $\Delta L.\Delta C \approx 0$ that is used, this expression can be obtained

$$(\frac{f}{f_{max}})^2 \leq \frac{LC + L\Delta C + C\Delta L}{LC} \leq (\frac{f}{f_{min}})^2$$

$$(\frac{f}{f_{max}})^2 - 1 \leq \frac{L\Delta C + C\Delta L}{LC} \leq (\frac{f}{f_{min}})^2 - 1$$

$$(\frac{f}{f_{max}})^2 - 1 \leq \frac{\Delta L}{L} + \frac{\Delta C}{C} \leq (\frac{f}{f_{min}})^2 - 1 (*)$$

After the utility grid is disconnected and islanding occurred, the reactive power mismatch can be derived as

$$\Delta Q = V^2[\frac{1}{2\pi.f.(L+\Delta L)} - 2\pi.f.(C+\Delta C)]$$

$$\Delta Q = V^2[\frac{1}{2\pi.f.L.\left(1+\frac{\Delta L}{L}\right)} - 2\pi.f.C.\left(1+\frac{\Delta C}{C}\right)]$$

$$\Delta Q = \frac{Q_L}{\left(1+\frac{\Delta L}{L}\right)} - Q_C.\left(1+\frac{\Delta C}{C}\right)$$

Where, $Q_L$ and $Q_C$ at the resonant frequency can be expressed by the quality factor $Q_f$:

$$Q_f = \frac{\sqrt{Q_L.Q_C}}{P}$$

$$Q_L = Q_C = Q_f.P$$

Hence,

$$\Delta Q = \frac{Q_f.P}{\left(1+\frac{\Delta L}{L}\right)} - Q_f.P.\left(1+\frac{\Delta C}{C}\right)$$

$$\frac{\Delta Q}{P} = Q_f[\frac{1}{\left(1+\frac{\Delta L}{L}\right)} - \left(1+\frac{\Delta C}{C}\right)]$$

$$\frac{\Delta Q}{P} = Q_f \frac{1-\left(1+\frac{\Delta L}{L}\right).\left(1+\frac{\Delta C}{C}\right)}{\left(1+\frac{\Delta L}{L}\right)}$$

$$\frac{\Delta Q}{P} = Q_f \frac{-\frac{\Delta L}{L}+\frac{\Delta C}{C}+\frac{\Delta L}{L}.\frac{\Delta C}{C}}{\left(1+\frac{\Delta L}{L}\right)}$$

If two approximations $\Delta L.\Delta C \approx 0$ and $1+\frac{\Delta L}{L} \approx 1$ are used, this equation can be obtained

$$\frac{\Delta Q}{P} \approx -Q_f\left(\frac{\Delta L}{L}+\frac{\Delta C}{C}\right)$$

$$-\frac{\Delta Q}{Q_f.P} \approx \left(\frac{\Delta L}{L}+\frac{\Delta C}{C}\right) (**)$$

Eventually, from (*) and (**), the following condition should be met

$$-Q_f[(\frac{f}{f_{max}})^2 - 1] \leq \frac{\Delta Q}{P} \leq -Q_f[(\frac{f}{f_{min}})^2 - 1]$$

$$Q_f[1-(\frac{f}{f_{max}})^2] \leq \frac{\Delta Q}{P} \leq Q_f[1-(\frac{f}{f_{min}})^2] (3.12)$$

***Similarly,*** the correlation between the active power and the voltage at point common of coupling can be represented as follows.

In the initial time, the power system is steady state, the load active power is calculated as

$$P = \frac{V^2}{R}$$

When the utility grid disconnects or opens, the mismatched load can be represented by $(R+\Delta R, L+\Delta L, C+\Delta C)$ , the DG active power matches with the load active power, which can be derived as

$$P' = \frac{V'^2}{(R+\Delta R)} = \frac{(V+\Delta V)^2}{(R+\Delta R)}$$

Supposing DG is in constant power control, hence, the active power balance gives

$$P = P' = \frac{V^2}{R} = \frac{(V+\Delta V)^2}{(R+\Delta R)}$$

$$\frac{R+\Delta R}{R} = \frac{(V+\Delta V)^2}{V^2}$$

$$\frac{\Delta R}{R} = \frac{\Delta V^2}{V^2} + \frac{2\Delta V}{V^2} (***)$$

Besides, the ΔP is derived from Ohm's Law that states the load voltage is the load resistance time the inverter output current, which is constant:

$$\Delta P = \frac{V^2}{(R+\Delta R)} - \frac{V^2}{R} = \frac{-V^2.\Delta R}{(R+\Delta R).R}$$

Normalize

$$\frac{\Delta P}{P} = \frac{\frac{-V^2.\Delta R}{(R+\Delta R).R}}{\frac{V^2}{R}} = \frac{-\Delta R}{(R+\Delta R)} = -\frac{\frac{\Delta R}{R}}{1+\frac{\Delta R}{R}}$$

$$\frac{\Delta P}{P} = -\frac{\frac{\Delta R}{R}}{1+\frac{\Delta R}{R}} (****)$$

*From (***) and (****),* simplifying the equation and can be obtained as follow

$$\frac{\Delta P}{P} = -\frac{\frac{\Delta V^2}{V^2} + \frac{2\Delta V}{V^2}}{1 + \frac{\Delta V^2}{V^2} + \frac{2\Delta V}{V^2}} = -\frac{1 + \frac{\Delta V^2}{V^2} + \frac{2\Delta V}{V^2} - 1}{1 + \frac{\Delta V^2}{V^2} + \frac{2\Delta V}{V^2}}$$

$$\frac{\Delta P}{P} = \frac{1}{(\frac{\Delta V}{V} + 1)} - 1 = \frac{V^2}{(V + \Delta V)^2} - 1$$

$$\frac{\Delta P}{P} = (\frac{V}{V + \Delta V})^2 - 1$$

Under the voltage amplitude thresholds [$V_{min}$; $V_{max}$] of Over/Under voltage method (OUV), the expression above must be met as follows

$$\left(\frac{V}{V_{max}}\right)^2 - 1 \leq \frac{\Delta P}{P} \leq \left(\frac{V}{V_{min}}\right)^2 - 1 (3.13)$$

Formulation of NDZ based on voltage phase displacement detection, in other words, the NDZ of voltage phase jump (PJ) can be represented as follows

$$\varphi_{load} = tan^{-1}\left\{(R + \Delta R)\left[\frac{1}{\omega(L + \Delta L)} - \omega(C + \Delta C)\right]\right\}$$

$$\varphi_{load} = tan^{-1}\left\{\frac{(R + \Delta R)}{R} R\left[\frac{1}{\omega(L + \Delta L)} - \omega(C + \Delta C)\right]\right\}$$

After the grid is disconnected, the reactive power mismatch can be taken from the equation

$$\Delta Q = V^2[\frac{1}{\omega(L + \Delta L)} - \omega(C + \Delta C)]$$

$$\frac{\Delta Q}{V^2} = [\frac{1}{\omega(L + \Delta L)} - \omega(C + \Delta C)]$$

$$P.R = V^2$$

$$\frac{\Delta Q}{P.R} = [\frac{1}{\omega(L + \Delta L)} - \omega(C + \Delta C)]$$

A formula is derived as

$$R\left[\frac{1}{\omega(L + \Delta L)} - \omega(C + \Delta C)\right] = \frac{\Delta Q}{P} (*****)$$

$$\frac{\Delta P}{P} = -\frac{\frac{\Delta R}{R}}{1+\frac{\Delta R}{R}}$$

$$\frac{\Delta P}{P} = -\frac{\Delta R}{R+\Delta R}$$

$$\frac{\Delta P}{P} + 1 = 1 - \frac{\Delta R}{R+\Delta R}$$

$$\frac{\Delta P}{P} + 1 = \frac{R}{R+\Delta R}$$

A formula is derived as

$$\frac{R+\Delta R}{R} = \frac{1}{\frac{\Delta P}{P}+1} (******)$$

The phase angle of impedance load can be expressed as

$$\varphi_{load} = tan^{-1}\left(\frac{\frac{\Delta Q}{P}}{\frac{\Delta P}{P}+1}\right)$$

*Given*

$$\varphi_{load} = tan^{-1}\left(\frac{\frac{\Delta Q}{P}}{\frac{\Delta P}{P}+1}\right) \leq \theta_{\text{threshold}} (3.14)$$

*Comparison of NDZ*

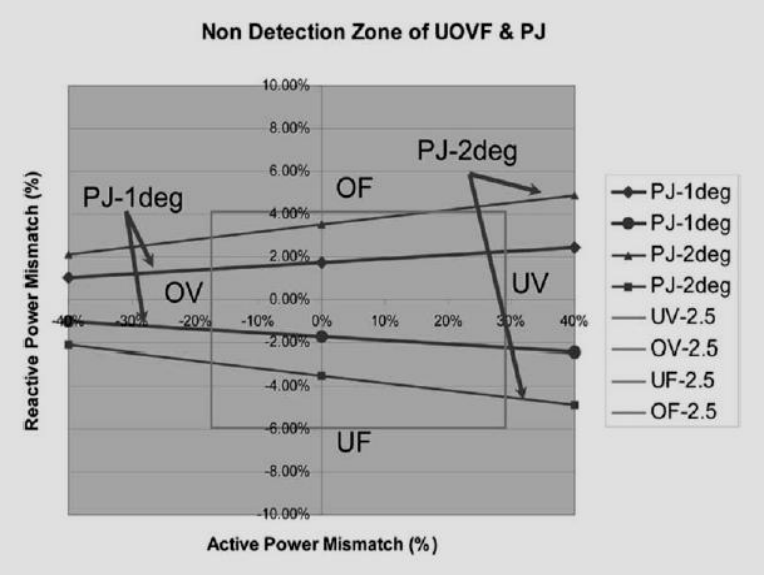


***Fig.3.6 Chart of OUV/OUF-NDZ and PJ-NDZ comparison[47]***

Some salient points from the formula above:

$$Q_f[1-(\frac{f}{f_{max}})^2] \leq \frac{\Delta Q}{P} \leq Q_f[1-(\frac{f}{f_{min}})^2] (3.12)$$

$$\left(\frac{V}{V_{max}}\right)^2 - 1 \leq \frac{\Delta P}{P} \leq \left(\frac{V}{V_{min}}\right)^2 - 1 (3.13)$$

$$\varphi_{load} = tan^{-1}\left(\frac{\frac{\Delta Q}{P}}{\frac{\Delta P}{P}+1}\right) \leq \theta_{\text{threshold}} (3.14)$$

- OUF-NDZ is dependent from the quality factor $Q_f$, otherwise, PJ-NDZ is independent from $Q_f$.
- The sensibility of OUV/OUF-NDZ also PJ-NDZ is all very low about the power mismatch (ΔP and ΔQ).
- NDZ of PJ increases with increased preset threshold value and vice-versa. There are practical issues related to using phase-jump thresholds on the order of a few degrees (i.e. 1 or 2 degree, maximum is 10 degree). Power system switching events, not resulting in islanding, can falsely trigger such schemes.

### 3.3.2 DISCUSSION

Calculating of the NDZ area from the power mismatches in order to preset the values of the threshold for working of frequency and amplitude of the voltage. The probability that ΔP and ΔQ fall into the NDZ can be significant. Because of this concern, the standard OUV/OUF protective devices alone are generally considered to be insufficient "anti-islanding protection". Therefore they must be combined with other islanding detection methods, as explained in the following.

When the utility grid disconnects or opens, if the active and reactive power mismatch is within the previous specified thresholds, which are also the function of voltage, voltage phase displacement (or voltage phase jump) and frequency thresholds, $V_{min}$ and $V_{max}$, $PJ_{max}$ and $PJ_{min}$, $f_{min}$ and $f_{max}$. If the variation of the voltage or frequency amplitude or voltage phase displacement goes beyond of the beforehand acceptable limits; the control accessories which work on OUV/OUF/PJ methods will be activated to prevent islanding. On the contrary, the change of the voltage and it's phase or frequency will remain inside of specified thresholds after the grid disconnects as an island may be formed and persist without being detected, that is defined as non-detection zone (NDZ).

## 3.4 PRELIMINARY SIMULATION ANALYSIS. SIMPLE CASE STUDY

A first series of simulations have been carried out on a simple case study (see figure 3.7), in which a DG is connected to the point of common coupling (PCC) between the grid and the load. In the simulated system, the load and the DG have been sort by type in order to have voltage and frequency variations before and after the opening of the circuit breaker (CB) (islanding) within the thresholds of, i.e. in the range of 0.8-1.15 of the rated voltage (230 V) and ± 0.5 Hz around the rated frequency (50 Hz), respectively. The parameters of study system are given in the table 3.1.

In such conditions, different scenarios have been simulated:

- Grid voltage sinusoidal and linear load (RLC load);
- Grid voltage nonsinusoidal (THD within the CEI EN 50160 limits) and linear load;
- Grid voltage sinusoidal and nonlinear load (a diode bridge rectifier feeding a DC load)
- Grid voltage nonsinusoidal and nonlinear load.

When the CB is closed, the DG and the local load are both connected to power grids and power produced by DG is injected. But when the CB is opened, islanding condition occurs, and DG along with a local load creates an independent power grid in which just DG supplies loads demand power. Inside, the DG source is a three-phase current source connects a Controlled Current Source (CCS). The sinusoidal current amplitude, the phase in degrees, and the frequency in hertz of the positive-sequence component of the source are programmed. In addition, the harmonics can be programmed and superimposed on the fundamental signal. In detail, the harmonic currents coming from the inverter (THD within the limit of 5%) have been simulated.

The scheme of the simulated system, in MATLAB/SIMULINK environment is reported in fig.3.8.

***Table 3.2: parameters of study system***

| **Parameters** | **Value** | **unit** |
|---|---|---|
| DG's Current Source ($I_1$) | 8 | A |
| Total harmonic distortion of DG | 5 | % |
| Utility Grid Voltage | 400 | V |
| Total harmonic distortion of grid | 8 | % |
| Resistance of line (R) | 1e-2 | Ω /phase |
| Inductance of line (L) | 300e-6 | H/phase |
| Real active Power of Load (P) | 5000 | W |
| Inductive Reactive Power of Load ($Q_L$) | 2000 | VAr |
| Capacitive Reactive Power of Load $Q_C$) | 500 | VAr |
| Diod rectified output inductor ($L_1$) | 1e-3 | H |
| Diod rectified output capacitor ($C_1$) | 1e-9 | F |
| Nonlinear load Resistance | 285 | Ω |
| Frequency (f) | 50 | Hz |

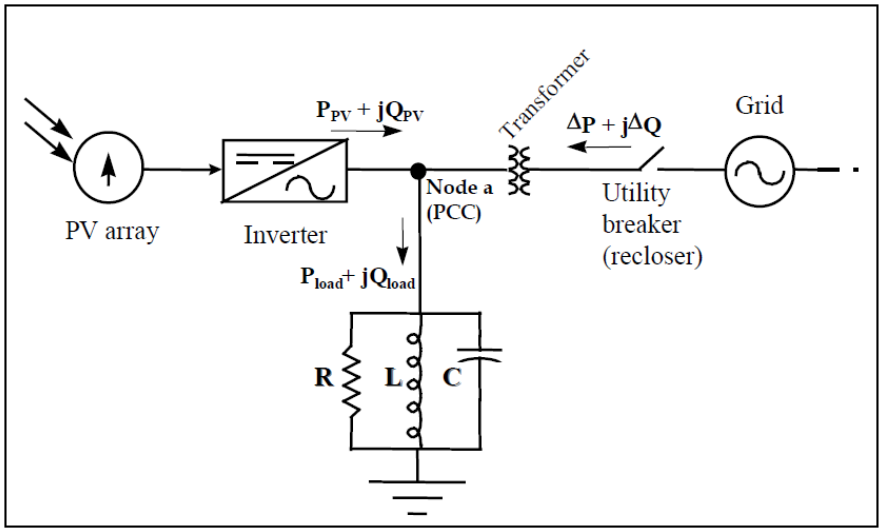


***Fig.3.7 Studied power system including DG and power grid***

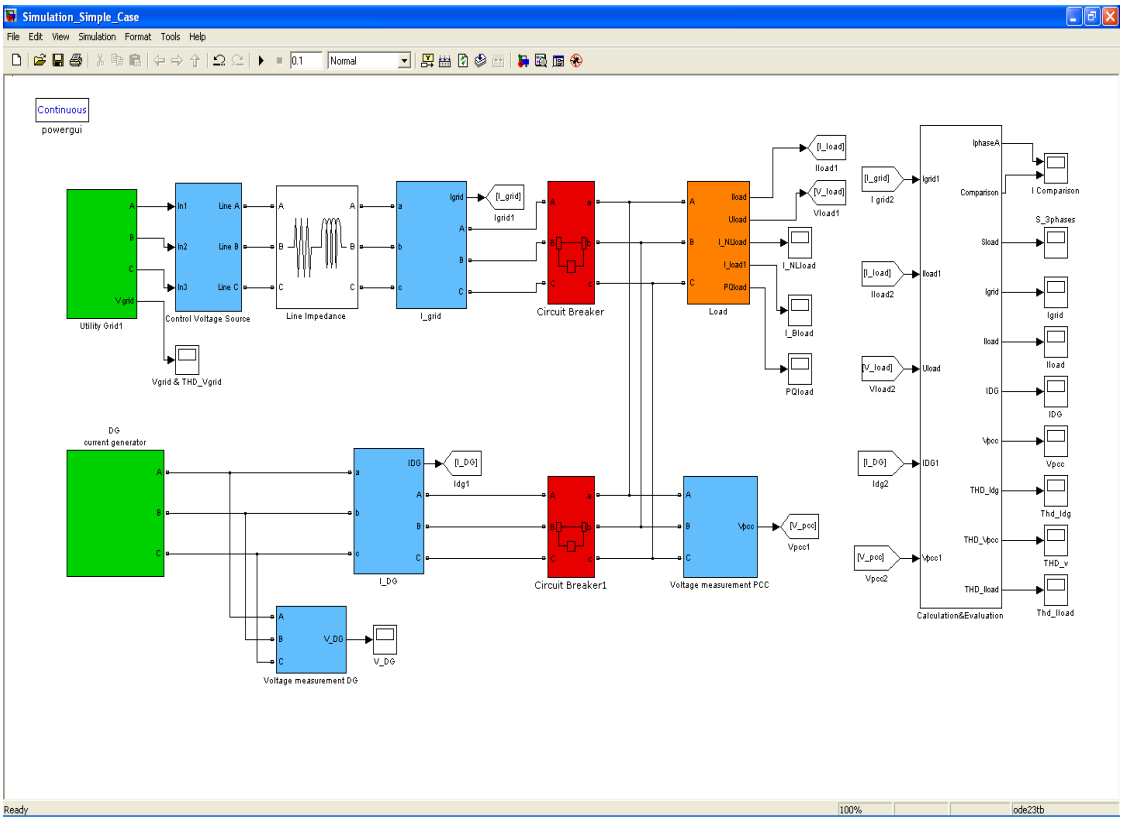


***Fig.3.8 The simulation of power system.***

### 3.4.1 SUMMARY OF SIMULATION RESULTS

In order to verify the theoretical analysis in the previous section, the time-domain simulations in MATLAB/SIMULINK are carried out. In this simulation, the harmonics always injected from the distributed generation source.

The simulations have been performed in order to verify the islanding detection capability and the operation under normal grid condition of the considered parameters. In this establishment, the operation factor of sources, the active and reactive power of inductance and capacitor of local load are 4kW and $Q_L$=2kVAr, $Q_C$=0.5kVAr, respectively, as reported in table 3.3, which summarizes the obtained results.

| **Sce** | THD $V_{Grid}$ | THD $I_{DG}$ | Load's Type | When the CB closes | | | | After CB is opened (t=0.5s) | | | | **Detect Islanding condition** |
|---|---|---|---|---|---|---|---|---|---|---|---|---|
| | | | | $THDi_{Load}$ | $THD_{Vpcc}$ | PJ | VU | $THDi_{Load}$ % | $THD_{Vpcc}$ % | PJ deg | VU_spike % | |
| Sce. 1 | 0 | 5 | Linear load | 0.5 | 0.7 | 0 | 0 | 4.8 | 8.3 | 16 | 5.9% | Yes |
| Sce. 2 | 0 | 5 | Non Linear load | 4.8 | 1 | 0 | 0 | 4.8 | 11.5 | 16 | 5.9% | Yes |
| Sce. 3 | 8 | 5 | Linear load | 4.5 | 7.8 | 0 | 0 | 4.8 | 8.3 | 16 | 5.9% | Yes |
| **Sce. 4** | 8 | 5 | Non Linear load | 4 | 8 | 0 | 0 | 4.8 | 11.5 | 16 | 5.9% | Yes |

***Table 3.3: Simulation results of Scenarios***

### 3.4.2 SCENARIO 1

In the simulation the limit of maximum harmonic distortion in percent of current and voltage at PCC is 5% according to the IEEE standard 1547 in [7]. Table 3.3 shows the simulation results. At t=0.05s, CB is opened, the utility grid disconnects to local load; thus DG and load are separated from power grid and an islanding condition occurs.

The figure 3.11 shows result of scenario 1. When the system operates under normal condition, the utility grid impedance is much lower than the load impedance at the harmonic frequency, hence the harmonic current flows through the utility grid and no abnormal voltage is detected at PCC[11],[12]. According to standard IEC61727, IEEE1547 while THD of voltage value at PCC is less than 5 ($THD_{Vpcc} \leq 5$), the system operates continuously.

The harmonics are injected and superimposed with a fundamental signal of DG source. The THD of output DG current and THD of the voltage at PCC in Fig. 3.9a, d is the evident, the amplitude increases after islanding has occurred, this instant variation meets the local load demand. When the grid is connected, the utility grid impedance is much lower than the load impedance at the harmonic frequency; thus the harmonic current flows into the utility and no abnormal voltage is detected. In Fig. 3.9c, the three phase current of load seems sinusoidal because the disturbance injection from DG is very small comparing with grid current and load current. The value of load current and the PCC voltage before the islanding condition can showed in fig. 3.9c and fig. 3.9f those are obvious that the three phase voltage is in balanced situation. On the other hand, when the grid is disconnected, the harmonic current can flow into the load. Therefore the load produces a harmonic voltage that showed in fig. 3.9b, e, islanding condition occurs, the THD of load current is showed in fig. 3.9a, which changes from 0.5% to 4.8%. Besides, the three phase voltage of PCC becomes non-sinusoidal, fig. 3.9d shows the harmonic voltage at PCC that alters from 0.7% to 8.3%; this variation is large enough to discover the island condition. Moreover, voltage phase jump and voltage unbalance change suddenly that are out of threshold values in fig. 3.9g, h (such as phase jumps from 0 to 16degree and VU jerks from 0% to 5.9%). Therefore islanding condition is detected very fast from this voltage after islanding has appeared, so islanding condition can be detected.

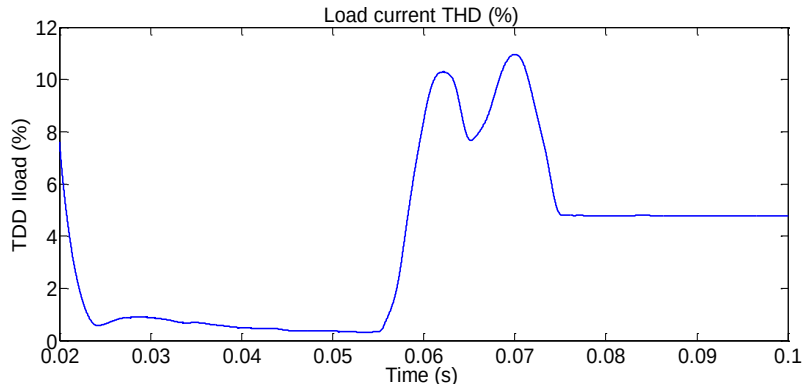


Load current THD

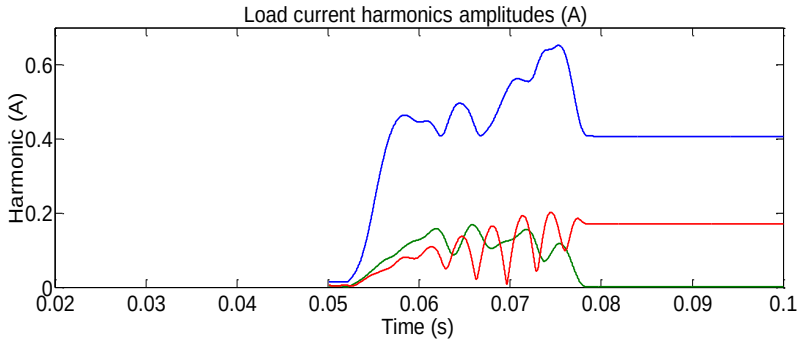


I_load harmonics amplitudes

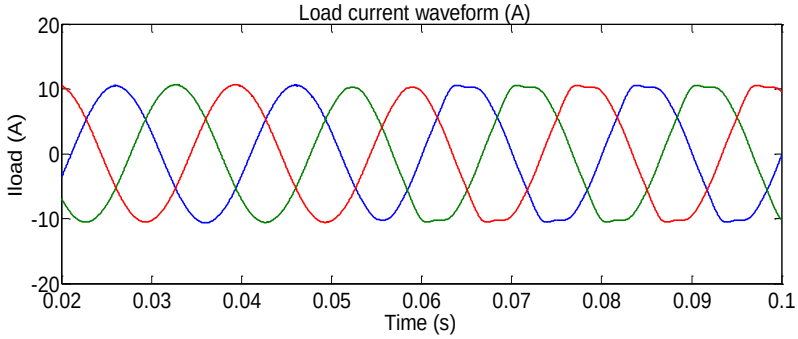


load current waveforms

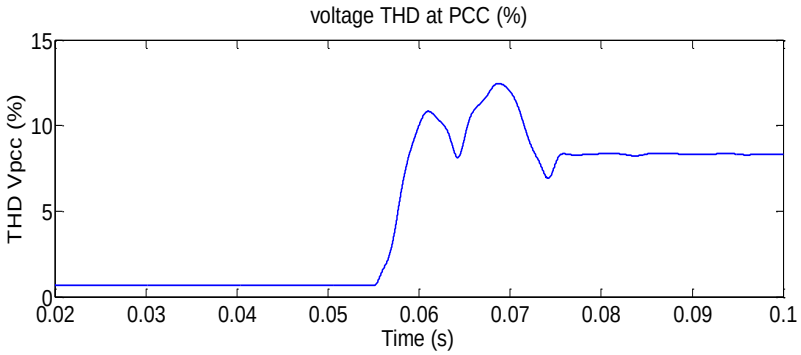


voltage THD at PCC

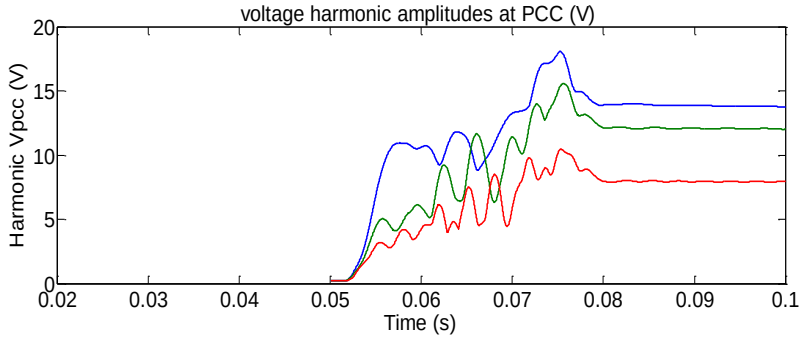


Vpcc harmonic amplitudes

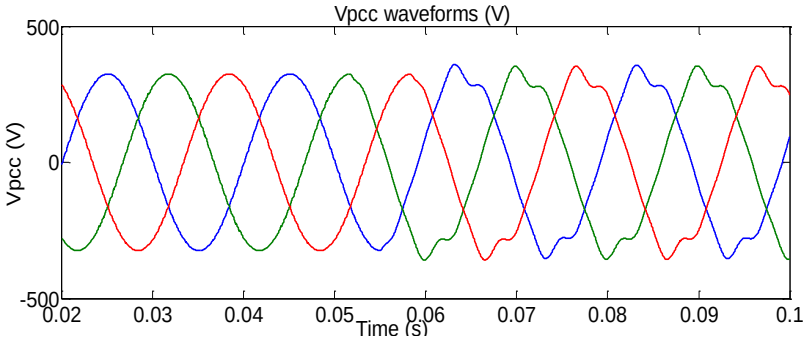


Vpcc waveforms

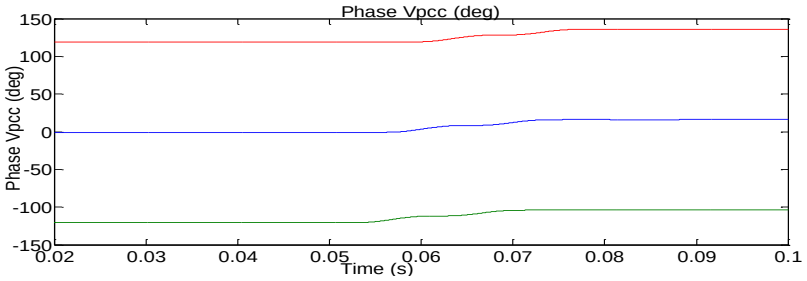


Voltage Phase at PCC

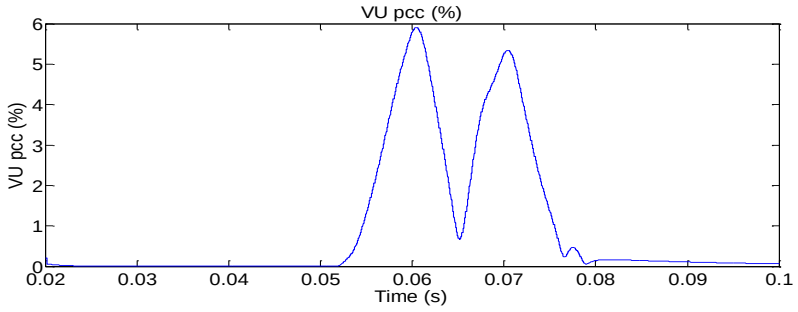


VU PCC

***Fig.3.9 the grid variations of Scenario 1***

### 3.4.3 SCENARIO 2

The harmonics are always injected and superimposed with a fundamental signal of DG source (THD = 5%). The local load is non-linear load. In fig. 3.10c-f, before the CB is opened (i.e. before the islanding condition), the three phase current of load and the voltage at the PCC are almost sinusoidal. The harmonic current flows into the utility and no abnormal voltage is detected. When the grid is disconnected, islanding condition occurs and the current load and the PCC voltage are non-sinusoidal due to the harmonic current can flow into the load. The deviation of THD of output DG current and THD of the voltage at PCC are marked. Therefore the load produces the harmonic voltage, the THD of load current seems constant, as shown in fig. 3.10a. Besides, the three phase voltage of PCC becomes non-sinusoidal; fig. 3.12f shows the harmonic voltage at PCC that increase from 4.8% to 11.5%.

The results of scenarios are shown below.

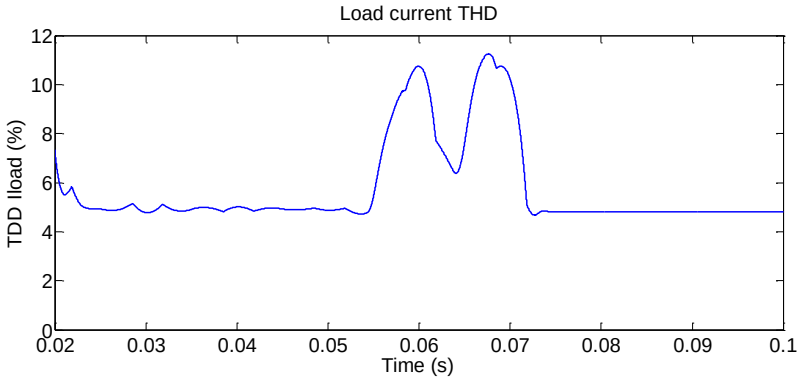


Load current THD

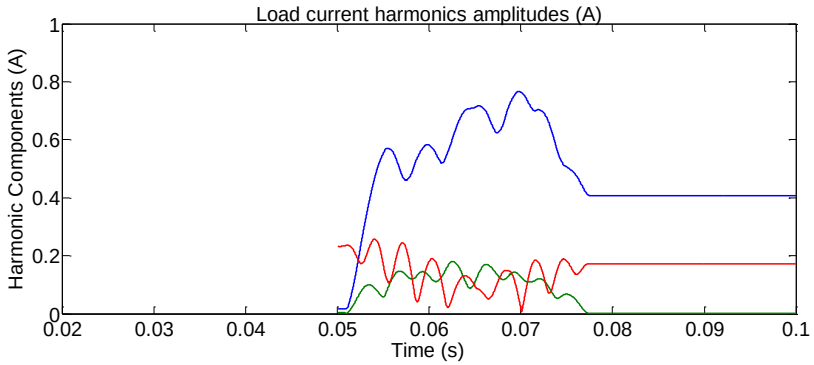


Iload harmonics amplitudes

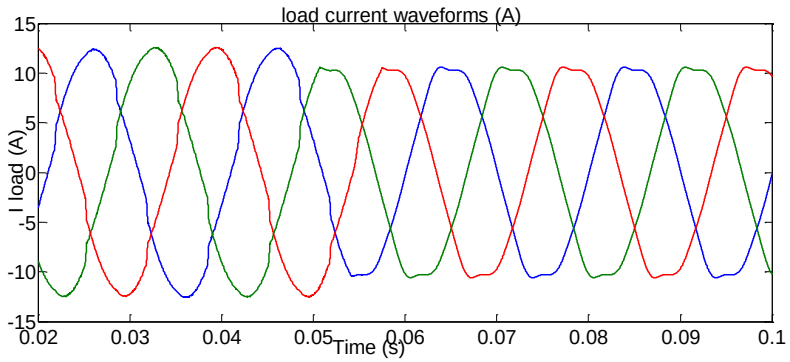


load current waveforms

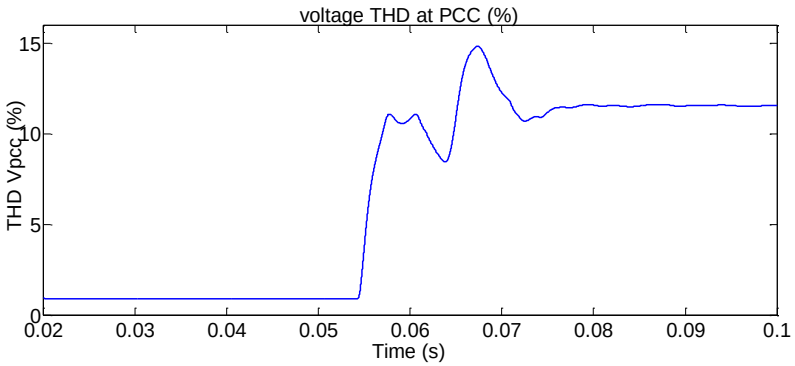


voltage THD at PCC

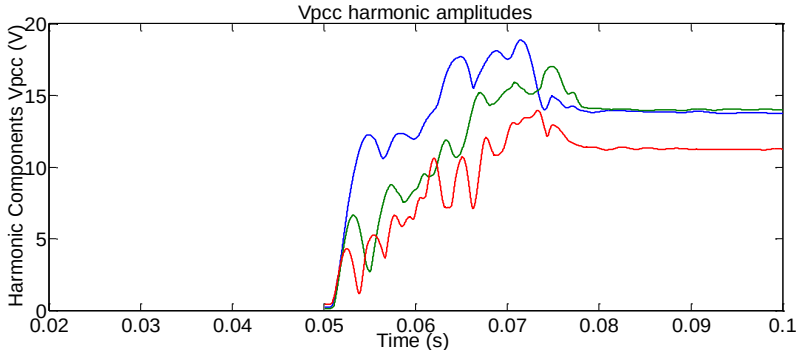


Vpcc harmonic amplitudes

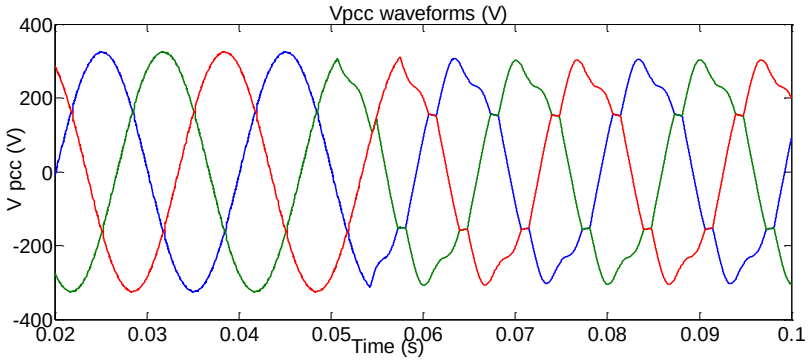


Vpcc waveforms

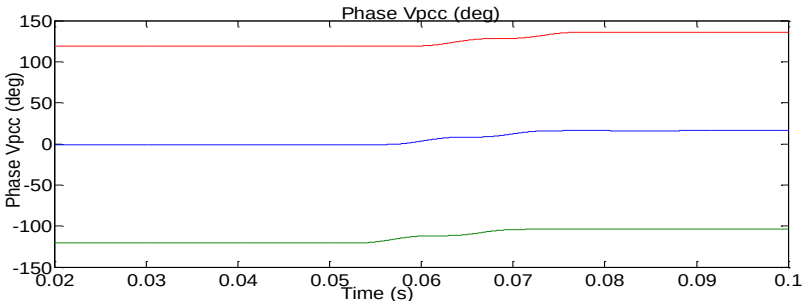


Voltage Phase at PCC

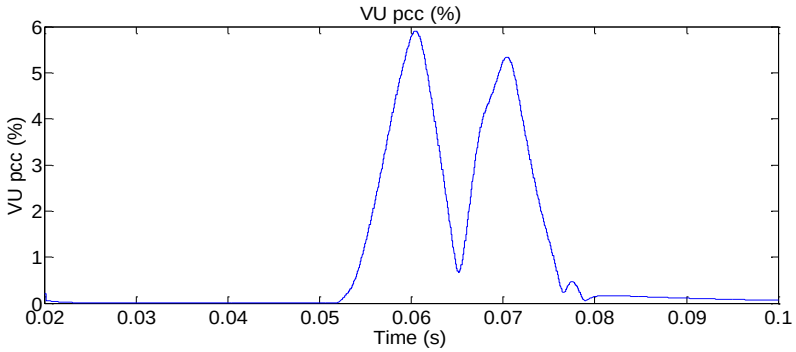


VU PCC

***Fig.3.10 the grid variations of Scenario 2***

### 3.4.4 SCENARIO 3

The harmonics are injected and superimposed with a fundamental signal of utility grid ($THD_V$ is 8%). Besides, the harmonics are always injected and superimposed with a fundamental signal of DG source ($THD_{DG}$ is 5%). The local load is linear load. The fig. 3.11 shows result of scenario 3. In the fig. 3.11c-f the three phase current of load and the voltage at the PCC before the islanding condition seems sinusoidal because the disturbance injection from DG is very small comparing with grid current and load current. While the grid is connected, the utility grid impedance is much lower than the load impedance at the harmonic frequency, the harmonic current flows into the utility and no abnormal voltage is detected. Whereas, when the grid is disconnected, islanding condition occurs and the current load and the PCC voltage are non-sinusoidal, as the harmonic current can flow into the load. Therefore the load produces the harmonic voltage, the THD of load current changes from 4.5% to 4.8% that are shown in fig. 3.11a. Besides, the three phase voltage of PCC becomes non-sinusoidal; fig. 3.11f shows the harmonic voltage at PCC that alters from 7.8% to 8.3%. The deviation of THD of output DG current and THD of the voltage at PCC are the evident, the amplitude increases after islanding has occurred, this instant variation meets the local load demand. Whereas, the THD voltage at PCC increases but the deviation is insignificant so no abnormal voltage is detected at PCC due to the system operates continuously. On the contrary, the phase jump and the voltage unbalance measurements can allow to detect the islanding occurrence.

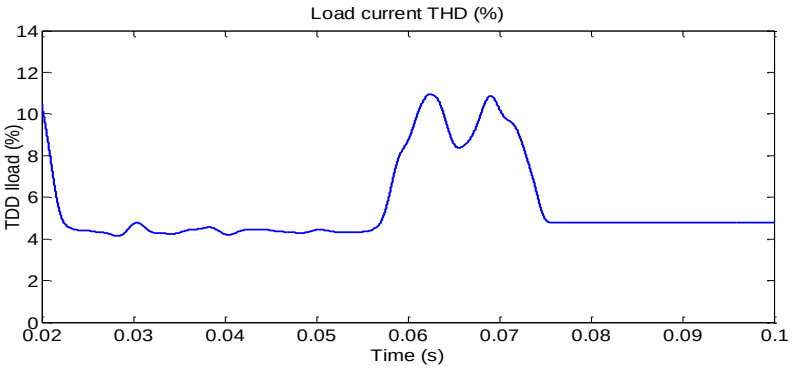


Load current THD

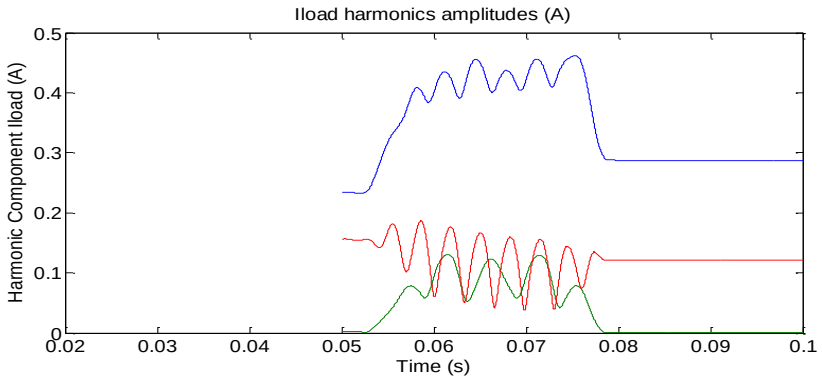


Iload harmonics amplitudes

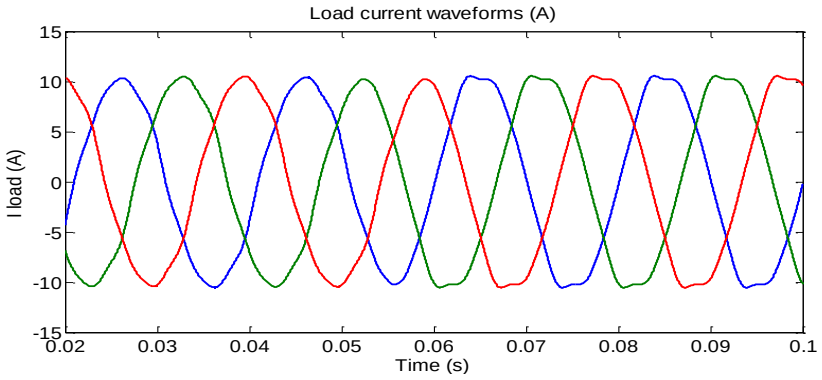


load current waveforms

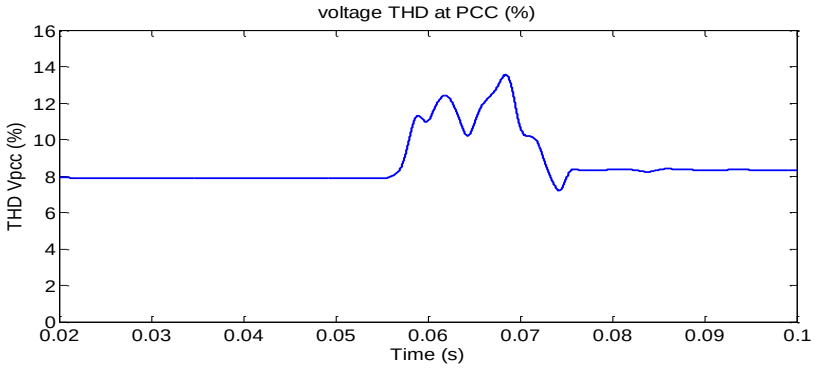


voltage THD at PCC

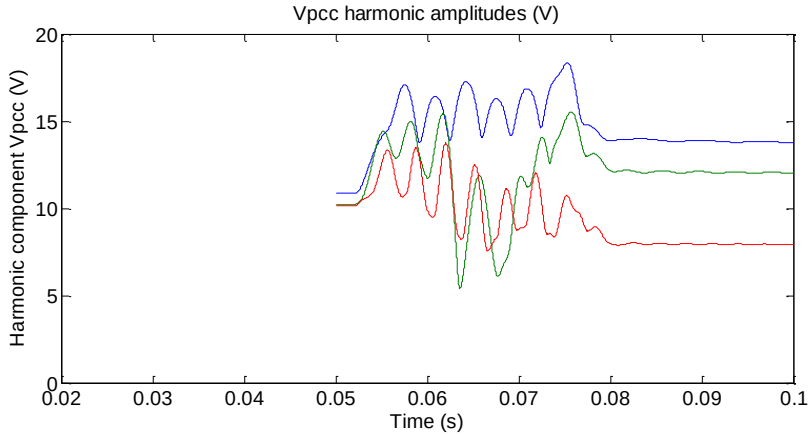


Vpcc harmonic amplitudes

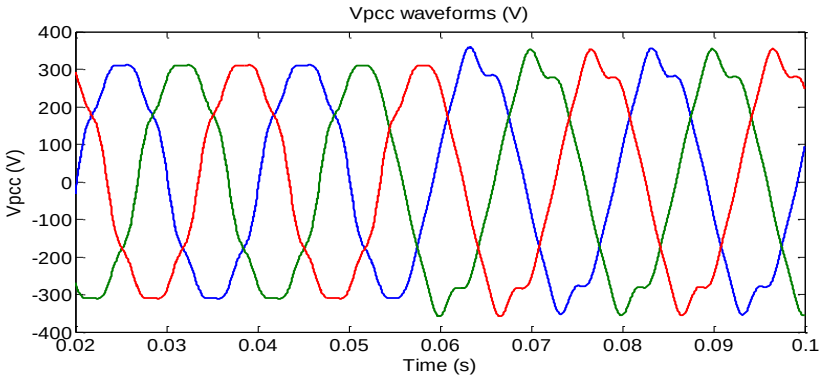


Vpcc waveforms

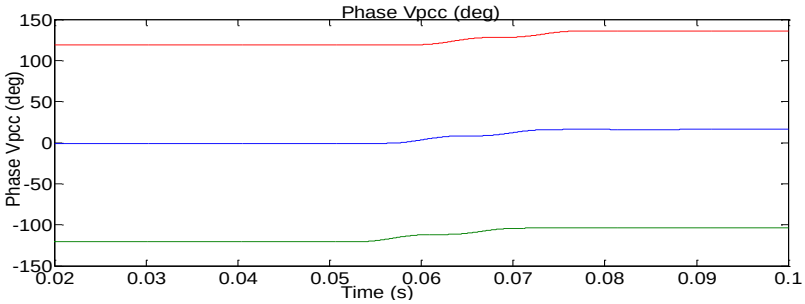


Voltage Phase at PCC

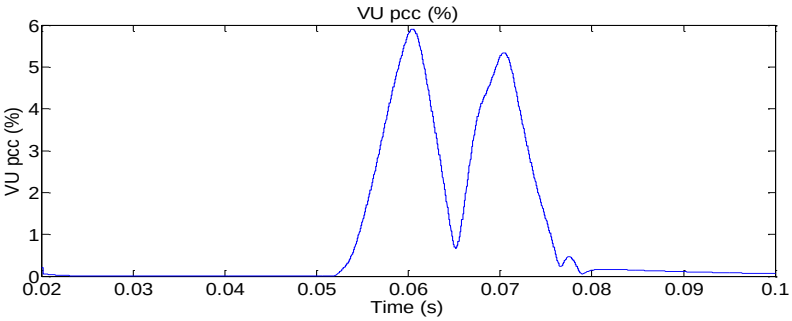


VU PCC

***Fig.3.11 the grid variations of Scenario 3***

### 3.4.5 SCENARIO 4

The harmonics are injected and superimposed with a fundamental signal of utility grid, $THD_V$ is 8%. Besides, the harmonics are always injected and superimposed with a fundamental signal of DG source, $THD_{DG}$ is 5%. The local load is non-linear load. In fig.3.12c, f, before the CB is opened, the three phase current of load and the voltage at the PCC before the islanding condition seems sinusoidal. Because the harmonic current flows into the utility and no abnormal voltage is detected. When the grid is disconnected, islanding condition occurs, the current load and the PCC voltage are non-sinusoidal. Therefore the load produces the harmonic voltage, the THD of load current increases from 4% to 4.8% that are shown in fig.3.12a. Besides, the three phase voltage of PCC becomes non-sinusoidal; fig.3.12d shows the harmonic voltage at PCC that alters from 8% to 11.5%. The deviation of THD of output DG current and THD of the voltage at PCC are the evident, the amplitude increases after islanding has occurred, this instant variation meets the local load demand. This variation is too high so the island condition is detected.

The results of scenarios are shown below.

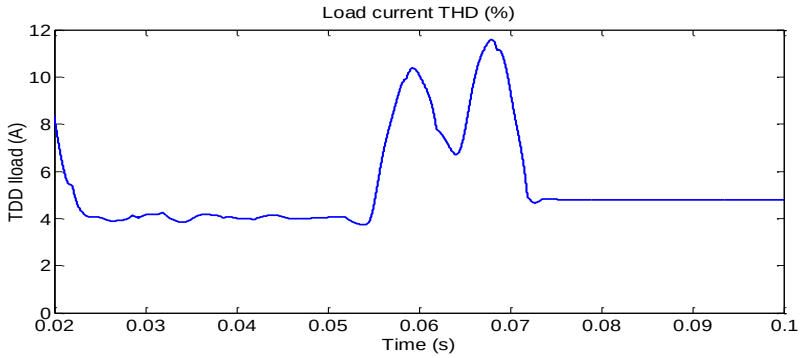


Load current THD

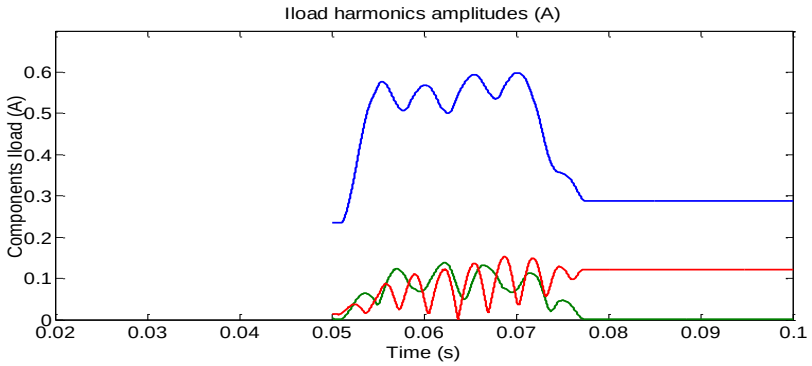


Iload harmonics amplitudes

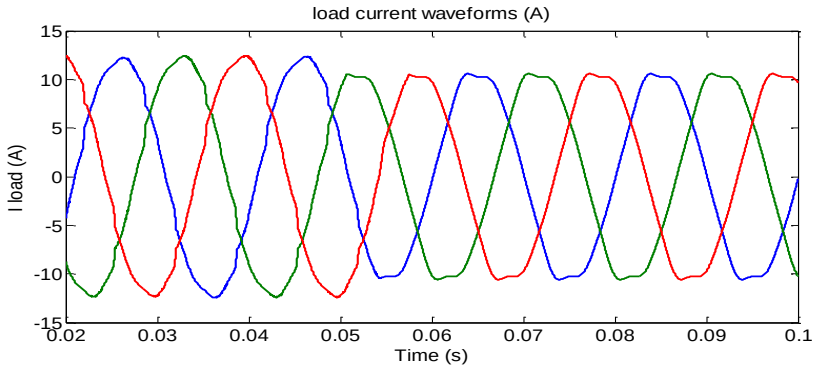


load current waveforms

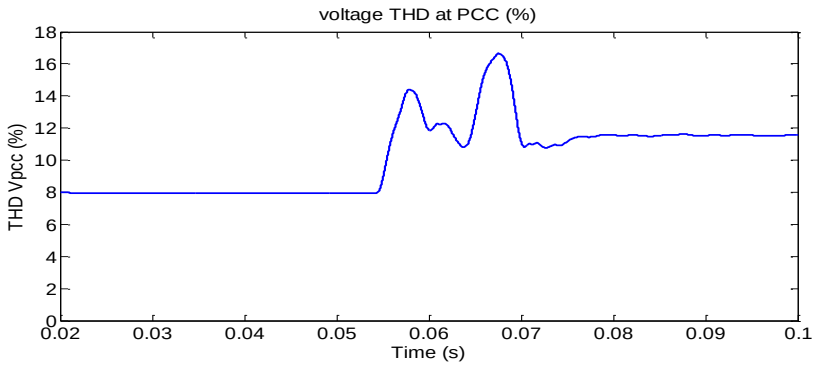


voltage THD at PCC

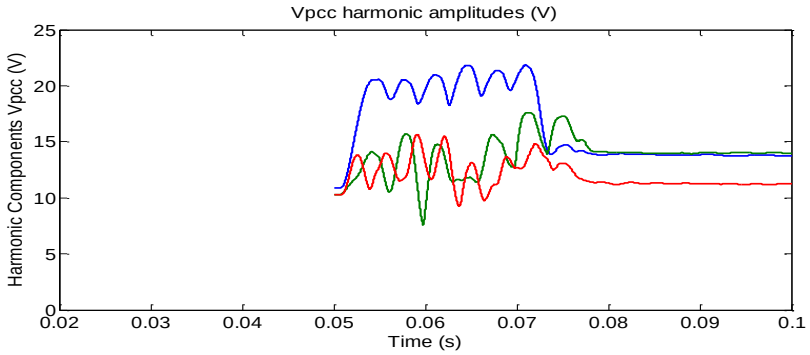


Vpcc harmonic amplitudes

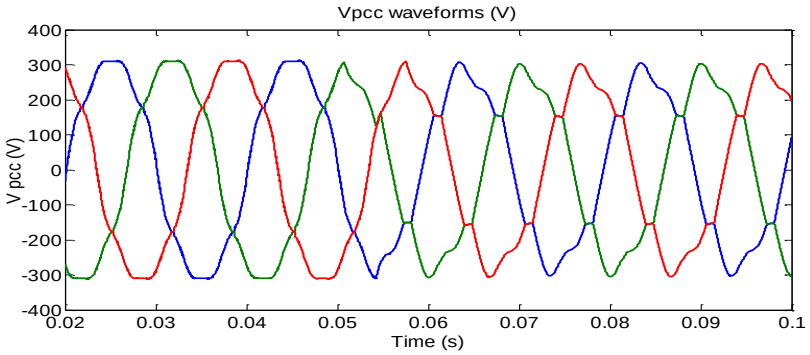


Vpcc waveforms

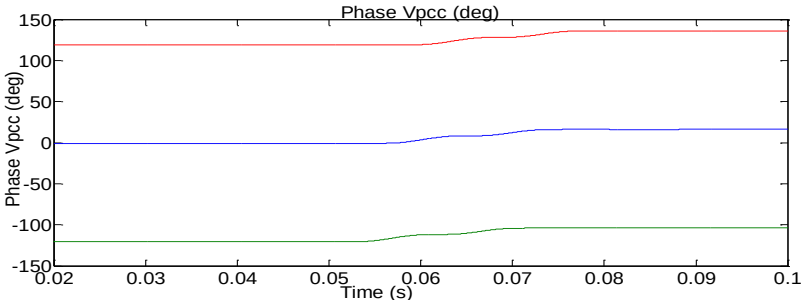


Voltage Phase at PCC

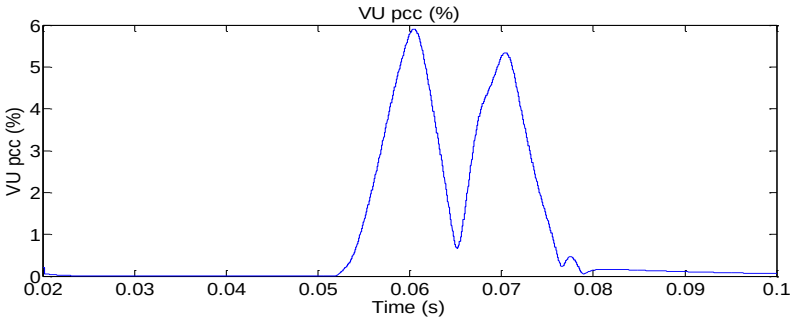


VU PCC

***Fig.3.12 the grid variations of Scenario 4***

### 3.5 THE PROPOSED COMBINED APPROACH BASED ON LOCAL MEASUREMENTS

The results of the previous sections show that the mix of the considered local measurements can correctly detect the islanding occurrence. On the other hand some of the considered parameters are redundant (for example, current distortion vs. voltage distortion) or they can be less meaningful in specific operating conditions (for example, single harmonics amplitudes in the presence of loads introducing such harmonics). Thus, a combined strategy can be defined, by using the evaluation of the following quantities:

- over/under voltage and over/under frequency (OUV and OUF in the following);
- voltage THD;
- voltage phase jump (PJ)
- Voltage unbalance (VU)

Each of the aforesaid quantities is compared with its own threshold and the result of such comparison is used to decide about the islanding occurrence.

As already mentioned, it has to be observed that, for the practical implementation of the proposed solution, it is necessary to fix the proper thresholds for the parameters variations, in order to provide a reliable islanding detection. For the considered parameters some limits are already fixed by the current standards concerning the voltage and power quality levels in distribution networks and they can be considered as a first reference for the thresholds. However, some "site-specific" conditions can occur, such as the starting of some typical loads (such as motors, which can cause transient phase jumps) or the presence of nonlinear and/or time-varying loads (which can modify the harmonic distortion level at PCC during their normal operation). Such conditions can cause significant variations on the monitored parameters and can lead to incorrect information for the islanding detection purpose. Thus, the islanding detection strategy should take into account these situations, in order to adjust itself to the measurement site. To solve this problem, the local measurements are implemented in a recursive algorithm, which can allow to properly fixing the thresholds. For each cycle, the algorithm starts with the signal acquisition and the calculation of the considered parameters. If the voltage or frequency of the network is beyond the values defined by standards requirements (in our case those defined in CEI 0-21); then algorithm will directly issue the trip command for DG disconnection, without any other calculations. On the contrary, if OUV or OUF are within the fixed limits (i.e. a possible NDZ situation is

occurred), the algorithm checks if THD, PJ and VU are out of range (with respect to their own thresholds). If yes, the islanding is detected and the trip command is given; otherwise the thresholds are updated and a new cycle begins. The proposed algorithm is shown in the chart below.

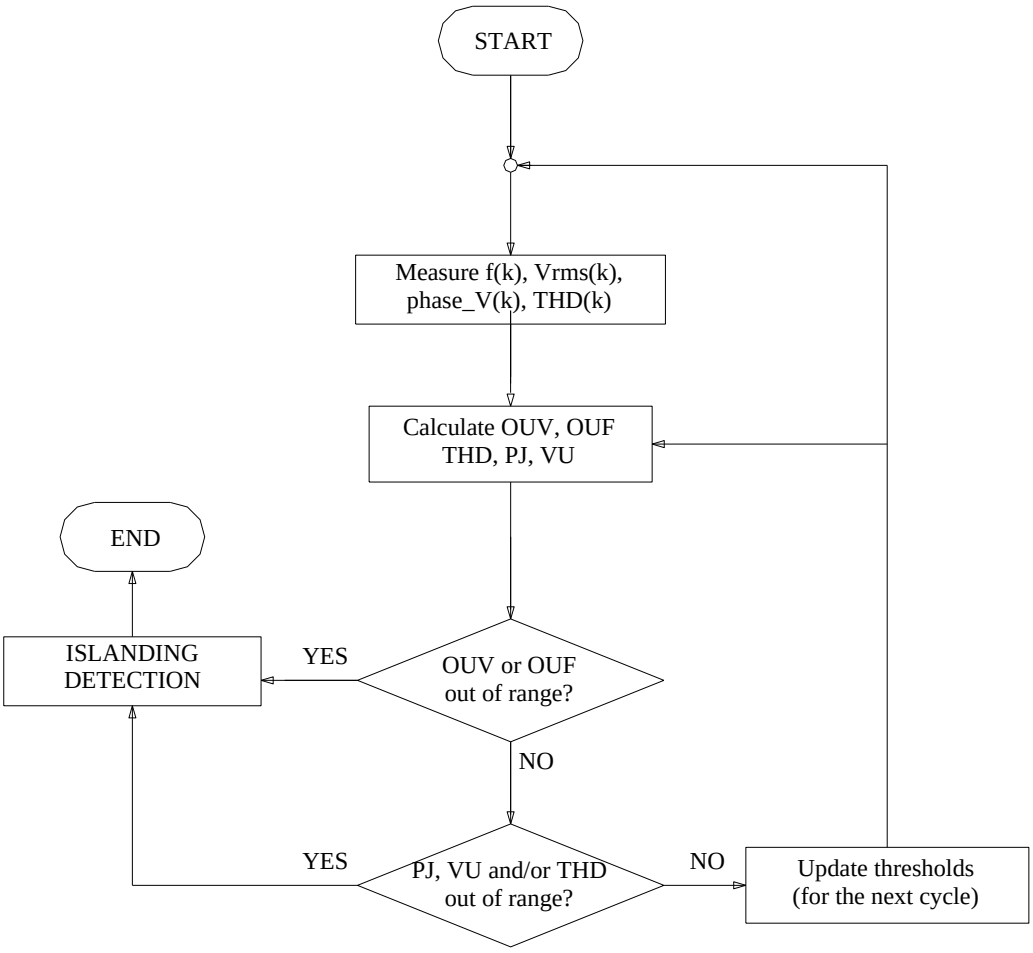


***Fig.3.13 Local mesurement combined detection method algorithm***

### 3.6 THE PROPOSED HYBRID METHOD

It has to be observed that, in some cases, the local measurements of the considered parameters can give an uncertain result; in fact the combined approach can allow to significantly reduce but not to totally avoid the NDZ situations. Furthermore, in some cases the variations of the aforesaid parameters could be too small, or within the measurement uncertainty range, causing again a NDZ condition. Further analyses and simulations and studies have shown that, in some cases, the local measurements of the considered parameters can give an uncertain result (i.e. the variations of some parameters could be too small, or within the measurement uncertainty range). This is also related to the fact that, for the practical implementation of the proposed solution, it is necessary to fix the proper thresholds for the

parameters variations, in order to provide a reliable islanding detection. To improve the effectiveness of the islanding detection in such cases, an hybrid method has been developed, which is based on both local measurements and communications between the DG and the grid. Furthermore, in the hybrid approach, when the local measurements give an uncertain result (i.e. in NDZ situations), communications between the grid and the DG can be used to send utility status information back to the DG (in order to detect the status of the PCC breaker). In such cases the communications are used to support the decision, in order to avoid the unwanted operation of DGs in islanded conditions. On the other hand, the local measurements could help if a communication fail occurs.

The complete flowchart of the hybrid method is represented in the figure below.

The system uses a PLCC (power line carrier communications) line whose support is the electric line of power [8, 14, 20, 27, 28, 48, 49]. Under normal conditions of operation a lower energetic signal is sent to the receiver. When a fault or intentional service interruption causes the disconnection of the grid line, the channel of communication is forced to stop the data transmission and commands the inverter to trip. The same goal can be achieved with a dedicated line of communication based on SPD (Signal produced by disconnect) [41, 50-57]. In another solution, wireless communications can be used [58-60].

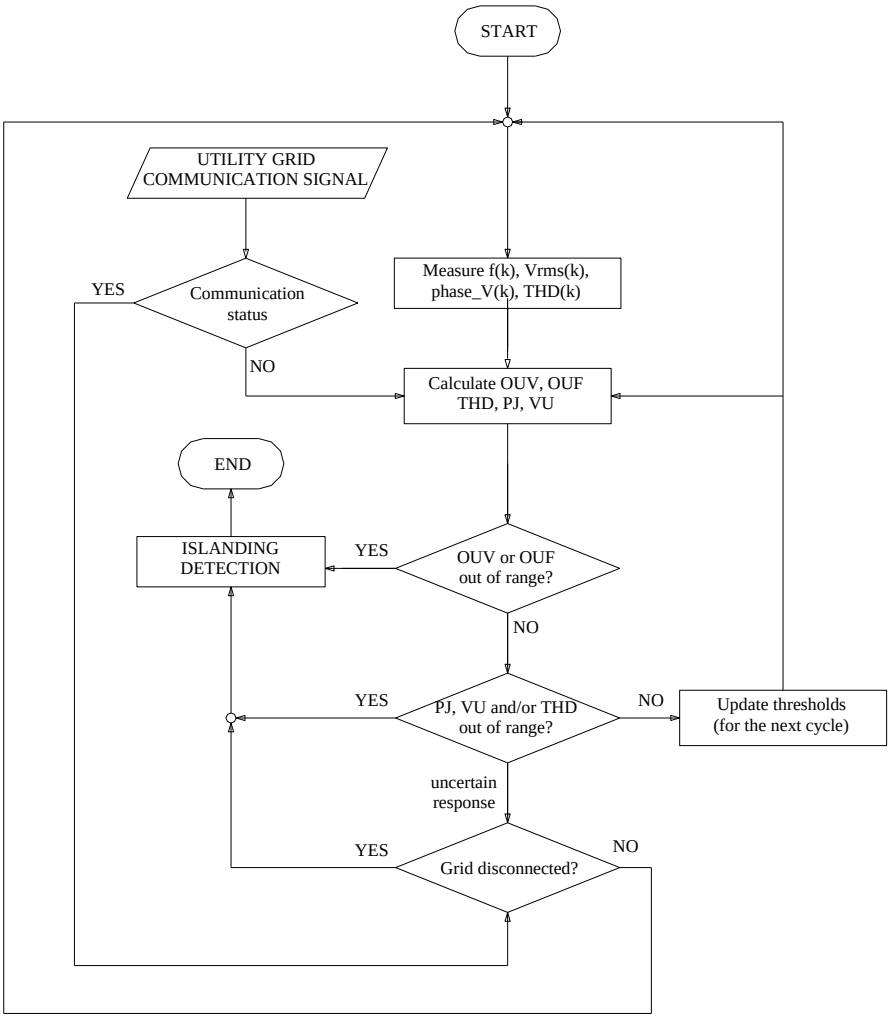


***Fig.3.14 Hybrid Islanding Detection Method Algorithm***

### 3.6.1 COMMUNICATION ARCHITECTURE AND INTERFACE DEVICES

The proposed hybrid solution for islanding detection can be implemented in a real system, by integrating local measurements and communication in the DG interface device (ID) and developing proper communication architecture for smart grid applications. The proposed approach can also allow the utility to remote control the DGs, in the perspective of their active participation to the power grid stability and control. In this way, it would be possible to move towards a complete integration of DGs with the utility systems, implementing not only protection functions, but even more, contributing to power grid stability and control. In this viewpoint, new IDs have to be developed, which should integrate measurement and communication functions. Moreover, a two-ways communication infrastructure is needed, to allow the information exchange between the IDs and their remote control.

As regards this, the work has been developed in conjunction with the following research projects (both under the Scientific Responsibility of prof. Antonio Cataliotti):

- PO FESR 2007-13 Sicily, Line 4.1.1.1, Project: REIPERSEI Title: “Reti Elettriche Intelligenti per la Penetrazione delle Energie Rinnovabili nei Sistemi Elettrici delle Isole minori” (Smart grids for the exploitation of renewable energy sources in the little islands of the Mediterranean Sea),
- PO FESR 2007-13 Sicily, Line 4.1.1.2, Project: SERPICO Title: “Sviluppo E Realizzazione di Prototipi di Inverter per impianti fotovoltaici a COncentrazione” (Development of new inverters prototypes for concentration photovoltaic systems).

In the framework of the aforesaid projects a new ID prototype has been developed for distributed generation, which is able to integrate both measurement and communication functions. Furthermore, different possible solutions have been investigated concerning the communication architecture, mainly using the power line communication technology, even integrated with other wireless solutions, in the framework of a SCADA (Supervisory Control and Data Acquisition) architecture.

A block diagram of the proposed ID is reported in Fig. 3.15. The ID has a metering section for the acquisition of voltage and current; these data are processed in order to perform the local measurements. Furthermore, the ID can operate on not only the basis of the local measurements but also by means of communications with the grid, in order to achieve the grid status information and also modify the thresholds for the Interface Protection Device (IPD) operation and the inverter functionalities. Currently, the firmware has been developed in order to implement the functions required by the CEI 0-21 Standard and its operation has been successfully verified by means of some experimental tests. This hardware solution allows one to easily implement further functionalities and measurements by reprogramming only the firmware. The new ID can communicate with the inverters through serial communication, i.e. RS232 port. Furthermore it can also exchange data with utility through the PLC port. For this purpose, the demo board is equipped with a ST7580 multi-mode power line networking system-on chip, based on single carrier modulation, (FSK, BPSK, QPSK and 8 PSK) up to 30 kbps.

As regards the communication architecture, two possible solutions are schematized in Fig. 3.16. The first one is based on the use of only PLCs. It is known that the PLCs are intrinsically not expensive for the electrical utilities, since they usually own the electrical

network. The authors have already investigated the feasibility of the employment of the PLC technology in MV and LV networks. Thus a possible solution for the communication between the Master unit and the IDs can be based on the use of PLC technology. A concentrator is connected to the LV side of each secondary substation, to collect the PLC data from the IDs (in analogy with the Automatic Meter Reading and Advanced Metering Infrastructure). On the other hand, a capacitive coupler is used to send the PLC signal to the MV bus-bars of the primary substation. In this way a MV-LV communication (by crossing the power transformer) is realized between the Master Unit and the secondary station concentrator. The second solution is a multi-level system, where PLCs are used in LV networks for the communication between the IDs and the concentrator, while the concentrator communicates with the master unit via a wireless connection (for example Hyperlan) or cable connection. In fig. 3.17 it is shown how the secondary station concentrator has been realized by means of low cost solution with a STM32 microcontroller of a STMicroelectronics E-meter demo board STEVAL-IPP001V2 and Arduino. In this way the concentrator communicates with IDs by power line (ST7580) and with utility by Modbus TCP/IP.

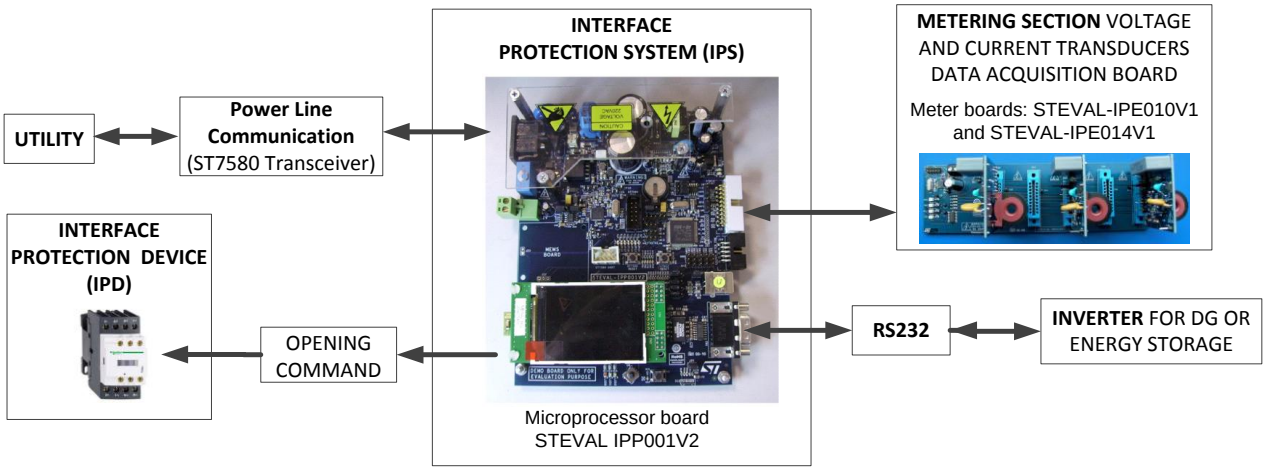


***Fig.3.15 Block diagram of the ID prototype***

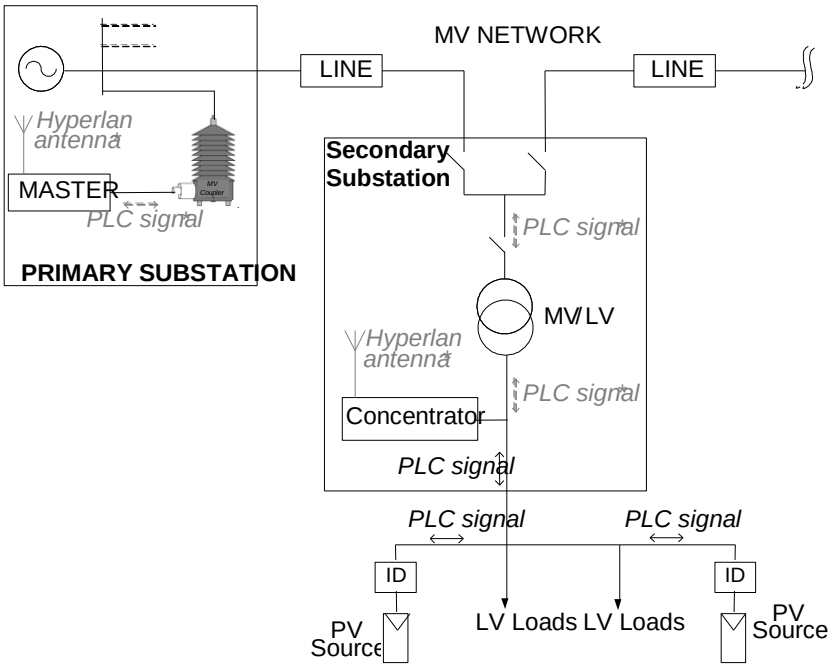


***Fig.3.16 Communication architecture. (The * indicates solutions that can be used alternatively)***

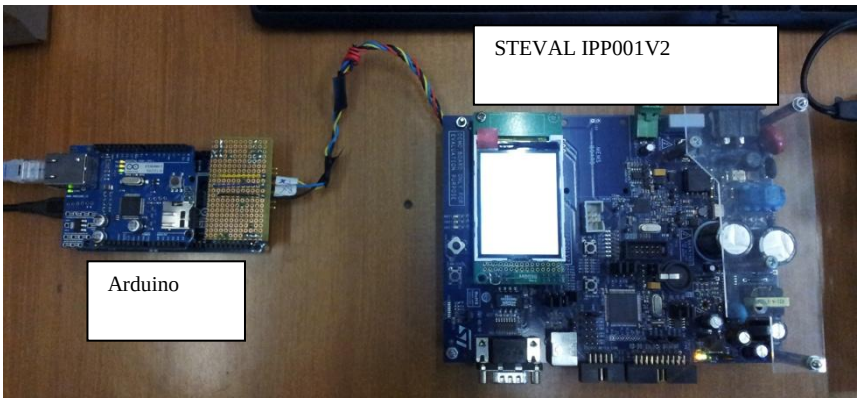


***Fig.3.17 Prototype of the secondary station concentrator.***

# CHAPTER 4. REAL NETWORK IN ISLANDING OPERATION. SIMULATION RESULTS

## 4.1 HYBRID IDM IMPLEMENTATION. GRAPHICAL USER INTERFACE (GUI)

The proposed hybrid islanding detection method (IDM) has been implemented in Matlab environment. According to the flow chart of the proposed strategy (see fig. 4.0-a), fig. 4.0-b shows the front panel of the MATLAB/SIMULINK GUI Interface programme, which has been used to detect islanding condition at PCC. In the appendix there is reported the source code of the implementation. The operation of the programme is described in the following.

- **Data entry**

The programme begins with the settings of the main simulation parameters (sampling time, stop-time simulation, power system frequency) and the choice of the network configuration for the simulated scenario (the details on the various simulated scenarios are reported in the following sections). These settings are reported in the "Data Entry" section of the GUI front panel.

- **Simulation running and figures**

After this, the simulation is run and the power system parameters at PCC are calculated. In detail, the programme allows to calculate not only the parameters which are used in the strategy, but also other power system quantities, in order to have a more complete information on the state of the simulated system. The considered quantities are Vpcc_rms, THD_vpcc, Phase_Vpcc, THDiload, Frequency, VU_pcc, I Grid, which are shown in the section "Figures". Such figures can be selected and viewed in the front panel.

- **Initial threshold values settings**

To evaluate if the considered parameters (OUV, OUF, THDv, PJ and VU) are within the range or not, the threshold value have to be initially set for each parameter. Such values can be the default values or they can be set manually. The settings details are the following:

- V_Threshold is the one-cycle average of Rated value of the phase to ground voltage at the steady state and normal loading conditions
- V_max_cyc_50: the allowed maximum loop number out of range if deltaV < 50%
- V_max_cyc_50_85: the allowed maximum loop number out of range 50% <= deltaV < 85%

- V_max_cyc_110_135: the allowed maximum loop number out of range 110% <= deltaV < 135%
- V_max_cyc_135: the allowed maximum loop number out of range deltaV >= 135%
- PhV_DeltaPhase: delta's lower limit.
- PhV_max_cyc: the allowed maximum loop number if theta continuously exceeds the threshold (limit value).
- THD_Threshold: the lower limit and upper limit of THD values.
- THD_max_cyc: the allowed maximum loop number if THD continuously exceeds the threshold (limit value).
- VU_max & VU_spike: Maximum unbalance and maximum permissible VU spike
- Communication method: to simulate the communication status acquisition and the grid status (disconnected or not), a dedicated line is used for communication based on SPD (Signal produced by disconnect).

➢ **Calculation and Results for the islanding detection method (IDM)**

By clicking the "Calculation" button, the IDM is simulated and, after the calculation is done, all the results of IDM can be selected and shown in the "Results" section of the front panel. Such results can be shown and analyzed one by one:

- Results of IDM based on the Over/Under Voltage method
- Results of IDM based on the phase displacement of Vpcc
- Results of IDM based on the Voltage Unbalance of Vpcc
- Results of IDM based on the THD of Vpcc
- Results of Hybrid Method

For each result, the following informations are shown:

1. The system is steady-state and normal loading condition
2. Islanding occurred
    - Out of range at:
    - Iteration(step):
    - trip time(s):
    - The value is:

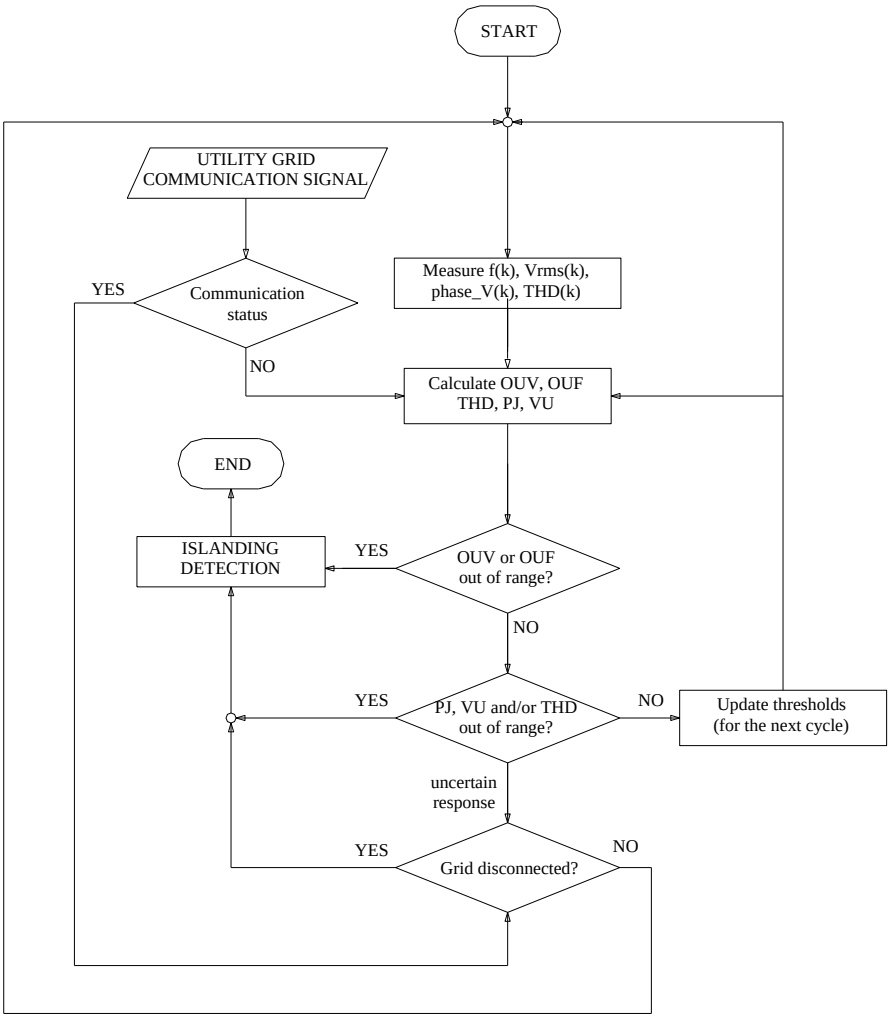


***Fig. 4.0-a. Flow chart of the implemented strategy***

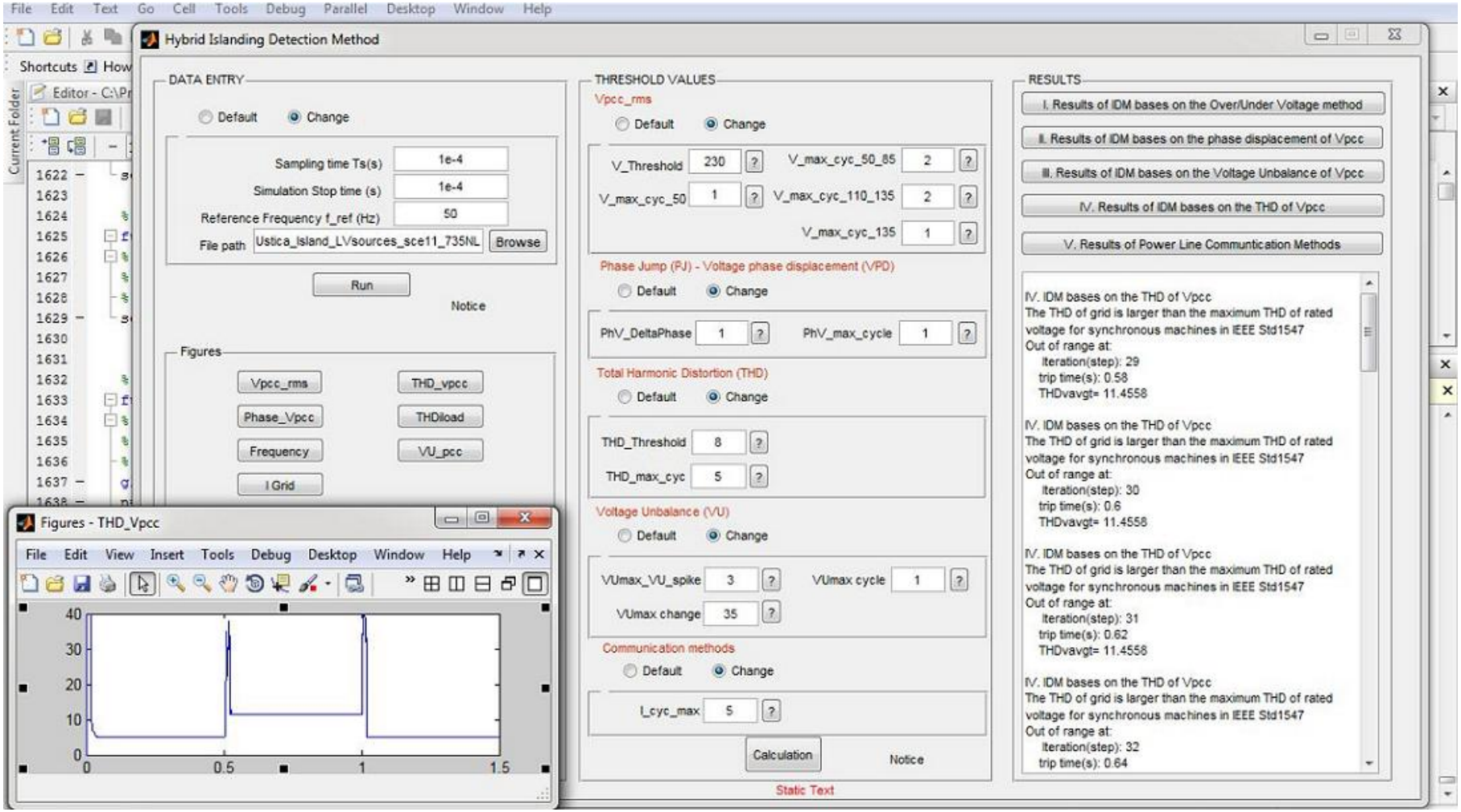


***Fig. 4.0-b. Hybrid Islanding Detection Graphical User Interface (GUI)***

## 4.2 INTRODUCTION. USTICA'S DISTRIBUTION NETWORK

An in-depth simulation study has been carried out in order to verify the islanding detection capability and the operation of the proposed method on a real power system.

The case study is the distribution network of the Island of Ustica. This network is composed by two MV radial branches departing from the generating substation. The rated voltage is 20 kV and 25 secondary substations, with MV/LV power transformers of different sizes, are connected to the MV branches.

The Ustica Island distribution network was simulated in Matlab/Simulink environment. A scheme of the simulated system is reported in figure 4.1. A DG was connected to the LV side of the power transformer at bus 22. The islanding condition was obtained by means of a circuit breaker (CB) connected to the MV side of the power transformer at bus 22. To carry out some simulations in the presence of harmonics coming from the grid, some harmonics were injected by the voltage generator which simulates the generating substation. To carry out some simulations in the presence of nonlinear loads, a nonlinear load was added to the LV side of the power transformer at bus 22. As done for the simple case study, the DG has been sized considering the power of the load at bus 22, in order to have voltage and frequency variations before and after the opening of the circuit breaker (CB) (islanding) within the thresholds of CEI:0-21[13]. In all the simulations, the CB at bus 22 was opened (*islanding*) at the instant t=0.1s and the behaviour of the voltage at PCC and the load current were studied during islanding operation.

In figure 4.1a there is reported a simplified scheme of the simulation, where the branches of the simulated network, upstream and downstream the bus 22, were replaced with single loads absorbing the same power of the real branches of the network.

In figure 4.1b there is reported the scheme of the simulation at the LV side of the power transformer at bus 22, where all the measurements have been carried out.

The simulation results are shown in the following sections. In all the simulation cases the limit of maximum harmonic distortion in percent of current is 5% and THD of the voltage at PCC is 8% according to the standard EN-50160. The simulations comply with standards IEC61727, IEEE 929&1547, VDE0126-1-1; the voltage is within the range of 85%-110% of the rated value; this limits define the NDZ normally defined by the current standards.

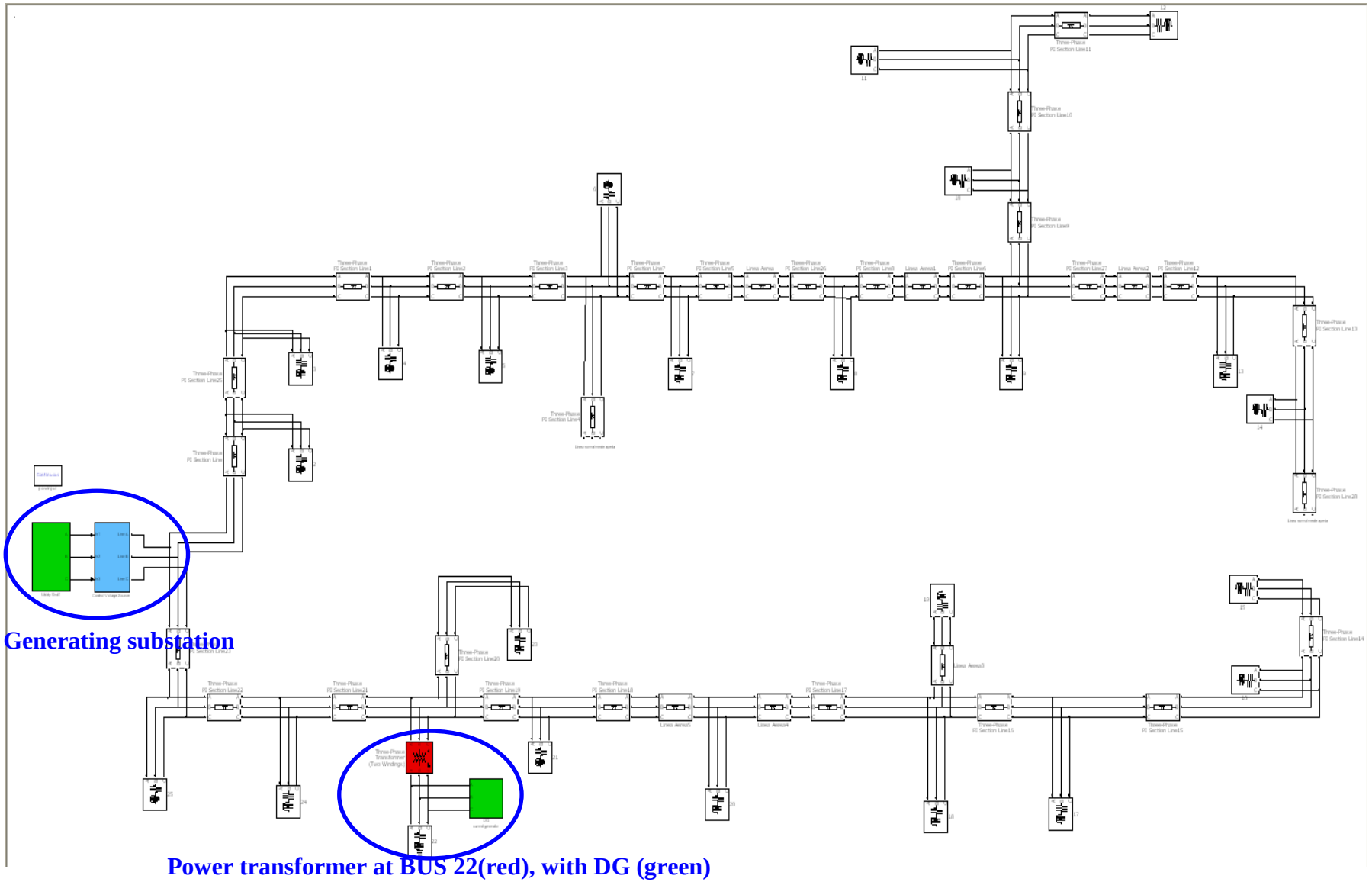


***Fig.4.1. The simulation of Utica's power system.***

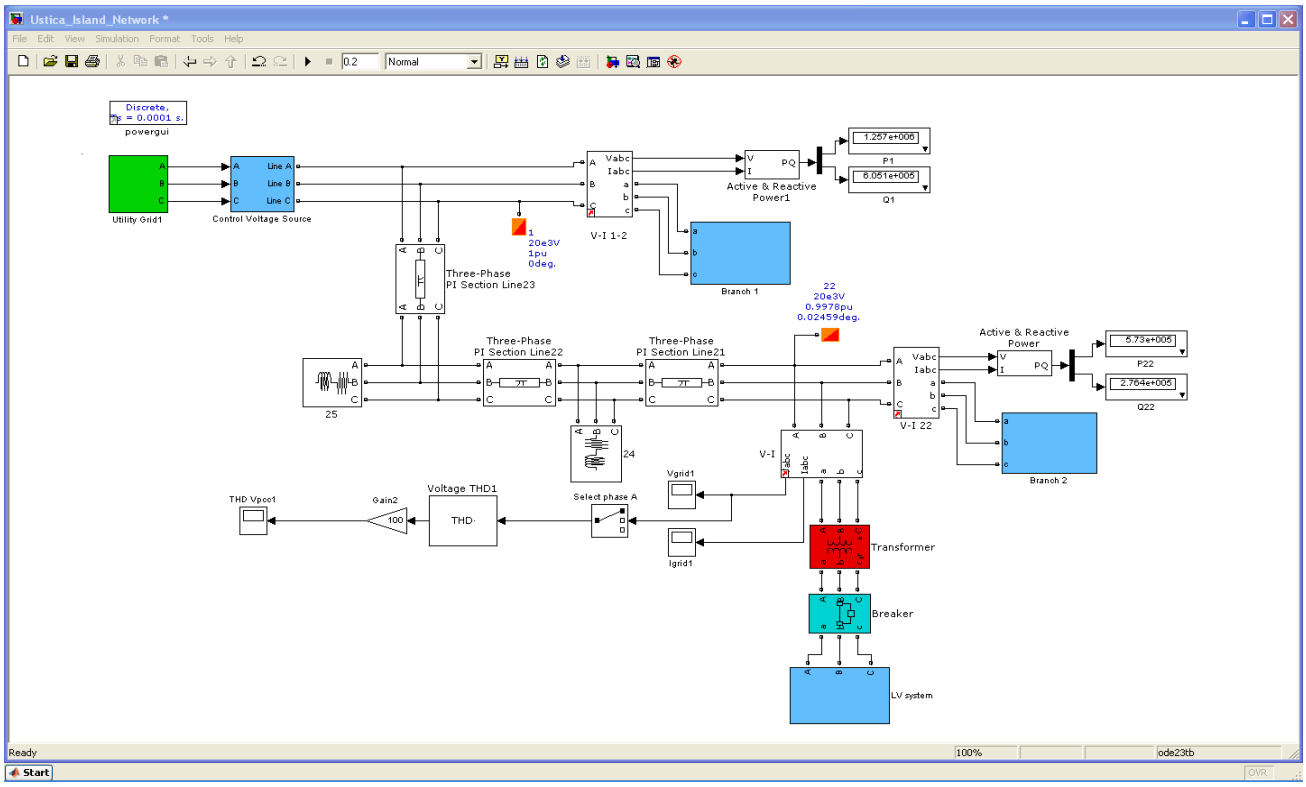


***Fig.4.2. the simulation of Ustica Island Network***

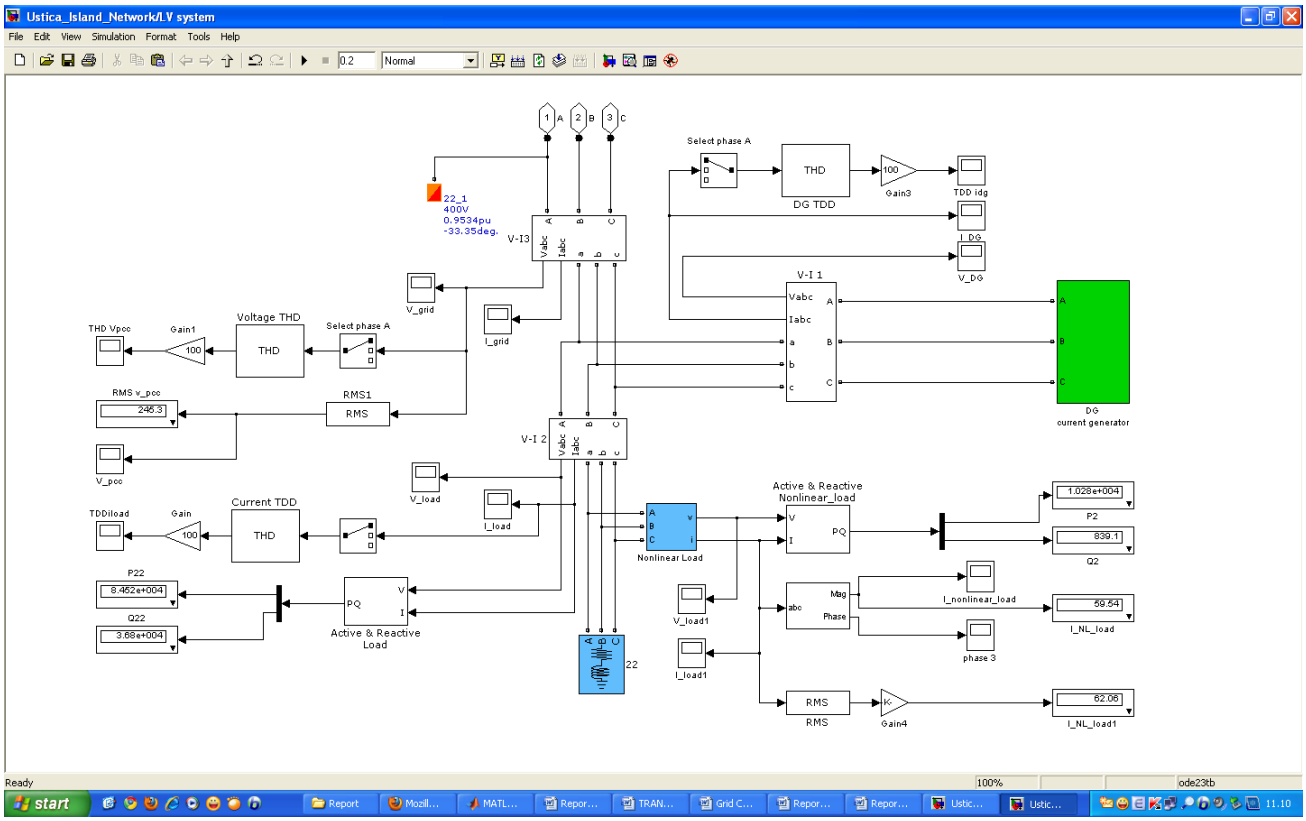


***Fig.4.3. the simulation of Low Voltage Network***

### 4.3 CASE 1

The figure 4.4 shows the simulation and the implementation of the Ustica network in the case 1. In this case, the bus 22-1 contains a linear-load (16kW and 8kvar) and a nonlinear-load (active power is 1.6kW), which are connected in parallel.

As regards the supply voltage, some harmonics can be injected and superimposed with the fundamental frequency voltage; the maximum amount of the disturbance is $THD_V$ = 7.3%; this limit has been set in order to have a THDv less than 5% at PCC (required standard value for DG connection).

Regarding the current distortion coming from the DG, harmonics are injected and superimposed with the fundamental current of the DG source; these harmonics are meant to simulate the harmonics injected by the DG inverter. For such current harmonics the standards fix a limit of 5%; however, for the aim of the present study the effect of higher distortion levels has been investigated; thus, the maximum considered total harmonic distortion has been set to $THDi_{DG}$ = 21.75%, in accordance with [34].

As already mentioned, the system has been sized in order to have a traditional non-detection zone (NDZ); small active and reactive power mismatches (ΔP and ΔQ) occur at PCC due to the change of frequency and voltage after the utility disconnected, which is not enough to detect islanding within a prescribed time period (in accordance with the different standards IEC61727, CEI 0-21, IEEE1547 ...). Thus frequency and voltage are insides of the acceptable quality range.

For this case, different scenarios have been analyzed, which have been obtained by varying the load, voltage supply and DG current harmonics, within the limits previously described. The different scenarios are summarized in table 4.1.

In all the simulations, at the initial time the circuit breaker at PCC is closed; it is opened at time t=0.5s and reclosed at time t=1s.

The simulation results for the considered scenarios are detailed in the following sections and they are summarized in table 4.2. From these results it can be observed that, in all the considered scenarios, the distortion of the load current and the PCC voltage is small before the islanding condition ($t < 0.5$ s). This happens the utility grid impedance is much lower than the load impedance, thus, the harmonic current flows into the utility and no abnormal voltage is detected at PCC. On the contrary, when the grid is disconnected, (i.e. islanding condition occurs, at $t = 0.5$ s, with the transient time of 0.02s), the harmonic currents can flow to the load and the PCC voltage distortion increases.

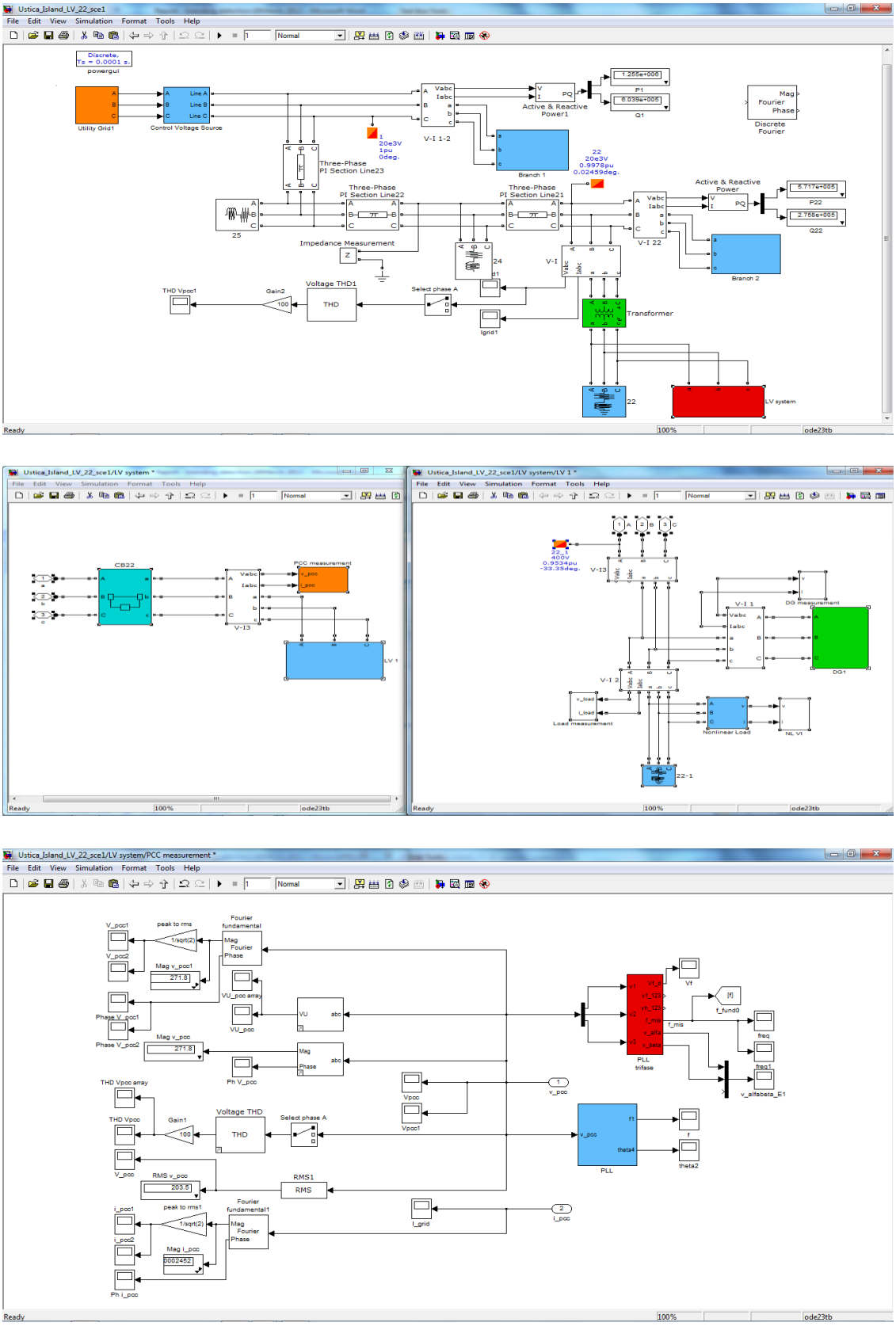


***Fig.4.4. the simulation and the measurement blocks in the Network of the CASE 1***

At the initial time, the circuit breaker at PCC closes, it is opened at time t=0.5s and reclosed at

time t=1s. Table 4.1 shows the implementation of the system. The three phase current of load and the voltage at the PCC before the islanding condition seems sinusoidal because the disturbance injection from DG is very small comparing with grid current and load current. As the utility grid impedance is much lower than the load impedance at the harmonic frequency while the grid is connected, the harmonic current flows into the utility and no abnormal voltage is detected. On the contrary, when the grid is disconnected, islanding condition occurs, the harmonic currents can flow to the load due to the current load and the PCC voltage is non-sinusoidal.

PJ (PJD-Phase jump detection) and VU method suffers from a serious implementation difficulty in that it is difficult to choose thresholds that provide reliable islanding detection but do not result in frequent nuisance trips. The starting of certain loads, particularly motors, often causes transient phase jumps of significant size, and these will cause nuisance trips of the PV inverter if the thresholds are set too low. PJD thresholds could be altered for a given installation site, but such site-specific parameters increase the difficulty in installing utility-interactive PV systems.

The disadvantage point of this hybrid method is setting up the threshold value. However, the threshold of VU, according to EN50160 standard, in has a value of 3%. Ustica network is simulated by MATLAB/SIMULINK, the trip signal is immediately sent when islanding occurs and this signal is completely accurate.

Conclusion, all of scenarios in which IDM based on VU, PJ always send the suspected signal as soon as islanding occurred however those techniques uncertain when islanding occurred or that is normally switching the load.

| CASE 1<br>Scenarios | Implementations | | | | | The Circuit Breaker Status<br>(Initial status of CB: Open/Close) | | | |
|---|---|---|---|---|---|---|---|---|---|
| | Grid | DG | | Load | | | | | |
| | THD<br>$V_{Grid}$<br>% | P<br>kW | THD $I_{DG}$<br>% | Linear<br>kVA | Non Linear<br>kW | CB-22 | CB-DG | CB-Load | CB-<br>NL load |
| Sce.1 | 0-7.3 | 20e3 | 5 | 16+j8 | 1.6 | C<br>(open at<br>t = 0.5-1 s | C | C | C |
| Sce.2 | 0-7.3 | 20e3 | 21 | 16+j8 | 1.6 | | | | C |
| Sce.3 | 0-7.3 | 20e3 | 0 | 16+j8 | 1.6 | | | | C |
| Sce.4 | 7.3 | 20e3 | 0 | 16+j8 | 1.6 | | | | O<br>(closed at<br>t =0.75 s) |

***Table 4. 1 Implementation for the simulated scenarios of the CASE 1***

| CASE 1 | Islanding Detection Methods responses (local measurements) | | | | Islanding Detected |
|---|---|---|---|---|---|
| | **Over/Under Voltage and Frequency (OUV/OUF)** | **Voltage Phase Jump (PJ)** | **Voltage Unbalance (VU)** | **Total Harmonic Distortion (THD)** | |
| Sce.1 | **No** | **Yes** | **Yes** | **Yes** | **Yes** |
| Sce.2 | **No** | **Yes** | **Yes** | **Yes** | **Yes** |
| Sce.3 | **No** | **Yes** | **Yes** | **Yes** | **Yes** |
| Sce.4 | **No** | **Yes** | **Yes** | **No** | **Yes** |

***Table 4.2: The results of the scenarios in the CASE 1***

### 4.3.1 SCENARIO 1.1

In this scenario, the simulation results show that measurements of OVF and OUV cannot detect islanding (i.e. a NDZ situation occurs). On the contrary, the islanding is detected by the other considered parameters monitoring. In fact, when the CB-22 opens at the time 0.5s (islanding occurrence), THDv at PCC increases from 1.012% to 11.456%; this value is greater than threshold value 5%. Therefore, the IDM based on THDv detect islanding although THDi of the current load is less than 5%. The voltage phase angle jumps from -27.5° to 14.236°, the average value of the phase jump in one cycle is ΔPJ=47.736°. Furthermore, VU jumps from 0 to 7.713%. These values are over the considered threshold of 10° and 3% for PJ and VU, respectively. The aforesaid thresholds for THDv, PJ (PJD) and VU have been set accordingly to the EN50160 standard. Thus, in this scenario, the islanding is detected by the combined passive method, (THDv=11.456%>5%, VU=7.713%>3%, ΔPJ =41.736°>10°).

The results obtained for this scenario are reported in the figure below.

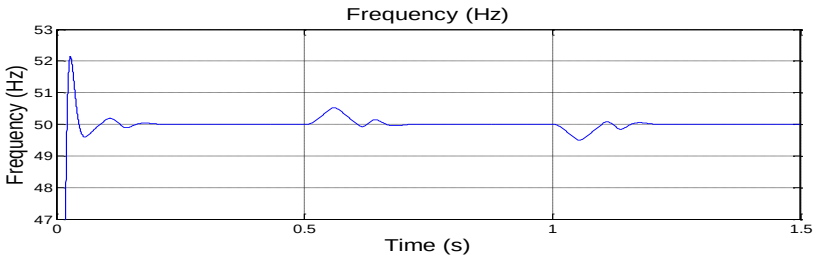


frequency

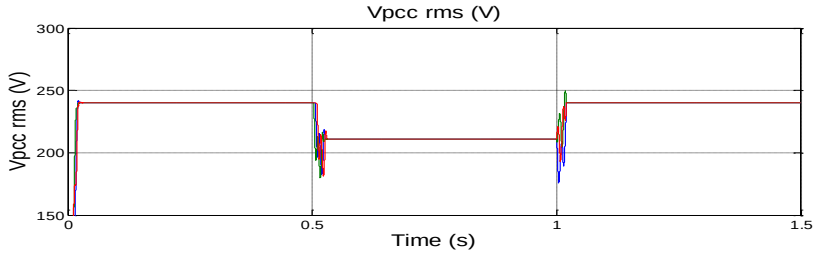


voltage rms at PCC

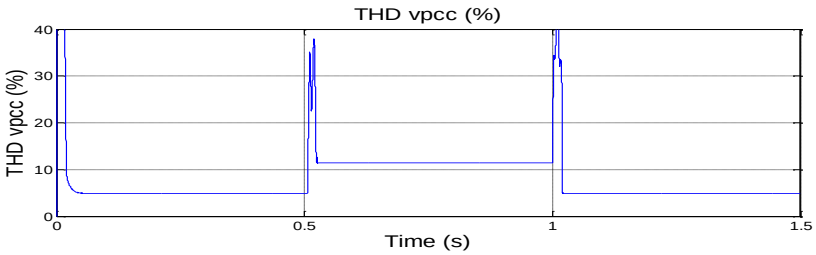


Voltage THD at PCC

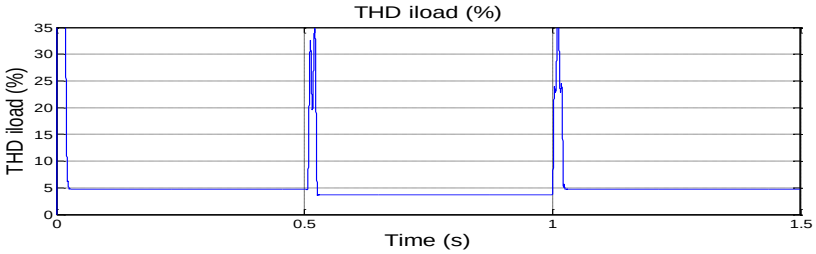


THD i load

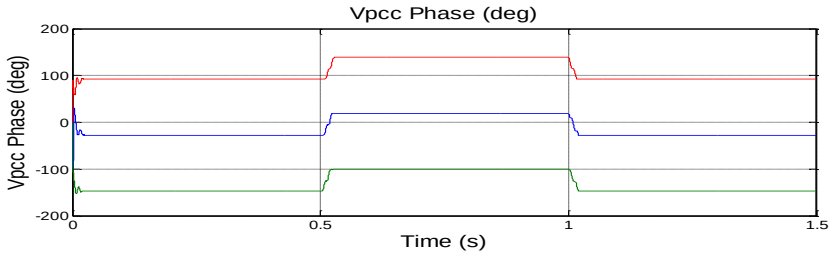


Voltage Phase at PCC

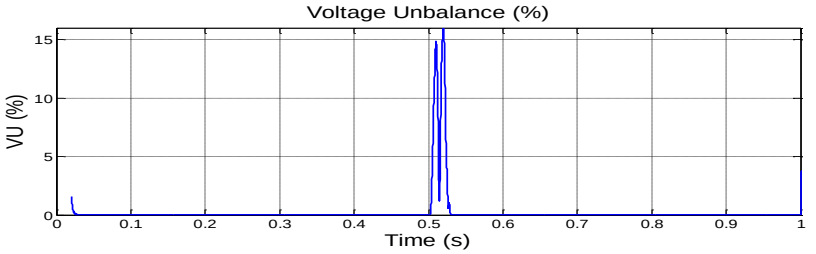


Voltage unbalance

***Fig.4.5. the variations of Scenario 1***

### 4.3.2 SCENARIO 1.2

In this scenario, the results for OUV, VU and PJ are similar to the previous case; on the other hand, THDv and THDi show higher variations after islanding (THDv=36.6%, THDi=16.65%). Also in this case the combined local measurements are able to detect the islanding occurrence. The results obtained for this scenario are reported in the figure below.

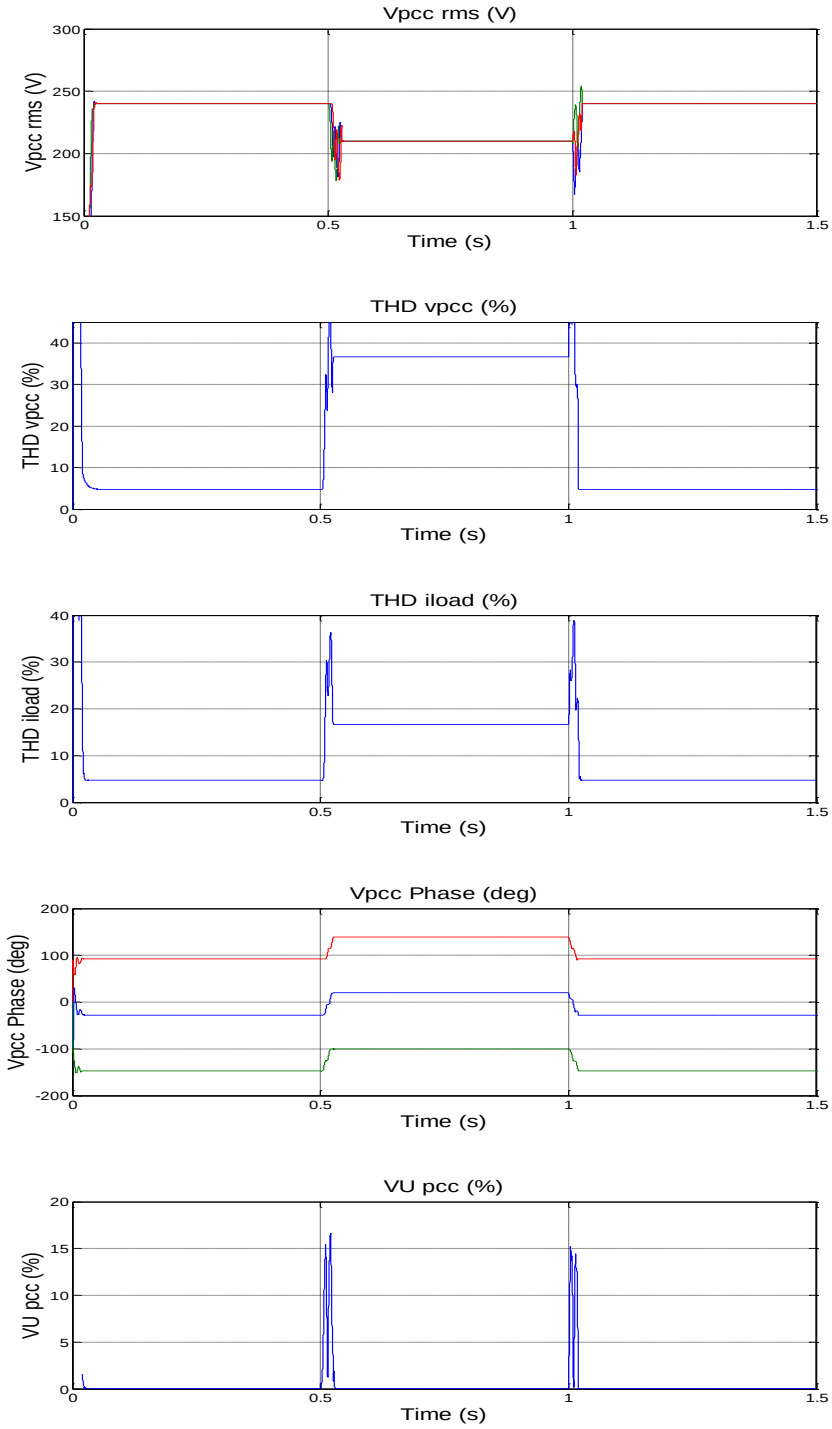


voltage rms at PCC

Voltage THD at PCC

THD i load

Voltage Phase at PCC

Voltage unbalance

***Fig.4.6. the variations of Scenario 2***

### 4.3.3 SCENARIO 1.3

Also in this scenario the combined measurements can detect islanding. In fact, after CB-22 opens, the voltage THD at PCC changes from 1.125% to 8%, and the other parameters show the same variations of the previous scenarios. Only the THDi of load current has a different behaviour (it decreases from 4.66% to 1.77%), because no harmonics are injected by the DG. The results obtained for this scenario are reported in the figure below.

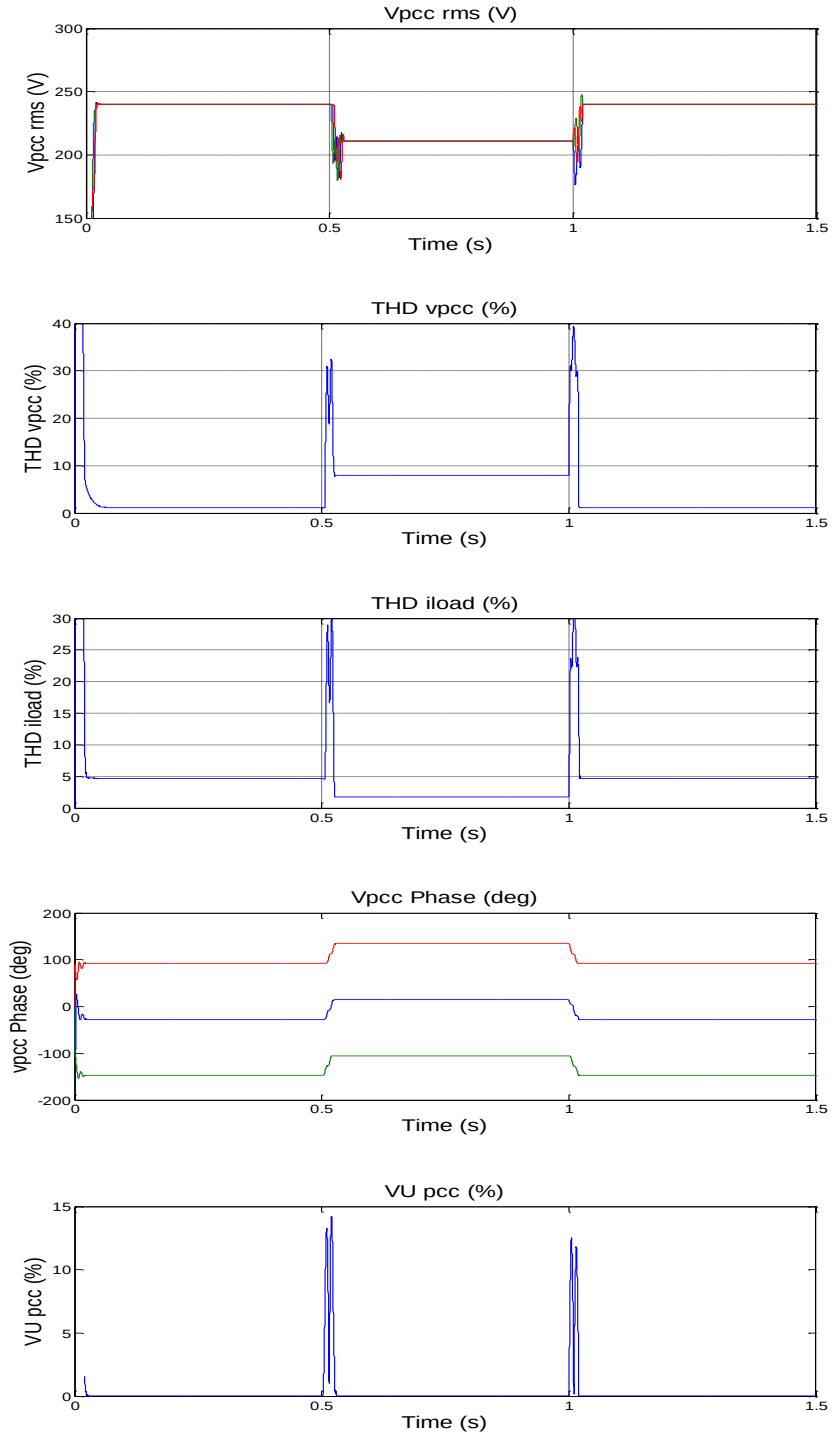


voltage rms at PCC

Voltage THD at PCC

THD i load

Voltage Phase at PCC

Voltage unbalance

***Fig.4.7. the variations of Scenario 3***

### 4.3.4 SCENARIO 1.4

This scenario is similar to the previous one, but the nonlinear load is inserted at t = 0.75s, while the CB-22 is opened at time 0.5s. The obtained results are show in the figure below. It can be observed that, when the CB-22 opens at the time 0.5s, THDv at PCC reduces from 4.6% to 1%; this is caused by sinusoidal supplies of DG current sources through linear load. The THD value is inside the range of acceptable limit (less than threshold 5%). Therefore, the method based on THDv cannot detect any abnormal state. Otherwise, when the nonlinear load in inserted (at the time 0.75s), the harmonic voltage at PCC increases from 1.012% to 8.434%. The deviation of THDv is greater than the threshold value However, this is a normal load switching status; hence this could lead to a false islanding detection. On the other hand, when the CB-22 opens at the time 0.5s, the voltage phase jumps from -27.4785° to 21.235°; VU jumps from 0 to 7.713 ($\Delta PJ$ =48.7135°>10°, VU=7.713%>3%). These values are over the thresholds, thus such parameters can correctly detect the islanding occurrence. Furthermore, the insertion of the nonlinear load determine small variations of such parameters (under the considered thresholds); thus the normal load switching does not produce a false islanding indication.

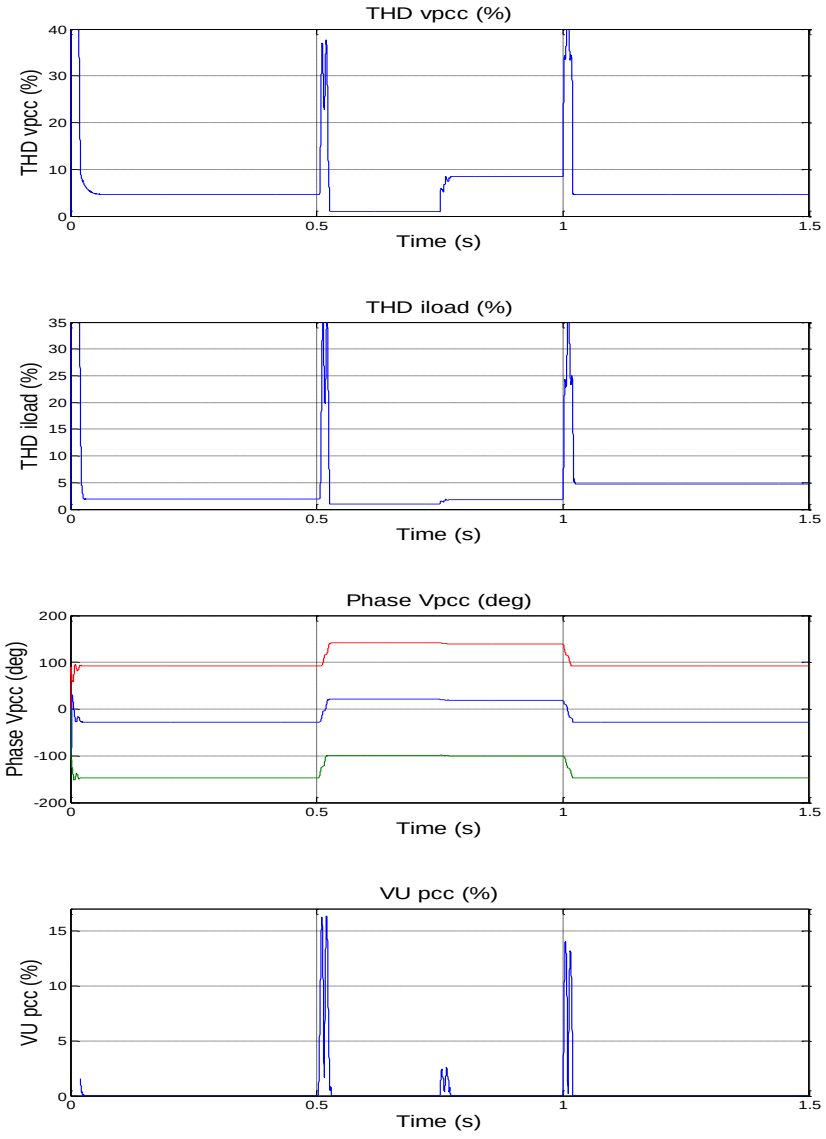


Voltage THD at PCC

THD i load

Voltage Phase at PCC

Voltage unbalance

***Fig.4.8. the variations of Scenario 4***

## 4.4 CASE 2

In this case the DG generator at bus 22 contains two branches operating in parallel (the active power is 10kW) and connected at PCC by the transformer 22/0.4kV. The harmonics are always injected and superimposed with a fundamental signal of DG1 source (harmonics $3^{rd}$, $5^{th}$ and $7^{th}$ with the amplitude are less than 4.5%). Furthermore, harmonics are also injected and superimposed with a fundamental signal of utility grid; the maximum of the disturbance is $THD_V$ = 7.3% and, for each scenario, it is set in order to have a value of THDv at PCC less than the preordained threshold value of 5%. In the following, table 4.3 shows the implementation of the system. The results of the programs are shown in the table 4.4 below.

| CASE 2 | Implement | | | | | The Circuit Breaker Status (Initial status of CB: Open/Close) | | | | | | |
|---|---|---|---|---|---|---|---|---|---|---|---|---|
| | Grid | Parallel DG & Load | | | | | | | | | | |
| | THD $V_{Grid}$ % | P kW | THD $I_{DG}$ % | Linear kVA | Non Linear kW | CB22 | CB-Br1 | CB-L1 | CB-NL1 | CB-Br2 | CB-L2 | CB-NL21 |
| Sce.1 | 7.3 | 2*10 | 21 | 2*(8+j3.87) | 2*0.8 | C (opens at t = 0.5 s; re-closes at t = 1.5 s) | C | C | C | O closes at t = 1s | C | C |
| Sce.2 | 0-7.3 | 2*10 | 5 | 2*(8+j3.87) | 0 | | | | C | O closes at t = 1s | | C |
| Sce.3 | 0-7.3 | 2*10 | 5 | 2*(8+j3.87) | 2*0.8 | | | | O closes at t = 1s | O closes at t = 1s | | C |
| Sce.4 | 0-7.3 | 2*10 | 0 | 2*(8+j3.87) | 2*0.8 | | | | O closes at t = 1s | C | | O closes at t = 1s |

***Table 4.3 Implementation for the simulated scenarios of the CASE 2***

| CASE 2 | Islanding Detection Methods responses (local measurements) | | | | |
|---|---|---|---|---|---|
| | Over/Under Voltage and Frequency (OUV/OUF) | Voltage Phase Jump (PJ) | Voltage Unbalance (VU) | Total Harmonic Distortion (THD) | Islanding Detected |
| Sce.1 | **No** | **Yes** | **Yes** | **Yes** | **Yes** |
| Sce.2 | **No** | **Yes** | **Yes** | **Yes** | **Yes** |
| Sce.3 | **No** | **Yes** | **Yes** | **Yes** | **Yes** |
| Sce.4 | **No** | **Yes** | **Yes** | **No** | **Yes** |

***Table 4.4 The results of scenarios of the CASE 2***

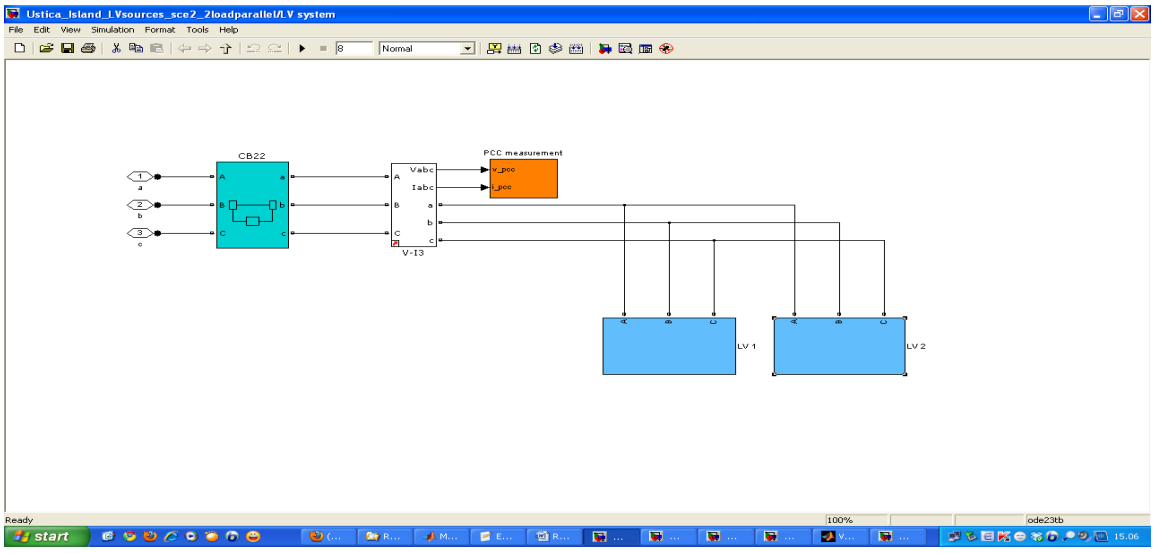


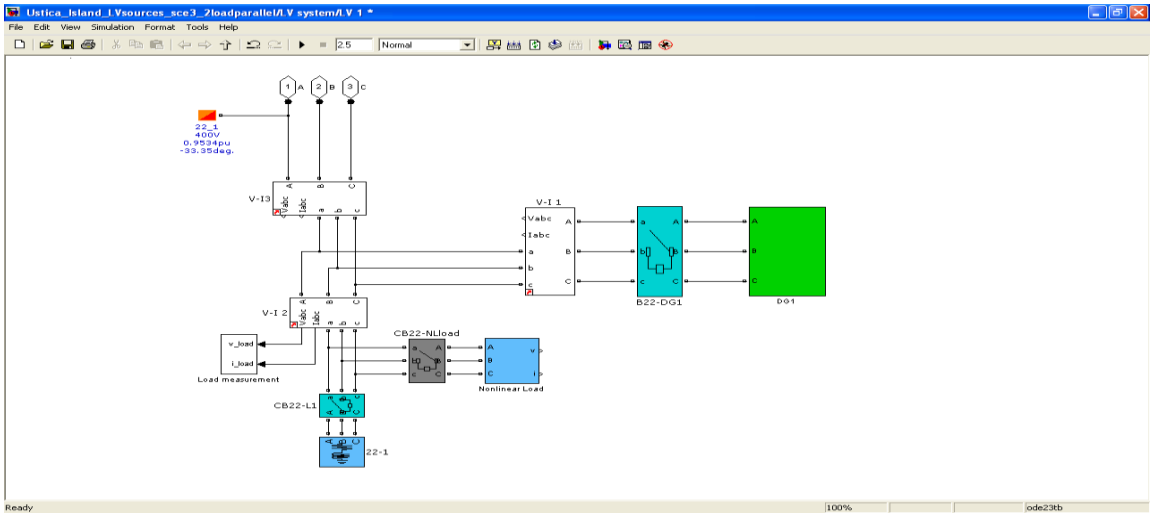


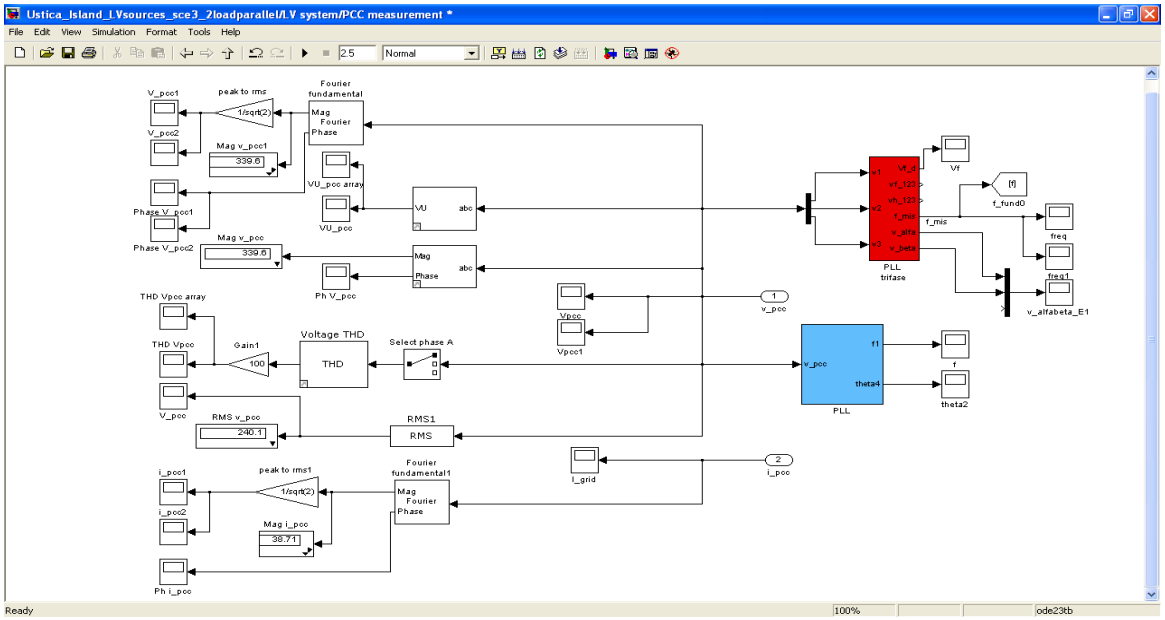


***Fig.4.9. the simulation and the measurement of Low Voltage Network***

### 4.4.1 SCENARIO 2.1

In this hypothesis, the DG's THD is very high (individual harmonics 3rd, 5th and 7th with 14%, 10% and 6% of the fundamental current, respectively). The results of the simulation are reported in fig.4.10. The frequency and the voltage at PCC are inside of the range of the acceptable limits, inversely, THDv=36.149%>5%, ΔPJ=44.43°>10°, VU=7.492%>3%. Thus, the islanding condition (at t = 0.5 s) is detected by the combined local measurements; in fact, the deviations of THD, PJ and VU at the PCC are out of the thresholds.

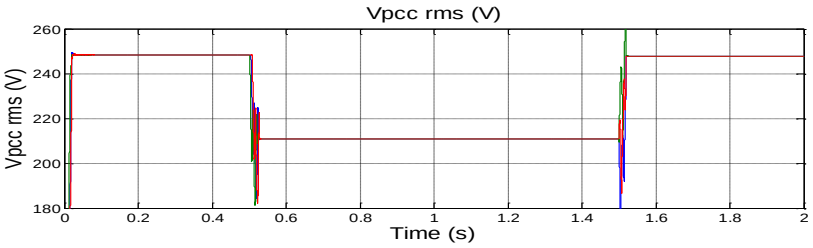


voltage rms at PCC

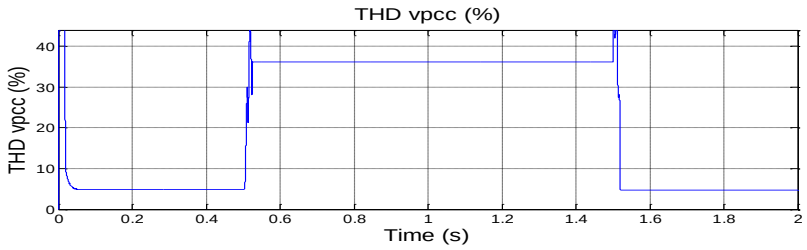


Voltage THD at PCC

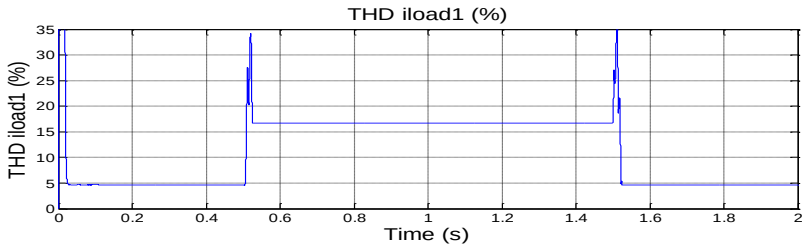


THD i load

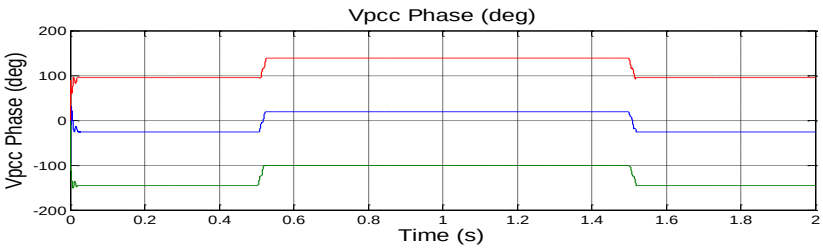


Voltage Phase at PCC

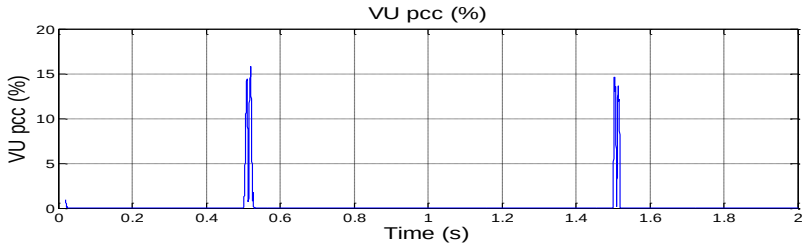


Voltage unbalance

***Fig.4.10. the variations of Scenario 2.1***

### 4.4.2 SCENARIO 2.2

In this case, one of the two DG/load groups (the branch 2 of fig. 4.9) joins in the system when the CB-Br2 closes (at time 1s); on the other hand the islanding occurs at t = 0.5 s. The IDM based on the combined measurements correctly operates. In fact, the following values are obtained at t = 0.5 s: THDv=8.22%>5%, VU=7.5%>3%, PJ=20.58°>10°. The simulation results are show in the figure below.

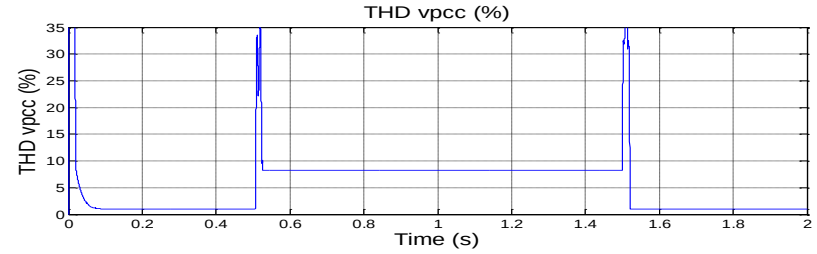


Voltage THD at PCC

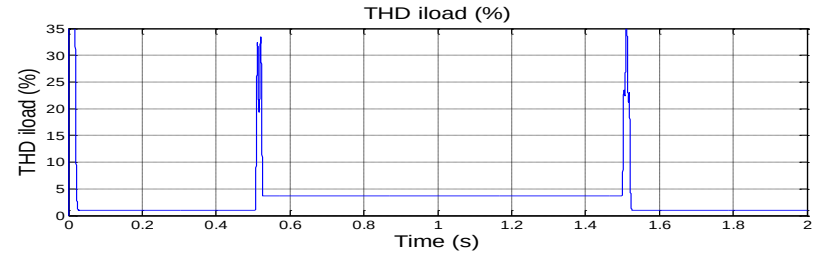


THD i load

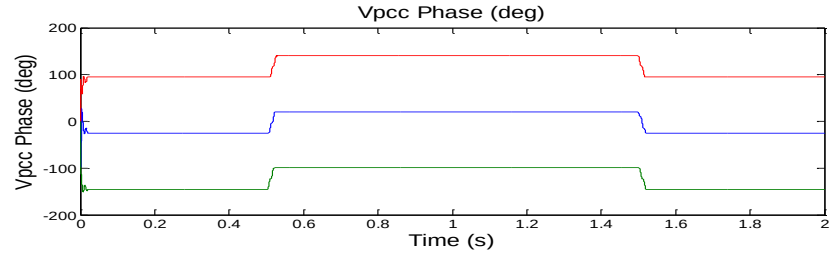


Voltage Phase at PCC

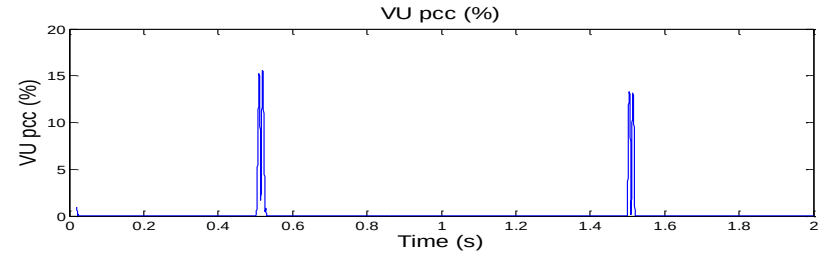


Voltage unbalance

***Fig.4.11. the variations of Scenario Sce22 (0_5_0)***

### 4.4.3 SCENARIO 2.3

In this case the circuit breaker at PCC CB-22 is opened at time t=0.5s and re-closed at t=1.5s; the nonlinear load 1 and the branch 2 join are both inserted at t=1s. The obtained values at the PCC when islanding occurs (at t = 0.5 s) are the following: THDv=11.456%>5%, VU=7.713%>3%, PJ=19.22°>10°. The simulation results are described in the fig.4.12.

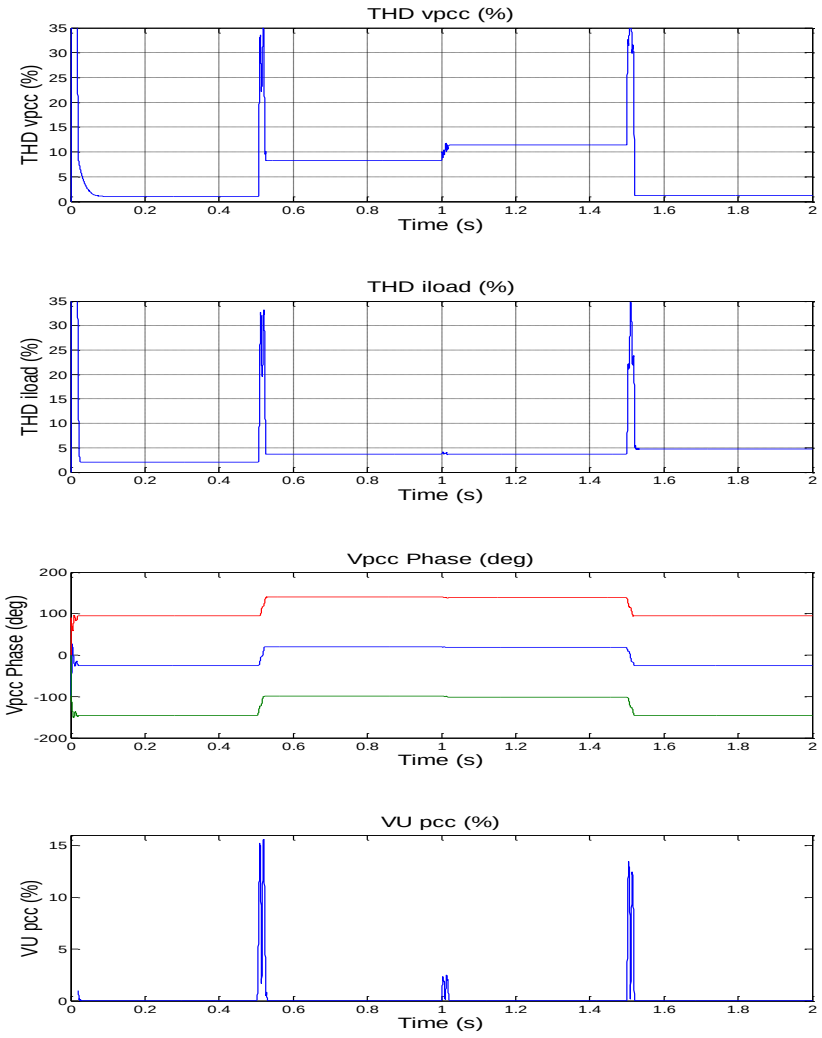


Voltage THD at PCC

THD i load

Voltage Phase at PCC

Voltage unbalance

***Fig.4.12. the variations of Scenario Sce2.3 (0_5_NL)***

### 4.4.4 SCENARIO 2.4

In this case, when the CB-22 opens at the time 0.5s, THDv at PCC reduces from 4.87% to 1%, theoretically, that is caused by sinusoidal supplies of DG current sources through linear load. The value taken from THDv method is inside the range of acceptable limit (less than threshold 5%). Therefore, the method based on THDv doesn't detect any abnormal state. Otherwise, at the time t = 1s , the nonlinear-loads are inserted and the THDv at PCC increases from 1% to 8.434%, this value is greater than the threshold value so that a warning signal about islanding occurrence is sent. However, this indication is false, because a normal switching occurred at t = 1 s. On the other hand, at the time 0.5s VU jumps from 0% to 7.52% and PJ jumps from -25.38° to 20.58°. These values are over the considered threshold values (3 % and 10 °, respectively), thus these parameters can allow to detect the islanding occurrence. Furthermore, the variations of VU and PJ at t = 1 s (when the nonlinear loads are inserted) are under the thresholds..

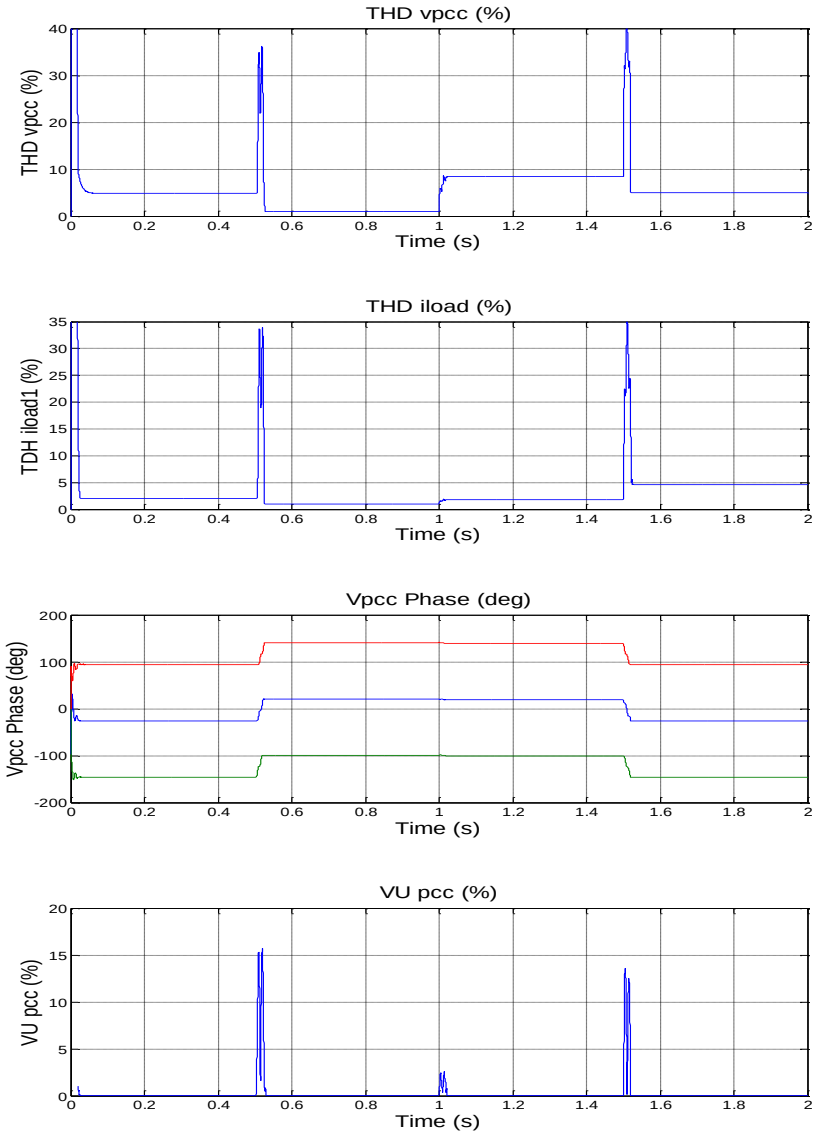


Voltage THD at PCC

THD i load

Voltage Phase at PCC

Voltage unbalance

***Fig.4.13. the variations of Scenario Sce2.4***

## 4.5 CASE 3

In this case, the islanding occurrence is simulated by opening the CB upstream the bus 17 of the Ustica's simulated network. The islanded portion of the network contains three DGs branches, at bus 17, 16 and 15, respectively. Each branch consists of a DG and load, which are connected at point common of coupling (PCC) to the MV network by the transformer 22/0.4kV. As for the previous cases, they are sized in order to meet the local load power, thus when islanding occurs the OUV and OUF values are within the CEI 0-21 limits (i.e. a traditional NDZ situation is always simulated). The simulated scenarios are synthesized in the table 4.5. As regards the utility grid supply voltage, some harmonics are injected and superimposed with the fundamental signal and the maximum of the disturbance is $THD_V$ = 7.3%; for each scenario, such supply voltage harmonics are sized in

order to have a value of THDv at PCC less than the considered threshold value of 5%. As for the previous cases the thresholds for THDv, PJ and VU are set to the values of 5%, 10° and 3%, respectively.

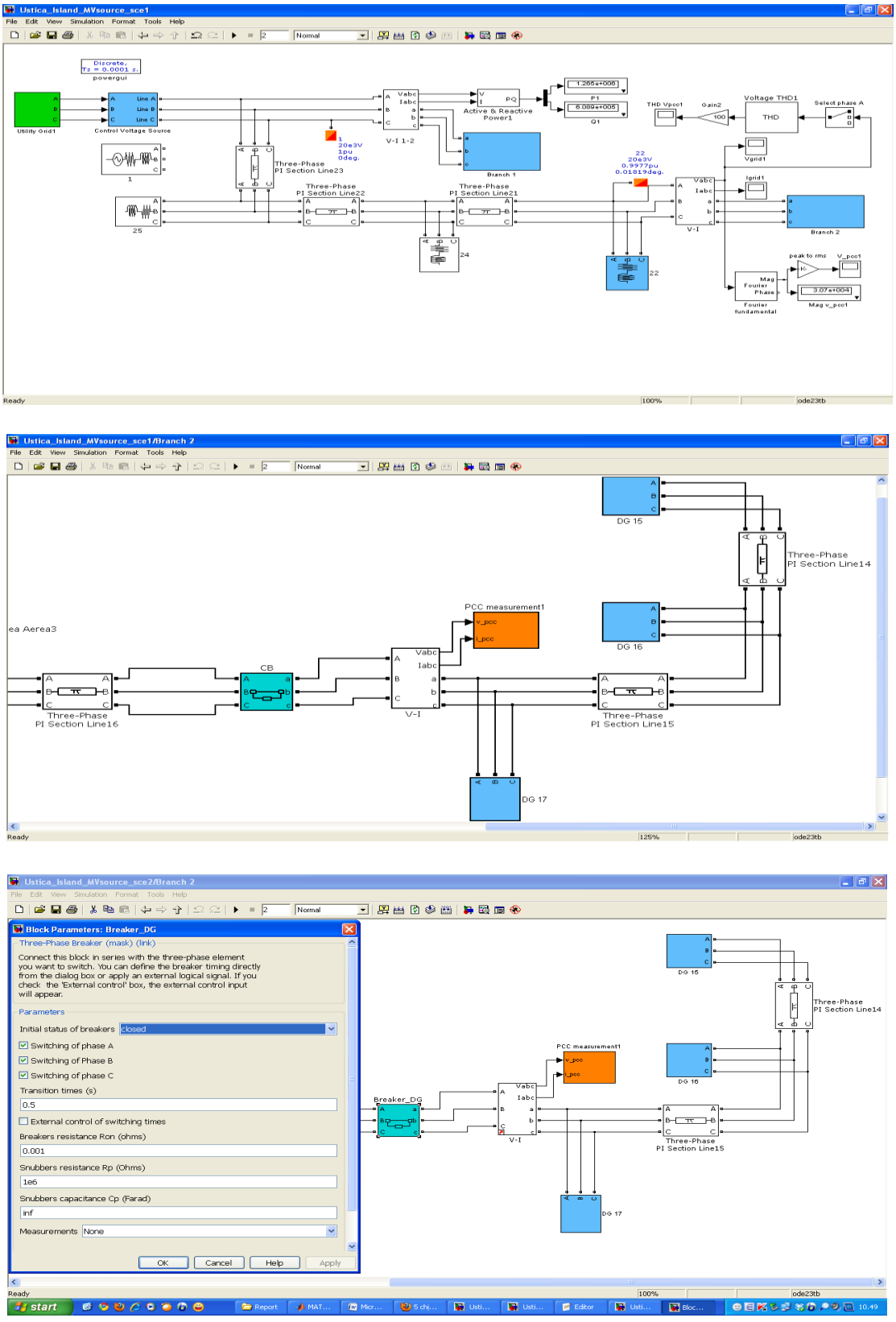


***Fig.4.14. The simulation and the measurement of Medium Voltage Network***

| *CASE 3* | **Implementation** | | | | | | **The Circuit Breaker Status** | | | |
|---|---|---|---|---|---|---|---|---|---|---|
| | *Branch 15* | | *Branch 16* | | *Branch 17* | | **(Initial status of CB: Open/Close)** | | | |
| | *THD-DG* | *Load* | *THD-DG* | *Load* | *THD-DG* | *Load* | **MV_CB** | **CB-15** | **CB-16** | **CB-17** |
| Sce.1 | *5%* *P=1.2*$P_{15}$* | *NonLinear* *($P_{15}$/5)* | *5%* *P=$P_{16}$* | *Linear* | *5%* *P=1.5*$P_{17}$* | *Linear* | C open at [0.5-1] s | O closes at t = 0.75s | C | C |
| Sce.2 | *5%* *P=1.2*$P_{15}$* | *NonLinear* *($P_{15}$/10)* | *5%* *P=$P_{16}$* | *NonLinear* *($P_{16}$/10)* | *5%* *P=1.5*$P_{17}$* | *NonLinear* *($P_{17}$/10)* | C open at [0.5 1] s | C | C | C |
| Sce.3 | *5%* *P=1.15*$P_{15}$* | *Linear* | *5%* *P=1.15*$P_{16}$* | *Linear* | *5%* *P=1.15*$P_{17}$* | *Linear* | C open at [0.5 1.25] s | O closes at t = 1s | O closes at t = 1s | C |

***Table 4.5 Implementation for the simulated scenarios of the CASE 2***

| | Islanding detection response of local measurements – PCC 17 | | | |
|---|---|---|---|---|
| **CASE 3** | **Voltage Phase Jump (PJ)** | **Voltage Unbalance (VU)** | **Total Harmonic Distortion (THD)** | **Islanding Detected** |
| **Sce.1** | **Yes** | **Yes** | **Yes** | **Yes** |
| **Sce.2** | **Yes** | **Yes** | **Yes** | **Yes** |
| **Sce.3** | **Yes** | **Yes** | **Yes** | **Yes** |

| | Islanding detection response of local measurements– PCC 16 | | | |
|---|---|---|---|---|
| **CASE 3** | **Voltage Phase Jump (PJ)** | **Voltage Unbalance (VU)** | **Total Harmonic Distortion (THD)** | **Islanding Detected** |
| **Sce.1** | **Yes** | **Yes** | **Yes** | **Yes** |
| **Sce.2** | **Yes** | **Yes** | **Yes** | **Yes** |
| **Sce.3** | **No** | **No** | **No** | **No** |

| | Islanding detection response of local measurements – PCC 15 | | | |
|---|---|---|---|---|
| **CASE 3** | **Voltage Phase Jump (PJ)** | **Voltage Unbalance (VU)** | **Total Harmonic Distortion (THD)** | **Islanding Detected** |
| **Sce.1** | **No** | **No** | **No** | **No** |
| **Sce.2** | **Yes** | **Yes** | **Yes** | **Yes** |
| **Sce.3** | **No** | **No** | **No** | **No** |

***Table 4.6 the results of scenarios of the CASE 3***

### 4.5.1 SCENARIO 3.1

In this scenario, the DG branches at buses 17 and 16 are connected to the grid and islanding occurs at t = 0.5 s. After islanding, the DG branch at bus 15 is connected to the insulated part of the grid, at t = 0.75 s. The simulation results for each branch are shown in fig. 4.15, 4.16 and 4.17. It can be observed that, when the MV-CB opens at the time 0.5s, THDv at PCC 17 increases from 1.46% to 7.22%; the PJ jumps from -25° to 21.5°, the average value of the phase jump in one cycle is ΔPJ=46.17°;VU jumps from 0 to 10.76%. These values are over the considered threshold of 10° and 3% for PJ and VU, respectively. Therefore, in this scenario, the islanding is detected by the combined passive method. On the other hand, at t = 0.75 s, the insertion of the DG branch at bus 15 causes small variations of the considered parameters. Similar results are obtained for the parameters at PCC 16 and 15. Obviously, for the PCC 15, the variations of the parameters are significant when the MV-CB re-closes, at t = 1 s, while no variations are measured at t = 0.5 s, since the brunch is not connected to the grid at this time. In practical cases, this could be a problem for the grid management and control. Thus in such cases the anti-islanding protection must use the communication method (between the DG's interface device and the utility, in order to achieve the correct information about the state of the system.

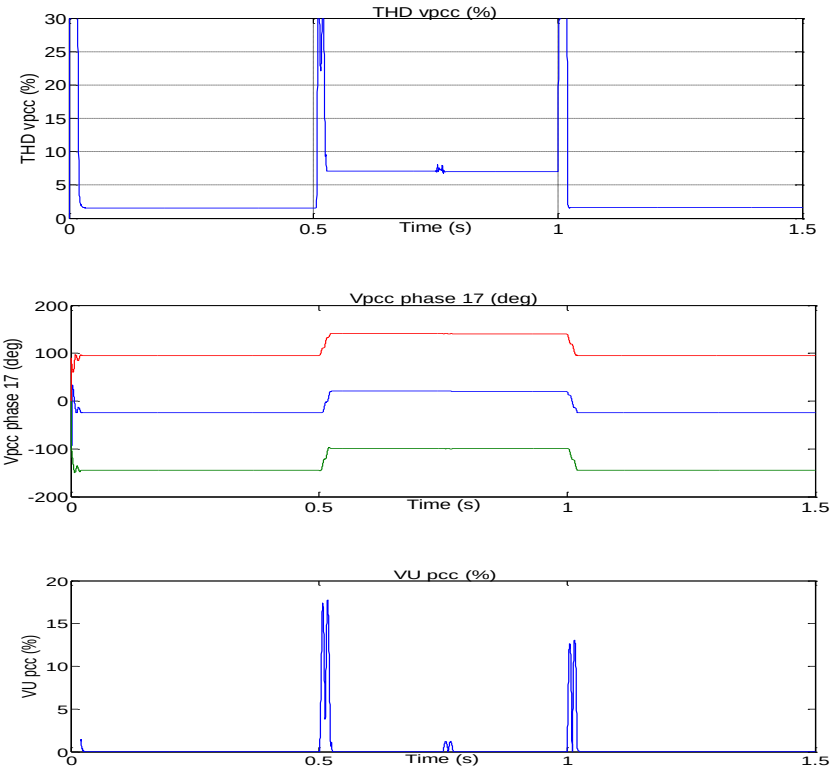


voltage THD at PCC

voltage Phase at PCC

voltage unbalance

***Fig.4.15. the grid variations at PCC 17 of Scenario 3.1***

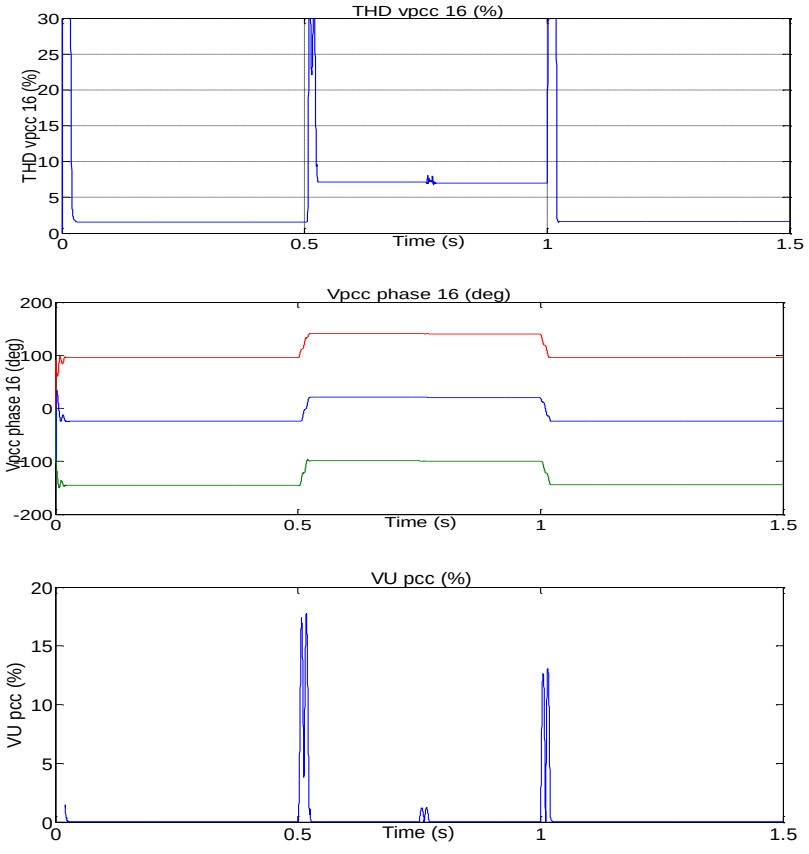


voltage THD at PCC

voltage Phase at PCC

voltage unbalance

***Fig.4.16. the grid variations at PCC 16 of Scenario 3.1***

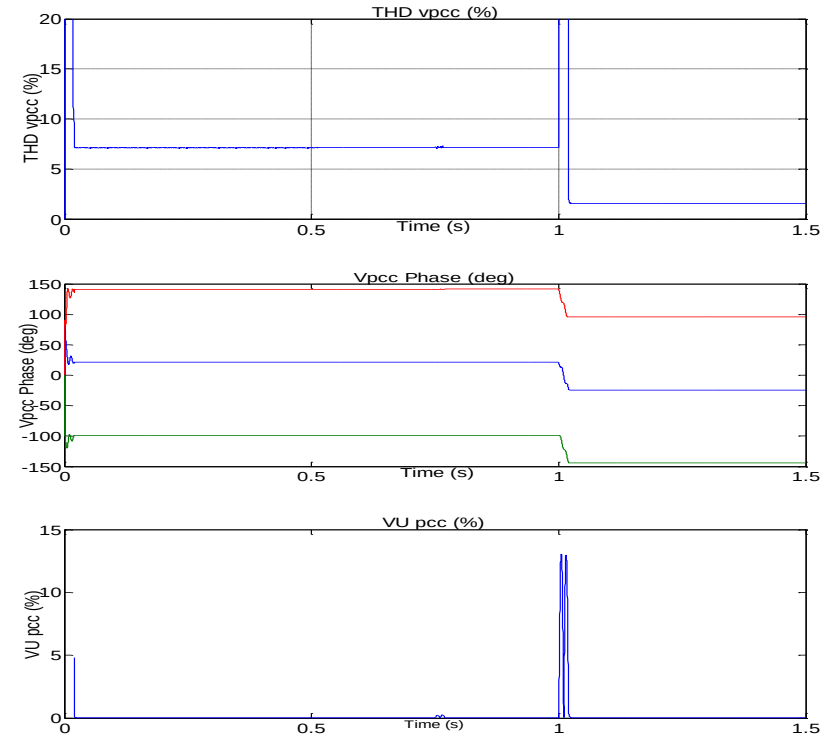


voltage THD at PCC

voltage Phase at PCC

voltage unbalance

***Fig.4.17. the grid variations at PCC 15 of Scenario 3.1***

### 4.5.2 SCENARIO 3.2

In this scenario, the results for OUV, VU and PJ are similar to the previous case for all the PCCs 15, 16 and 17, since all the DGs branches are connected to the grid when islanding occurs. The results obtained for this scenario are reported in the figure below.

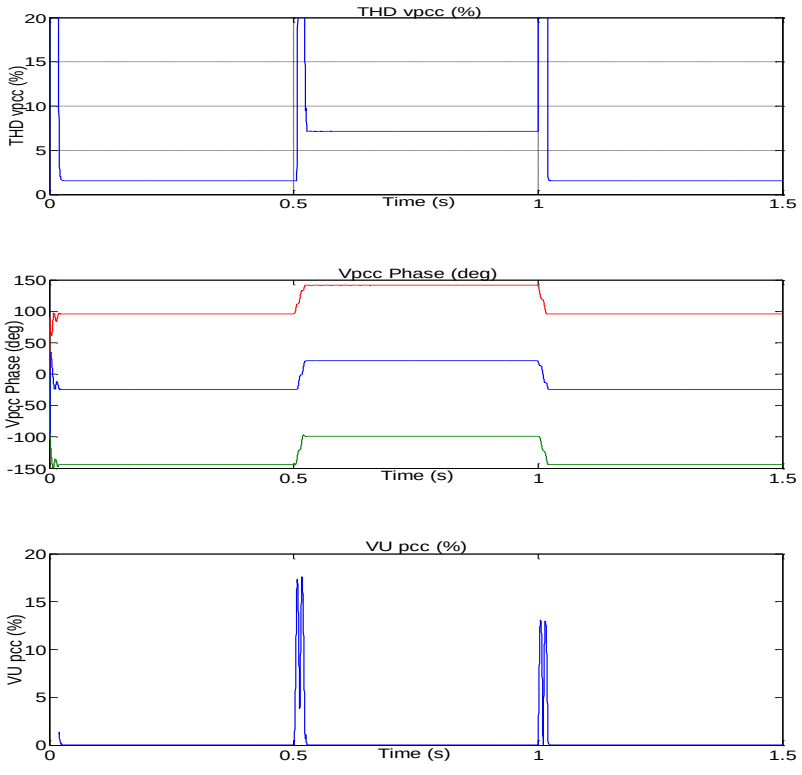


voltage THD at PCC

voltage phase

VU at PCC

***Fig.4.18. the grid variations at PCC 17 of Scenario 3.2***

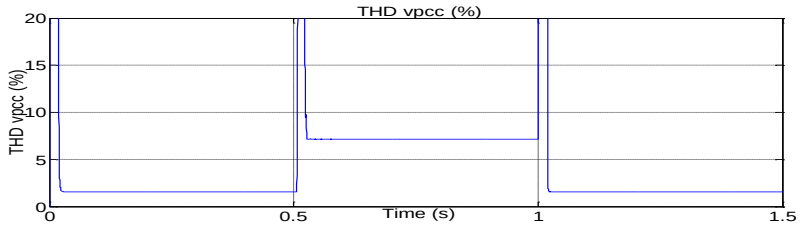


voltage THD at PCC

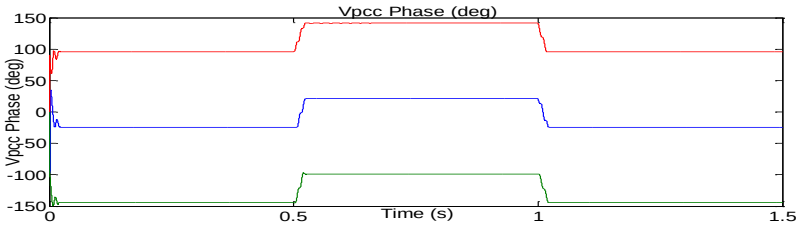


voltage phase

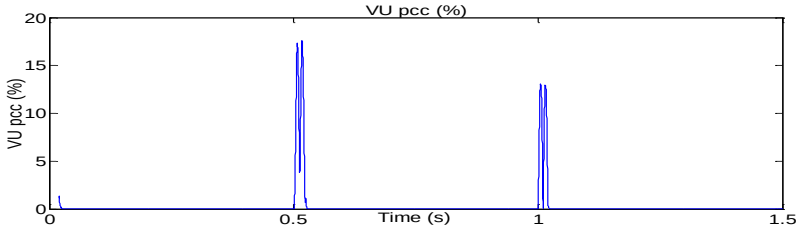


VU at PCC

***Fig.4.19. the grid variations at PCC 16 of Scenario 3.2***

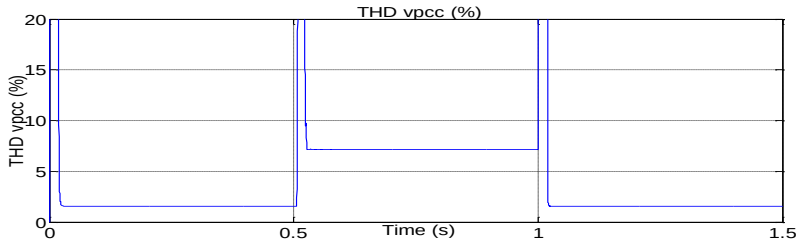


Voltage THD at PCC

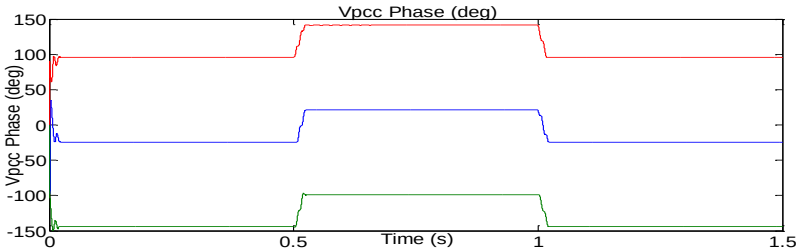


Voltage Phase at PCC

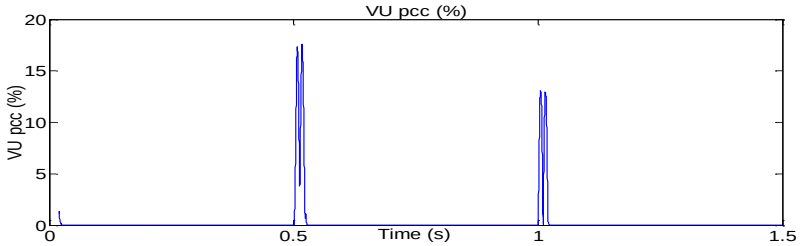


Voltage unbalance

***Fig.4.20. the grid variations at PCC 15 of Scenario 3.2***

### 4.5.3 SCENARIO 3.3

In this scenario, when the CB-22 opens at the time 0.5s, THDv at PCC 17 increases from 1.012% to 7.22%; this value is greater than threshold value 5%. Therefore, the IDM based on THDv detect islanding although THDi of the current load is less than 5%. Besides, the PJ jumps suddenly, the average value of the phase jump in one cycle is ΔPJ=46.48°. Furthermore, VU jumps from 0 to 10.86%. These values are over the considered threshold of 10° and 3% for PJ and VU, respectively. Thus, in this scenario, the islanding is detected at PCC 17 by the combined passive method, (THDv=7.22%>5%, VU=10.86%>3%, ΔPJ =46.48°>10°). On the other hand, for the PCCs 15 and 16, the parameters show significant variations only when the islanding is extinguished, while, when the DGs are connected to the grid, the system is already islanded and no variations are detected, because of the balance between the local load and the DG power.

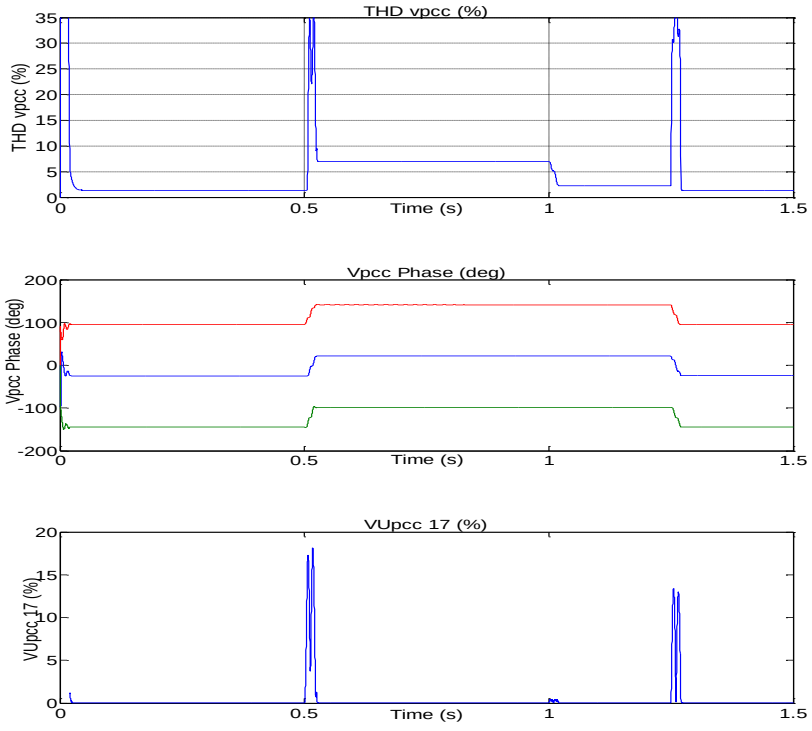


voltage THD at PCC

voltage Phase at PCC

voltage unbalance

***Fig.4.21. the grid variations at PCC 17 of Scenario 3.3***

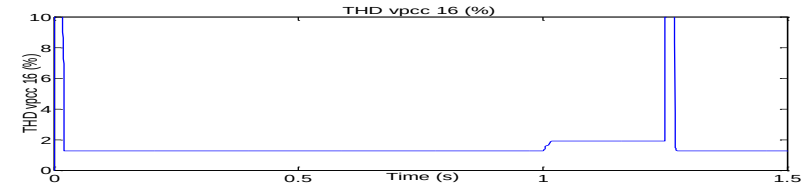


voltage THD at PCC

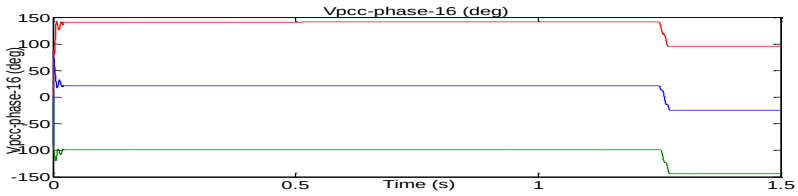


voltage Phase at PCC

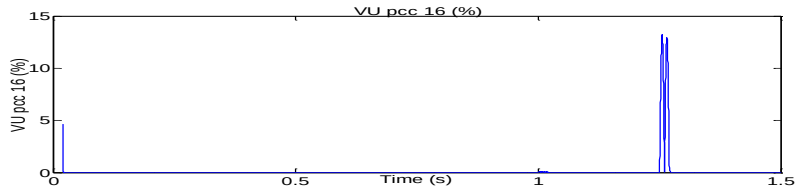


voltage unbalance

***Fig.4.22. the grid variations at PCC 16 of Scenario 3.3***

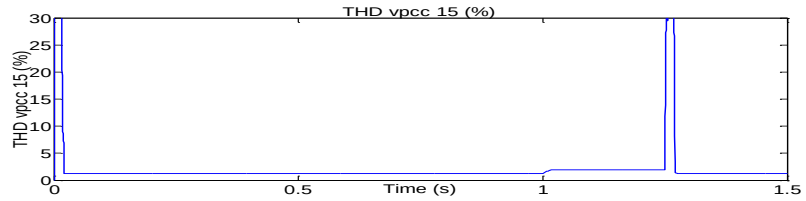


voltage THD at PCC

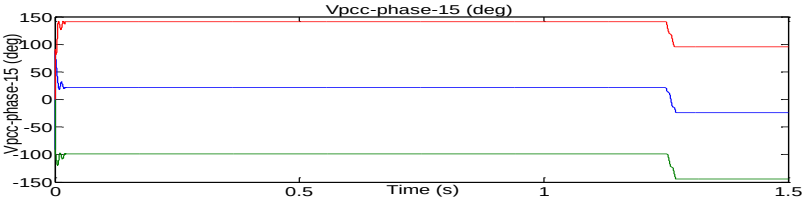


voltage Phase at PCC

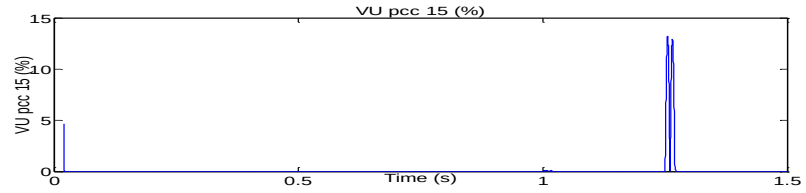


voltage unbalance

***Fig.4.23. the grid variations at PCC 15 of Scenario 3.3***

## CONCLUSIONS

This work has been focused on the development of a hybrid solution for the islanding detection, which makes use of both passive methods (local measurements) and communications between the DGs and the distribution grid. More in detail, the proposed solution has been developed starting from some existing standard requirements for local measurements and improving their effectiveness by both monitoring more than one parameter (combined local measurements) and integrating the measurements with the communications between the grid and the DG. The feasibility of the proposed solution has been investigated discussed, by means of some simulation tests, which are carried out on a real test system (the Ustica Island's distribution network).

The proposed hybrid solution for islanding detection can be implemented in a real system, by integrating local measurements and communication in the DG interface device (ID) and developing a proper communication architecture for smart grid applications. In this viewpoint, the study herein presented has been carried out in conjunction with the following research projects (both under the Scientific Responsibility of prof. Antonio Cataliotti):

- PO FESR 2007-13 Sicily, Line 4.1.1.1, Project: REIPERSEI Title: "Reti Elettriche Intelligenti per la Penetrazione delle Energie Rinnovabili nei Sistemi Elettrici delle Isole minori" (Smart grids for the exploitation of renewable energy sources in the little islands of the Mediterranean Sea),
- PO FESR 2007-13 Sicily, Line 4.1.1.2, Project: SERPICO Title: "Sviluppo E Realizzazione di Prototipi di Inverter per impianti fotovoltaici a COncentrazione" (Development of new inverters prototypes for concentration photovoltaic systems).

In the framework of the aforesaid projects a new ID prototype has been developed for distributed generation, which is able to integrate both measurement and communication functions. Furthermore, different possible solutions have been investigated concerning the communication architecture, mainly using the power line communication technology, even integrated with other wireless solutions, in the framework of a SCADA (Supervisory Control and Data Acquisition) architecture.

The implementation of the proposed hybrid anti-islanding protection in such systems can help to improve the effectiveness of the traditional anti-islanding protection, without introducing power quality problems; moreover the proposed solution is not affected by the number of inverters on the system and it would be effective at any penetration level, with any size

system, and with any type of DGs. The proposed approach can also allow the utility to remote control the DGs, in the perspective of their active participation to the power grid stability and control. In this way, it would be possible to move towards a complete integration of DGs with the utility systems, implementing not only protection functions, but even more, contributing to power grid stability and control.

# APPENDIX: MATLAB/SIMULINK - GUI

## 1. SOURCE CODE

```
%Data entry
Ts=1e-4;  %the sampling time
tpwm=1e-4  %
f_ref=50  % the frequency
load('var_P_Q_mod_simulink.mat');
sim('Ustica_Island_LVsources_sce15_850',1.5);

%Data entry (Initialize the input values)
k = 0;   %the number of iteration-initial value k=0
i = 0;   %the variable initialization for browsing the THDt arrays
t = 0.02;  %time of one cycle

%---Input----------------Ustica_THDvpcc----------------------%
THD_n = 400;      %the sampling number of one cycle
THD_vt = THDvpcc123;  %input variable THDvt array that is assigned as the data input of
PCC voltage THD at the time t
THD_vavgs = 0;     %initialize data of THDavgs
THD_Threshold = 8;
THD_ThetaLeft = -100;  %Theta's lower limit
THD_ThetaRight = 75;  %Theta's upper limit
THD_max_cyc = 5;     %the allowed maximum loop number if theta continuously exceeds the
threshold (limitted value)
THD_at = 1;         %ability test - examine the possibility of occurence of the issue
supposed
%Initialize
THD_cyc = 0;      %Initialize the checked value of the iteration (step_cycle)
THD_err = 1;      % allowed limit of error in 1/4 cycle
THD_stop = 0;      %.....................................
THD_i = 0;       %.....................................

%---Input----------------Ustica_Vpcc----------------------%
V_n = 400;       %the sampling number of one cycle
V_t = vpcc_rms;      %input variable Vt array that is assigned as the data input of PCC
voltage at the time t
V_avgs = 230;       %the one-cycle average of Rated value of the phase to ground voltage
at the steady state and normal loading conditions(Volt)
V_Threshold = 230;
V_max_cyc_50 = 1;    %the allowed maximum loop number out of range if deltaV < 50%
V_max_cyc_50_85 = 2;  %the allowed maximum loop number out of range 50% <= deltaV < 85%
V_max_cyc_110_135 = 2; %the allowed maximum loop number out of range 110% <= deltaV <
135%
V_max_cyc_135 = 1;   %the allowed maximum loop number out of range deltaV >= 135%
V_cyc_50 = 0;
V_cyc_50_85 = 0;
V_cyc_110_135 = 0;
V_cyc_135 = 0;
V_at = 1;          %ability test - examine the possibility of occurence of the issue
supposed
%Initialize
V_i = 0;        %the variable initialization for browsing the Vpcct arrays
V_err = 0.1;      %limit of errors in 1/4 cycle
V_MaxVt = 0;
V_MinVt = 100000;    %=))

%---Input----------------Ustica_vpcc_phase_displacement----------------------%
%Data entry (Initialize the input values)
PhV_n = 400;      %the sampling number of one cycle
PhV_t = Phase_vpcc11;  %input variable Phvt array that is assigned as the data input of
PCC voltage-phase at the time t
PhV_avgs = 0;          %initialize data of the one-cycle average of the Vpcc-phase
displacement at the steady state and normal loading conditions
PhV_DeltaPhase = 1;   %delta's lower limit
PhV_max_cyc = 1;     %the allowed maximum loop number if theta continuously exceeds the
threshold (limitted value)
%Initialize
PhV_i=0;        %the variable initialization for browsing the Phvt arrays
PhV_cyc=0;       %Initialize the checked value of the iteration (step_cycle)
PhV_err = 0.5;     %allowed limitation of voltage-phase displacement in 1/4 cycle
PhV_at = 1;         %ability test - examine the possibility of occurence of the issue
supposed

%---Input----------------Ustica_VUpcc----------------------%
%Data entry (Initialize the input values)
VU_n = 200;       %the sampling number of one cycle
```

```
VU_t = VU_pcc;      %input variable Voltage Unbalance array that is assigned as the data input of PCC Voltage Unbalance at the time t
VU_avgs = 0;      %initialize data of VUavgs
VU_max_VU_spike  =  3;    %ACCORDING  TO  EN50160  "Voltage  unbalance  for  three-phase inverters. Maximum unbalance is 3%"-REF: Grid converters for PV.
          %maximum permissible VU spike = 35*VUavg
VU_max_cyc = 1;      %the allowed maximum loop number if theta continuously exceeds the threshold (limitted value)
%Initialize
VU_i = 0;        %the variable initialization for browsing the VUt arrays
VU_cyc = 0;       %Initialize the checked value of the iteration (step_cycle)
VU_err = 0.05;     %allowed limit of error in 1/4 cycle
VU_at  =  0;          %ability  test  -  examine  the  possibility  of  occurence  of  the  issue supposed

%BEGIN
while (1)
  k = k + 1;
%---Main----------------Ustica_THDvpcc---------------------%
  THD_Sta = 0;
  THD_s = 0;
  THD_i = THD_i + 1;
  for THD_i = THD_i:1:(THD_i + THD_n - 1);
    THD_s = THD_s + THD_vt(THD_i,2);end%main variable
  THD_vavgt = THD_s / THD_n;
  THD_Theta = abs((THD_vavgs - THD_vavgt) / THD_vavgs) * 100;
  THD_vavgs = THD_vavgt;
  if (THD_Theta <= THD_ThetaLeft || THD_Theta >= THD_ThetaRight) %out of RANGE;
    if (THD_vavgt > THD_Threshold)  %out of range of THD's limitation in the IEEE Std
      THD_cyc = THD_cyc + 1;
      if (THD_cyc >= THD_max_cyc) THD_Sta = 1;end
    else THD_cyc = 0;end %inside of range of THD's limitation in the IEEE Std
  else
    if (THD_vavgt > THD_Threshold)  %out of range of THD's limitation in the IEEE Std
      fprintf('\nIV. IDM bases on the THD of Vpcc');
      fprintf('\nThe THD of grid is larger than the maximum THD of rated voltage for synchronous machines in IEEE Std1547 \n');
      fprintf('Out of range at: \n \t Iteration(step): %d \n \t trip time(s): %f \n \t THDvavgt= %f \n',k,k*0.02,THD_vavgt);
      THD_stop = 1;
      THD_Sta = 1;
    end
    THD_cyc = 0; %Inside of range;
  end
%---Main----------------Ustica_Vpcc---------------------%
  V_Sta = 0;
  V_sv = 0;
  V_i = V_i + 1;
  for V_i = V_i:1:(V_i + V_n - 1);
    V_sv = V_sv + V_t(V_i,2);end %main variable
  V_avgt = V_sv/V_n;
  %the one-cycle average of the voltage at the time t
  if (V_avgt > V_MaxVt) V_MaxVt = V_avgt; end;
  if (V_avgt < V_MinVt) V_MinVt = V_avgt; end;
  V_deltaV = (V_avgt / V_avgs) * 100; %compute V% by the measurement values (Vavgt) and the initial values (Vavgs) in the cycle calculation.
  V_pp = V_avgt / V_Threshold;
  if (V_deltaV < 135) V_cyc_135=0; end
  if (V_deltaV < 50) %check the condition deltaV < 50%
    V_cyc_50 = V_cyc_50 + 1;
    if (V_cyc_50 >= V_max_cyc_50)
      if ((V_pp > 1.1) || (V_pp < 0.85))
        V_Sta = 1;end end
  else
    V_cyc_50 = 0; %inside of range
    if (V_deltaV < 85) %check the condition deltaV >=50 and deltaV <85
      V_cyc_50_85 = V_cyc_50_85+1;
      if (V_cyc_50_85 >= V_max_cyc_50_85)
        if ((V_pp > 1.1) || (V_pp < 0.85))
          V_Sta = 1;end end
    else
      V_cyc_50_85=0;
      if (V_deltaV < 110) %check the condition deltaV >=85 and deltaV <110
        V_avgs  =  V_avgt;  %Update  the  initial  values  Vavgs  by  the  measurement  values Vavgt
        V_cyc_50 = 0;
        V_cyc_50_85 = 0;
        V_cyc_110_135 = 0;
```

```
        V_cyc_135 = 0;
      else if (V_deltaV < 135) %check the condition deltaV >=110 and deltaV < 135
          V_cyc_110_135 = V_cyc_110_135 + 1;
          if (V_cyc_110_135 >= V_max_cyc_110_135)
            if ((V_pp > 1.1) || (V_pp < 0.85))
              V_Sta = 1;end end
        else %check the condition deltaV >=135
          V_cyc_110_135 = 0;
          V_cyc_135 = V_cyc_135 + 1;
          if (V_cyc_135 >= V_max_cyc_135)
            if ((V_pp > 1.1) || (V_pp < 0.85))
              V_Sta = 1;end end end
      end
    end
  end
%---Main----------------Ustica_vpcc_phase_displacement---------------------%
  PhV_Sta = 0;
  PhV_s = 0;
  PhV_i = PhV_i + 1;
  for PhV_i = PhV_i:1:(PhV_i + PhV_n - 1);
    PhV_s = PhV_s + PhV_t(PhV_i,2);end
  PhV_avgt = PhV_s/PhV_n;
  PhV_Delta = PhV_avgs - PhV_avgt;
  if abs(PhV_Delta) <= PhV_DeltaPhase;
    PhV_cyc = 0;     %Inside of range
  else  %Out of range of the voltage-phase's limitation
    PhV_cyc = PhV_cyc + 1;
    if (PhV_cyc >= PhV_max_cyc) PhV_Sta = 1;end
  end
  PhV_avgs = PhV_avgt; %Update the initial values Phavgs by the measurement values
Phavgt
%---Main----------------Ustica_VUpcc---------------------%
  VU_Sta = 0;
  VU_s = 0;
  VU_i = VU_i + 1;
  VU_at = VU_at + 1;
  for VU_i = VU_i:1:(VU_i + VU_n - 1);
    VU_s = VU_s + VU_t(VU_i,2);end%main variable
  VU_avgt = VU_s/VU_n;
  VU_ref = 0;
  if (VU_avgt > VU_avgs * VU_max_VU_spike)
    VU_ref = VU_at;
    VU_Sta = 1;end
  if (VU_avgt * VU_max_VU_spike < VU_avgs)
    VU_ref = VU_at - 1;
    VU_Sta = 1;end
  VU_avgs = VU_avgt;
%---Output----------------Ustica_THDvpcc---------------------%
  if (THD_Sta==1)
    if (THD_stop~=1)
      fprintf('\nIV. IDM bases on the THD of Vpcc \n');
      if (THD_cyc >= THD_max_cyc)
        fprintf('Islanding situation occurred \n ')
        fprintf('Out of range at: \n \t Iteration(step): %d \n \t trip time(s): %f \n \t
THDvavgt= %f \n \t Theta= %f',k,k*0.02,THD_vavgt,THD_Theta);
      else fprintf('The system is steady-state')end end end
%---Output----------------Ustica_Vpcc---------------------%
  if (V_Sta==1)
  fprintf('\nI. IDM bases on the Over/Under Voltage method \n');
  if (V_at==1)
    fprintf('Islanding situation occurred \n')
    fprintf('Out of range at: \n \t Iteration(step): %d \n \t trip time(s): %f \n \t
Vpcc(V) = %f \n \t deltaV = %f',k,k*0.02,V_avgt,V_deltaV);
  else fprintf('The system is steady-state \n \t Vpcc(V) = %f \n \t deltaV = %f \n \t
MaxVt = %f \n \t MinVt = %f',V_avgt,V_pp*100',V_MaxVt,V_MinVt);end end
  %In all cases, when 0.85*Vavgs<Vavgt<1.1*Vavgs, print "The system is steady-state and
normal loading condition"
%---Output----------------Ustica_vpcc_phase_displacement---------------------%
  if (PhV_Sta==1)
  fprintf('\nII. IDM bases on the phase displacement of V_pcc \n');
  if (PhV_cyc >= PhV_max_cyc)
    fprintf('Islanding situation occurred \n ')
    fprintf('Out of range at: \n \t Iteration(step): %d \n \t trip time(s): %f \n \t
Phavgt = %f \n \t Delta = %f',k,k*0.02,PhV_avgt,PhV_Delta);
  else fprintf('The system is steady-state and normal loading condition') end end
%---Output----------------Ustica_VUpcc---------------------%
  if (VU_Sta==1)
  fprintf('\nIII. IDM bases on the Voltage Unbalance of Vpcc \n');
```

```
  if (VU_ref >= 0)
    fprintf('Islanding situation occurred \n ')
    fprintf('Out of range at: \n \t Iteration(step): %d \n \t trip time(s): %f \n \t
VUavgt= %f',k,k*0.02,VU_avgt);
  else fprintf('The system is steady-state')end end
end
```

## REFERENCES


1. IEEE 929 Std, *Recommended Practice for Utility Interface of Photovoltaic (PV) Systems*, 2000, IEEE, Published 3 April 2000.: The Institute of Electrical and Electronics Engineers, Inc. 3 Park Avenue, New York, NY 10016-5997, USA.
2. Europe 2020, *A strategy for smart sustainable and inclusive growth*, 2010 available at http://ec.europa.eu/eu2020/index_en.htm: Brussels, COM(2010) 2020.
3. Ipakchi A. and Albuyal, *Grid of the future.* IEEE Power Energy Mag., Mar./Apr. 2009. **7**(2): p. 52-62.
4. European Technology Plarform. *Smart grids – Strategic Deployment Document for the Electricity Network of the Future,* . April 2010 [cited 2010; Available from: http://www.smartgrids.eu.
5. European Commission M/490 EN, *Smart Grid Mandate. Standardization Mandate to European Standardisation Organisations (ESOs) to support European Smart Grid deployment*, March 2011, European Commission M/490 EN: Brussels, Belgium.
6. ENTSOE. *European Network Code Development: The importance of network codes in delivering a secure, competitive and low carbon European electricity market*. March 2013 [cited 2013 15 March].
7. IEEE 1547 Standard, *IEEE Standard for Interconnecting Distributed Resources with Electric Power Systems*, in *IEEE Application Guide for IEEE Std 1547™*2003.
8. Cataliotti, A., et al. *Hybrid passive and communications-based methods for islanding detection in medium and low voltage smart grids*. in *Proceedings of International Conference on Power Engineering, Energy and Electrical Drives, POWERENG-2013*. 2013. Istanbul, Turkey: IEEE.
9. *Technology Action Plan: Smart Grids* 2009, Report to the Major Economies Forum on Energy and Climate.
10. Teodorescu, R., M. Liserre, and P. Rodriguez, *Grid converter for PV and wind power systems*2011.
11. Timbus, A., A. Oudalov, and C.N.M. Ho, *Islanding detection in smart grids*, in *Energy Conversion Congress and Exposition (ECCE), 2010 IEEE* 2010, IEEE. p. 3631 - 3637
12. Standard, E., *Standard EN 50160- Voltage Characteristics in Public Distribution Systems*, in *Voltage Disturbances*2004.
13. Standard, C.-. *Reference technical rules for the connection of active and passive users to the LV electrical Utilities*, in *Regola tecnica di riferimento per la connessione di utenti attivi e passivi alle reti BT delle imprese distributrici di energia elettrica (In Italian).*2011, CEI Standard, december 2011 (In Italian). Italy.
14. Bower, W. and M. Ropp, *Evaluation of islanding detection for PV utility-interactive inverters in Photovoltaic Systems*, 2002, Sandia National Laboratories Albuquerque, New Mexico 87185 and Livermore, California 94550.
15. Tran-Quoc, T., et al., *Behaviour of Grid-Connected Photovoltaic Inverters in Islanding Operation*, in *IEEE Trondheim PowerTech*2011, IEEE.
16. Liserre, M., *Islanding detection for Low Power DPGS.*
17. Chowdhury, S.P., et al. *Islanding protection of distribution systems with distributed generators-A comprehensive survey report*. in *Power and Energy Society General Meeting - Conversion and Delivery of Electrical Energy in the 21st Century*. 2008. IEEE.
18. Jouybari-Moghaddam, H., S.H. Hosseinian, and B. Vahidi. *Automatic Local State Detection for Synchronous Distributed Generators*. in *Electrical Power Distribution Networks (EPDC)*. 2012. Proceedings of 17th Conference on.

19. Aljankawey, A.S., et al., *Passive Method-Based Islanding Detection of Renewable-Based Distributed Generation: The Issues*, in *IEEE Electrical Power & Energy Conference*2010, IEEE.
20. Ropp, M., et al. *Using Power Line Carrier Communications to Prevent Islanding*. in *Proc. of the 28th IEEE Photovoltaic Specialist Conference*. 2000. IEEE.
21. Balaguer I. J., et al., *Survey of Photovoltaic Power Systems Islanding Detection Methods*, in *IEE IECON*2008. p. 2247-2252.
22. De Mango F, et al., *Overview of Anti-Islanding Algorithms for PV Systems. Part I: Passive Methods*, in *Power Electronics and Motion Control Conference, 12th International, EPE-PEMC.* 2006, IEEE. p. 1878-1883.
23. De Mango, F., M. Liserre, and A. Dell'Aquila, *Overview of anti-islanding algorithms for PV system. Part II: Active methods*, in *EPE-PEMC, Portoro2, Slovenia*2006. p. 1884-1889.
24. Etxegarai, A., P. Eguía, and I. Zamora, *Analysis of Remote Islanding Detection Methods for Distributed Resources*, in *International Conference on Renewable Energies and Power Quality (ICREPQ'11)*2011.
25. Maher, G., M. Abdolrasol, and S. Mekhilef, *Robust hybrid anti-islanding method for inverter-based distributed generation*, in *TENCON*2010.
26. Menon V. and M.H. Nehrir, *A Hybrid Islanding Detection Technique Using VU and Frequency Set Point*, in *IEEE TRANSACTIONS ON POWER SYSTEMS*2007. p. 442-.
27. Xu, W., et al., *A power line signaling based technique for anti-islanding protection of distributed generators — Part I: scheme and analysis*, in *IEEE TRANSACTIONS ON POWER DELIVERY*2007.
28. Abarrategui O., et al., *Power line carrier communications and its interest in the current power grid scenario*, in *ICREPQ*. 2008.
29. Jeraputra, C. and P.N. Enjeti, *Development of a robust anti-islanding algorithm for utility interconnection of distributed fuel cell powered generation.* Ieee Transactions on Power Electronics, 2004. **19**(5): p. 1163-1170.
30. Hanif M., M. Basu, and K. Gaughan, *Development of EN50438 compliant wavelet-based islanding detection technique for three-phase static distributed generation systems*, in *IET Renewable Power Generation*2012, The Institution of Engineering and Technology 2012. p. 289-301.
31. Bertling F. and Soter S., *A novel converter integrable impedance measuring method for islanding* Institute of Electrical Drives and Mechatronics, University of Dortmund, 44227 Dortmund, (Germany).
32. Timbus, A., et al. *Line impedance estimation using active and reactive power variations*. in *Proc. IEEE Power Electronics Specialists Conference*. 2007.
33. Jang S. I. and Kim K. H., *An islanding detection method for distributed generations using VU&THD*, in *IEEE TRANSACTIONS ON POWER DELIVERY*2004. p. 745-752.
34. Aiello, M., et al., *Theoretical and Experimental Comparison of Total Harmonic Distortion Factors*, in *IEEE TRANSACTIONS ON POWER DELIVERY*2006, IEEE.
35. Ciobotaru, M., et al., *Online grid impedance estimation for single-phase grid-connected systems using PQ variations*, in *Proc. IEEE Power Electronics Specialists Conference*2007. p. 2306-2312.
36. Timbus A., Teodorescu R., and Rodriguez P., *Grid impedance identification based on active power variations and Grid Voltage Control*, in *in Conference Record of the 2007 IEEE 42nd IAS Annual Meeting Industry Applications Conference*2007, IEEE. p. 949–954.
37. Ciobotaru, M., et al., *Accurate and less-disturbing active anti-islanding method based on PLL for grid-connected converters*, in *IEEE Trans. Power Electronic*2010. p. 1576-1584.

38. Mahat P., Z. Chen, and B. Bak-Jensen, *Review of Islanding Detection Methods for Distributed Generation*, in *Electric Utility Deregulation and Restructuring and Power Technologies, DRPT 2008*2008, IEEE: April 2008 Nanjing China. p. 2743-2748.
39. Ropp, M.E., et al., *Determining the Relative Effectiveness of Islanding Detection Methods Using Phase Criteria and Nondetection Zones*, in *IEEE TRANSACTIONS ON ENERGY CONVERSION*2000, IEEE. p. 290-296.
40. Artale, G., et al. *Measurement and Communication Interfaces for Distributed Generation in Smart Grids*. in *Proc. 2013 IEEE International Workshop on Applied Measurements for Power Systems, AMPS 2013*. 2013. Aachen, Germany: IEEE.
41. Cataliotti A., et al., *Power-line communication in medium-voltage system: simulation model and onfield experimental tests*, in *IEEE Transactions on Power Delivery*2012. p. 62-69.
42. Kim, J.-H., et al., *An Islanding Detection Method for a Grid-Connected System Based on the Goertzel Algorithm*, in *IEEE transactions on Power electronics*April 2011. p. 1049-1055.
43. Velasco, D., et al., *An Active Anti-Islanding Method Based on Phase-PLL Perturbation*, in *IEEE transactions on Power electronics.*2011. p. 1056-1066.
44. Gonzalez G. H. and Iravani R., *Current Injection for Active Islanding Detection of Electronically-Interfaced Distributed Resources.* IEEE transactions on Power delivery, 2006. **21**(3).
45. Karimi H., Yazdani A., and Iravani R. *Negative-Sequence Current Injection for Fast Islanding Detection of a Distributed Resource Unit*. in *IEEE transactions on Power electronics*. 2008.
46. Karimi, H., A. Yazdani, and R. Iravani, *Negative-Sequence Current Injection for Fast Islanding Detection of a Distributed Resource Unit*, in *IEEE transactions on Power electronics*January 2008.
47. Ye, Z., et al., *Evaluation of Anti-Islanding Schemes Based on Nondetection Zone Concept*, in *IEEE transactions on power electronics*2004, IEEE. p. 1171-1176.
48. Benato F., Caldon R., and Cesena F., *Carrier signal-based protection to prevent dispersed generation islanding on mv systems*, in *CIRED, 17th International Conference on Electricity Distribution*2003: Barcelona, Spain. .
49. Biglieri E., et al., *Power Line Comunications (Guest Editorial)*, in *IEEE JOURNAL ON SELECTED AREAS IN COMMUNICATIONS.* July 2006, IEEE. p. 1261–1266.
50. Cataliotti A., A. Daidone, and G. Tinè, *A medium- voltage cables model for power-line communication*, in *IEEE Transactions on Power Delivery.* 2009. p. 129-135.
51. Cataliotti A., Di Cara D., and Tinè G. *Model of line to shield power line communication system on a Medium Voltage network*. in *Proc. 2010 IEEE International Instrumentation and Measurement Technology Conference.* 2010. Austin.
52. Cataliotti A., et al. *Simulation of a power line communication system in medium and low voltage distribution networks*. in *Proc. 2011 IEEE International Workshop on Applied Measurements for Power Systems. .* 2011. Aachen, Germany.
53. Cataliotti A., et al., *Simulation and laboratory experimental tests of a line to shield medium-voltage powerline communication system*, in *IEEE Transactions on Power Delivery.* 2011. p. 2829-2836.
54. Cataliotti A., et al., *Oil filled MV/LV power transformer behavior in narrow-band power-line communication systems*, in *IEEE Transactions on Instrumentation and Measurement.*Oct. 2012. p. 2642-2652.
55. Cataliotti A., et al. *On the use of narrow band power line as communication technology for medium and low voltage smart grids*. in *Proc. 2012 IEEE International*

*Instrumentation and Measurement Technology Conference, I2MTC.* May 13-16, 2012. Graz, Austria.

56. Artale G., et al. *Secondary substation power line communications for medium voltage smart grids*. in *Proc. IEEE International Workshop on Applied Measurements for Power Systems, AMPS 2012*. Sept 2012. Aachen, Germany: IEEE.
57. Castello P., et al., *An IEC 61850-Compliant distributed PMU for electrical substations,* in *IEEE International Workshop onApplied Measurements for Power Systems (AMPS 2012)*Sept 2012: Aachen, Germany.
58. Parikh P.P., Kanabar M. G., and Sidhu T.S. *Opportunities and challenges of wireless communication technologies for smart grid applications*. in *Proc. IEEE Power and Energy Society General Meeting.* Jul. 25-29, 2010. Minneapolis, MN.
59. Gungor V.C., et al., *Opportunities and Challenges of Wireless Sensor Networks in Smart Grid,* in *Industrial Electronics, IEEE Transactions on.*Oct, 2010. p. 3557 - 3564.
60. El Brak M. and Essaaidi M., *Wireless sensor network in smart grid technology: Challenges and opportunities,* in *Sciences of Electronics, Technologies of Information and Telecommunications (SETIT), 2012 6th International Conference on*2012. p. 578-583.